REPORT DOCUMENTATION PAGE

1a. REPORT SECURITY CLASSIFICATION UNCLASSIFIED	1b. RESTRICTIVE MARKINGS
2a. SECURITY CLASSIFICATION AUTHORITY	3. DISTRIBUTION/AVAILABILITY OF REPORT Approved for public release; distribution is unlimited.
2b. DECLASSIFICATION/DOWNGRADING SCHEDULE	
4. PERFORMING ORGANIZATION REPORT NUMBER(S)	5. MONITORING ORGANIZATION REPORT NUMBER(S)
6a. NAME OF PERFORMING ORGANIZATION Naval Postgraduate School 6b. OFFICE SYMBOL (*If applicable*) 55	7a. NAME OF MONITORING ORGANIZATION Naval Postgraduate School
6c. ADDRESS (*City, State, and ZIP Code*) Monterey, CA 93943-5000	7b. ADDRESS (*City, State, and ZIP Code*) Monterey, CA 93943-5000
8a. NAME OF FUNDING/SPONSORING ORGANIZATION 8b. OFFICE SYMBOL (*If applicable*)	9. PROCUREMENT INSTRUMENT IDENTIFICATION NUMBER
8c. ADDRESS (*City, State, and ZIP Code*)	10. SOURCE OF FUNDING NUMBERS Program Element No / Project No / Task No / Work Unit Accession Number

11. TITLE (*Include Security Classification*)
MONTE CARLO ANALYSIS OF ENERGY DEPOSITION IN SOLID STATE MATERIALS BY 400 AND 200 MEV ELECTRONS

12. PERSONAL AUTHOR(S) YAW, RICHARD N.

13a. TYPE OF REPORT	13b. TIME COVERED	14. DATE OF REPORT (*year, month, day*)	15. PAGE COUNT
Master's Thesis	From To	920618	142

16. SUPPLEMENTARY NOTATION
The views expressed in this thesis are those of the author and do not reflect the official policy or position of the Department of Defense or the U.S. Government.

17. COSATI CODES			18. SUBJECT TERMS (*continue on reverse if necessary and identify by block number*)
FIELD	GROUP	SUBGROUP	ELECTRON TRANSPORT; PHOTON TRANSPORT; RADIATION; ENERGY DEPOSITION

19. ABSTRACT (*continue on reverse if necessary and identify by block number*)

Radiation dose distribution measurements have been carried out by the Naval Surface Warfare Center (NSWC) using 200 and 391 MeV electron beams completely penetrating layers of Aluminum, Lead and Aluminum, Polymethyl Melthacrylate (PMMA), and PMMA sandwiching an air gap. For the case of 391 MeV electrons, the results have been compared previously to the corresponding distributions predicted by the Monte Carlo simulation codes EGS3 and ACCEPT [Ref. 1]. Those measurements/predictions for 391 MeV are here compared to predictions by the CYLTRAN electron/photon transport code, and the 200 MeV measurements done by NSWC are compared to CYLTRAN calculations. The CYLTRAN code predictions agree well with measurements at 391 MeV. Comparison of CYLTRAN calculations with the NSWC results for 200 MeV indicates possible saturation of the detectors used to take the measurements. The distribution of energy dose within the target has a large dependence on the location of the air gap. The variation in dose distribution is caused by the change in target geometry resulting from insertion of the air gap.

20. DISTRIBUTION/AVAILABILITY OF ABSTRACT	21. ABSTRACT SECURITY CLASSIFICATION	
☒ UNCLASSIFIED/UNLIMITED ☐ SAME AS REPORT ☐ DTIC USERS	UNCLASSIFIED	
22a. NAME OF RESPONSIBLE INDIVIDUAL MARUYAMA, XAVIER K.	22b. TELEPHONE (*Include Area code*) 408/646-2431	22c. OFFICE SYMBOL Ph/Mx

DD FORM 1473, 84 MAR 83 APR edition may be used until exhausted
All other editions are obsolete

T259320

Approved for public release; distribution is unlimited.

MONTE CARLO ANALYSIS OF ENERGY DEPOSITION IN SOLID STATE MATERIALS BY 400 AND 200 MEV ELECTRONS

by

Richard N. Yaw
Captain, United States Army
B.S., Louisiana State University

Submitted in partial fulfillment
of the requirements for the degree of

MASTER OF SCIENCE IN PHYSICS

from the

NAVAL POSTGRADUATE SCHOOL
June 1992

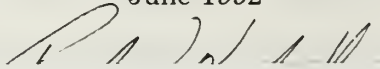

ABSTRACT

Radiation dose distribution measurements have been carried out by the Naval Surface Warfare Center (NSWC) using 200 and 391 MeV electron beams completely penetrating layers of Aluminum, lead and aluminum, polymethyl methacrylate (PMMA), and PMMA sandwiching an air gap. For the case of 391 MeV electrons, the results have been compared previously to the corresponding distributions predicted by the Monte Carlo simulation codes EGS3 and ACCEPT [Ref. 1]. Those measurements/predictions for 391 MeV are here compared to predictions by the CYLTRAN electron/photon transport code, and the 200 MeV measurements done by NSWC are compared to CYLTRAN calculations. The CYLTRAN code predictions agree well with measurements at 391 MeV. Comparison of CYLTRAN calculations with the NSWC results for 200 MeV indicates possible saturation of the detectors used to take the measurements. The distribution of energy dose within the target has a large dependence on the location of the air gap. The variation in dose distribution is caused by the change in target geometry resulting from insertion of the air gap.

T0313
Y328
C.1

TABLE OF CONTENTS

I. INTRODUCTION 1

A. BACKGROUND 1

B. SOME CONSIDERATIONS IN ELECTRON TRANSPORT MODELING 5

1. Electron Step Size 5

2. Electron Radiation Length 7

3. Thin Film Scattering 8

C. OVERVIEW OF ITS 8

1. CYLTRAN 9

2. ACCEPT 10

II. SIMULATION PROCEDURE 12

A. GENERAL PROCEDURAL APPROACH 12

B. NEW ANALYSIS FOR 200 MEV ELECTRONS 18

III. RESULTS AND DISCUSSIONS OF PREVIOUSLY ANALYZED DATA AT 391 MEV 19

A. RESULTS WITH CYLTRAN CORRECTED FOR THIN FILM SCATTERING 19

B. GENERAL COMPARISON OF CYLTRAN TO ACCEPT AND NSWC DATA 19

C. EFFECT OF AIR GAP LOCATION ON TARGET DOSE DISTRIBUTION 26
D. NUMBER OF PRIMARY ELECTRON HISTORIES 28
E. DOSE BREAKDOWN BY ELECTRON TYPE 29
F. EFFECT OF REPLACING THE AIR GAP BY A VOID . . . 45
G. AIR GAP STEP SIZE EFFECTS 47
H. RANDOM NUMBER EFFECTS 47

IV. RESULTS FOR PREVIOUSLY UNANALYZED 200 MEV DATA . . 49

V. CONCLUSIONS 55

APPENDIX A. USING ITS ON THE DEC VAXStation 3200 COMPUTER 57
A. BOOTING AND USING THE VAXSTATION 3200 57
1. Turning the Computer On 57
2. Logging on to the Computer 58
3. Turning the Computer Off 59
4. Miscellaneous Comments on Operation of the Computer 60
B. ITS OVERVIEW 62
C. RUNNING ITS ON THE VAXSTATION 3200 64
1. Batch Mode Submission of an ITS Run 65
2. Running ITS Interactively on the VAXStation 3200 67
D. SAMPLE CYLTRAN INPUT FILE 68

E. SAMPLE CYLTRAN OUTPUT FILE 70

APPENDIX B. INTERACTIVE DATA LANGUAGE (IDL) DATA MANIPULATION AND PLOTTING PROGRAM 98

A. RUNNING IDL AND EXECUTING PROGRAMS 98

B. RUNNING PLOT.PRO TO ANALYZE CYLTRAN OUTPUT . 100

APPENDIX C. SUPPLEMENTARY FIGURES 117

LIST OF REFERENCES 126

INITIAL DISTRIBUTION LIST 128

LIST OF FIGURES

Figure 1. Schematic drawing of a target stack as configured for the NSWC measurements. [Ref. 1] . 4

Figure 2. Low Resolution Target With a 39cm Air Gap Downstream of One PMMA Target Section. This target is called a low resolution target because the target material itself is not resolved into zones in which the dose is evaluated. 14

Figure 3. Low Resolution Target Section and Dosimeter Array 16

Figure 4. High Resolution Target Section and Dosimeter Array 16

Figure 5. Low Resolution 391 MeV CYLTRAN Dose Distribution in PMMA with 39cm Air Gap Downstream of 1st PMMA Target Section, 10,000 primary electrons. Note close agreement of CYLTRAN and data. Compare with Figure 10. 21

Figure 6. Low Resolution 391 MeV CYLTRAN Dose Distribution in PMMA with 39cm Air Gap Downstream of 4th PMMA Target Section, 10,000 primary electrons. 22

Figure 7. Low Resolution 391 MeV CYLTRAN Dose Distribution in PMMA Target with No Air Gap, 10,000 primary electrons. 23

Figure 8. Low Resolution 391 MeV CYLTRAN Dose Distribution in Aluminum Target, 10,000 primary electrons. . . . 24
Figure 9. Low Resolution 391 MeV CYLTRAN Dose Distribution in Target of Lead followed by Aluminum, 10,000 primary electrons. 25
Figure 10. High Resolution 391 MeV CYLTRAN Dose Distribution in PMMA with 39cm Air Gap Downstream of 1st PMMA Target Section, 10,000 primary electrons. Compare to figure 5. Note reduced disagreement with data. 30
Figure 11. High Resolution 391 MeV CYLTRAN Dose Distribution for PMMA with 39cm Air Gap Downstream of 4th PMMA Target Section, 10,000 Primary Electrons. CYLTRAN agrees very well with data here. 31
Figure 12. High Resolution 391 MeV CYLTRAN Dose Distribution for PMMA Target, 10,000 Primary Electrons. CYLTRAN agrees very well with data. . . 32
Figure 13. High Resolution 391 MeV CYLTRAN Dose Distribution for Aluminum Target, 10,000 Primary Electrons. CYLTRAN agrees very well with data. . . 33
Figure 14. High Resolution 391 MeV CYLTRAN Dose Distribution for Target of Lead Followed by Aluminum, 10,000 Primary Electrons. CYLTRAN agrees very well with data. 34
Figure 15. High Res. 391 MeV CYLTRAN Dose Distribution in PMMA with Air Gap Downstream of 1st PMMA Target

Section, 100,000 primary electrons. Compare to previous figure to note drastic decrease in statistical uncertainty. 35

Figure 16. Uncertainty in Total Dose by Radius for 10,000 Primary Electrons in Target of Figure 9. Compare to following figure where 100,000 electrons are used. Note the improvement in statistics with a large number of electrons. 36

Figure 17. Uncertainty in Total Dose by Radius for 100,000 Primary Electrons in Target of Figure 10. Compare with the previous figure for 10,000 electrons. Note the improvement in statistics with a larger number of primary electrons. 37

Figure 18. Classification of Dose Deposition by Type of Electron Depositing the Dose. 39

Figure 19. Dose Breakdown by Electron Type on Beam Axis for Target of Figure 10 with 100,000 Electrons, 391 MeV. Most of the dose is due to primary electrons in the first 15cm depth. The next figure expands the region beyond 20cm depth. 40

Figure 20. Dose Breakdown on Beam Axis (Expanded View Beyond 20cm Depth) for 100,000 Electrons at 391 MeV. Photon processes cause rapid increase in gamma-secondaries at air gap boundary, so beyond 48cm dose is mostly from low energy g-secondaries. 41

Figure 21. Dose Breakdown by Electron Type at 2cm Radius for Target of Figure 10 with 100,000 Electrons, 391 MeV. Dose at this radius is mostly from primaries and is highest at mid-depth after electrons have scattered to that radius. 42

Figure 22. Dose Breakdown by Electron Type at 5cm Radius for Target of Figure 10 with 100,000 Electrons, 391 MeV. Statistics in the air gap begin to decrease because few electrons reach that radius inside the gap. 43

Figure 23. Dose Breakdown by Electron Type at 20cm Radius for Target of Figure 10 with 100,000 Electrons, 391 MeV. Dose from knock-ons overshadows others in the air gap. Uncertainty in the air gap is very high due to the few collisions occurring. 44

Figure 24. CYLTRAN Dose Distribution for Target of Figure 10 with a 39cm Void Replacing the Air Gap. This figure and figure 10 are very similar, showing that dose distribution dependence on air gap location is a geometry effect. 46

Figure 25. High Res. CYLTRAN Dose Dist. for 200 MeV Electrons in PMMA Target. CYLTRAN agrees well with data except on beam axis and large depth. Linearity of NSWC data past 25cm depth suggests saturation of TLD's on axis. Compare with figure 12. 51

Figure 26. High Resolution CYLTRAN Dose Distribution for 200 MeV Electrons in Aluminum Target, 10,000 Primary Electrons. CYLTRAN agrees well with data for this case. Compare to figure 13 at 391 MeV. 52

Figure 27. High Res. CYLTRAN Dose Distribution for 10,000 200 MeV Electrons in Target of Lead followed by Aluminum. CYLTRAN agrees with data except on axis at large depth. Again, TLD saturation is suggested. Compare to figure 14. 53

Figure C1. Dose Breakdown on Beam Axis for Target of Figure 11 with 10000 Electrons. On the centerline the dose is almost completely due to primary electrons. Note the lack of dose after a radiation length, which is 34.4 cm in PMMA. 118

Figure C2. Dose Breakdown at 2cm Radius for Target of Figure 11 with 10,000 Electrons. There is very little energy deposited in the first 20cm. Note the reduction in scale from the previous figure, i.e the dose is reduced quickly off-axis. 119

Figure C3. Dose Breakdown at 5cm Radius for Target of Figure 11 with 10,000 Electrons. Dose is negligible until electrons reach the air gap. Photon processes obviously play a more important role off-axis. . 120

Figure C4. Dose Breakdown at 20cm Radius for Target of Figure 11 with 10,000 Electrons. Note reduction in scale from previous figures. Also note that the dose

from primary, gamma-secondary, and knock-on electrons is roughly equal. 121

Figure C5. Low Resolution 391 MeV Dose Distribution for Target of Figure 4. Comparison of CYLTRAN calculations using 2 different random number seeds, all other parameters remaining the same. 122

Figure C6. High Resolution Dose Distribution for Target of Figure 10 with Different Random Number Seed. Compare to figure 10 to see that the random number seed can cause the results to fluctuate about 20-50%. . . 123

Figure C7. Dose Breakdown at 20cm Radius for Target of Figure 10 with Different Random Number Seed. Notice the small number of collisions experienced in the air gap. The change in random number seed causes a drastic change in the distribution in the air. 124

I. INTRODUCTION

The objective of this work is to test the ability of a computer model, using the Integrated Tiger Series (ITS) code, to accurately predict the behavior of radiation cascades caused when a high energy electron beam traverses a solid target. The approach used has been to study experimental measurements, construct a computer model suitable for use as input to the ITS simulation code system, run the code, and compare the results to the measurements. In order to understand the approach taken in the construction of the computer model forming the basis of this work, some details of the experiments to which the model will be compared must be examined.

A. BACKGROUND

Researchers from the Naval Surface Warfare Center (NSWC) have conducted experiments at the Massachusetts Institute of Technology, Bates Linear Accelerator Center to measure the three-dimensional spatial distribution of energy deposited by radiation showers in a multilayer, multi-element target stack when the target is bombarded by a high energy electron beam [Ref. 1, 2, and 3]. The experiment by NSWC was conducted using 200 MeV and 391 MeV electrons incident on four separate target stack configurations. The results of the 391 MeV experiment were compared with energy deposition distributions calculated

using two different Monte Carlo electron transport model computer codes, EGS3 (Electron-Gamma Shower, Version 3) and ACCEPT. The EGS (for Electron-Gamma-Shower) system of computer codes is a general purpose package developed by the Stanford Linear Accelerator Center (SLAC) for the Monte Carlo simulation of coupled electron and photon transport in arbitrary geometry. ACCEPT is one of a series of codes based on ETRAN [Ref. 5] called the Integrated Tiger Series (ITS), developed by Sandia National Laboratory [Ref. 4].

The target materials examined in the NSWC work were Aluminum, Lead followed by Aluminum, Polymethyl Methacrylate (PMMA, also known as Lucite or Plexiglass), and PMMA sandwiching an air gap. Target plates of roughly equal thickness were constructed of each type of target material. These 5 or 6 plates were stacked together to make target stacks. Each target stack was configured so that the total target thickness, expressed as the areal mass density, was approximately 50 g/cm^2. A schematic of a target stack as configured for the NSWC experiments is shown in Figure 1.

Interspaced at regular intervals in the target stack were planar arrays of Lithium Fluoride Thermoluminescent Dosimeters (TLDs). The TLD arrays consisted of 88 individual dosimeters, 0.1cm in diameter, 0.3cm in length, arranged in concentric annular patterns with their centers along the beam axis, and were designed so as to measure the amount of energy deposited

(dose) as a function of radial distance from the beam at several positions along the length of the target stack.

The target stacks were irradiated by electron beams of 200 and 391 MeV. The results obtained in the work by the NSWC form the basis of this work and are reported in references 1 and 2 for 391 MeV, and in Reference 3 for 200 MeV.

The work by NSWC included a comparison of the 391 MeV measurements to predictions by two Monte Carlo electron/photon shower simulation codes, EGS3 and ITS/ACCEPT. This comparison led the researchers at NSWC to three specific conclusions (these conclusions pertained only to the 391 MeV data). The NSWC conclusions are summarized below. [Ref. 1-3]

- CYLTRAN and EGS3 both predicted values for the dose distribution that agreed well with measurements except in the PMMA target configurations with an air gap.
- Neither ACCEPT nor EGS3 was able to accurately predict the dose distribution in the PMMA configurations with an air gap. The codes predicted doses as much as 100% larger than the measurements.
- The dose distribution in the PMMA target stacks was largely dependent on the location of the air gap within the stack.

In comparison of the results from the present work to those from the NSWC work, the following conclusions have been reached.

- CYLTRAN predictions agreed well with the 391 MeV data taken by NSWC with no exceptions. Even though the dose distribution in the target configuration with an air gap varied with the location of the air gap, CYLTRAN was able to predict the dose.
- The variation in dose distribution caused by changing the location of the air gap seems to be a geometry effect.

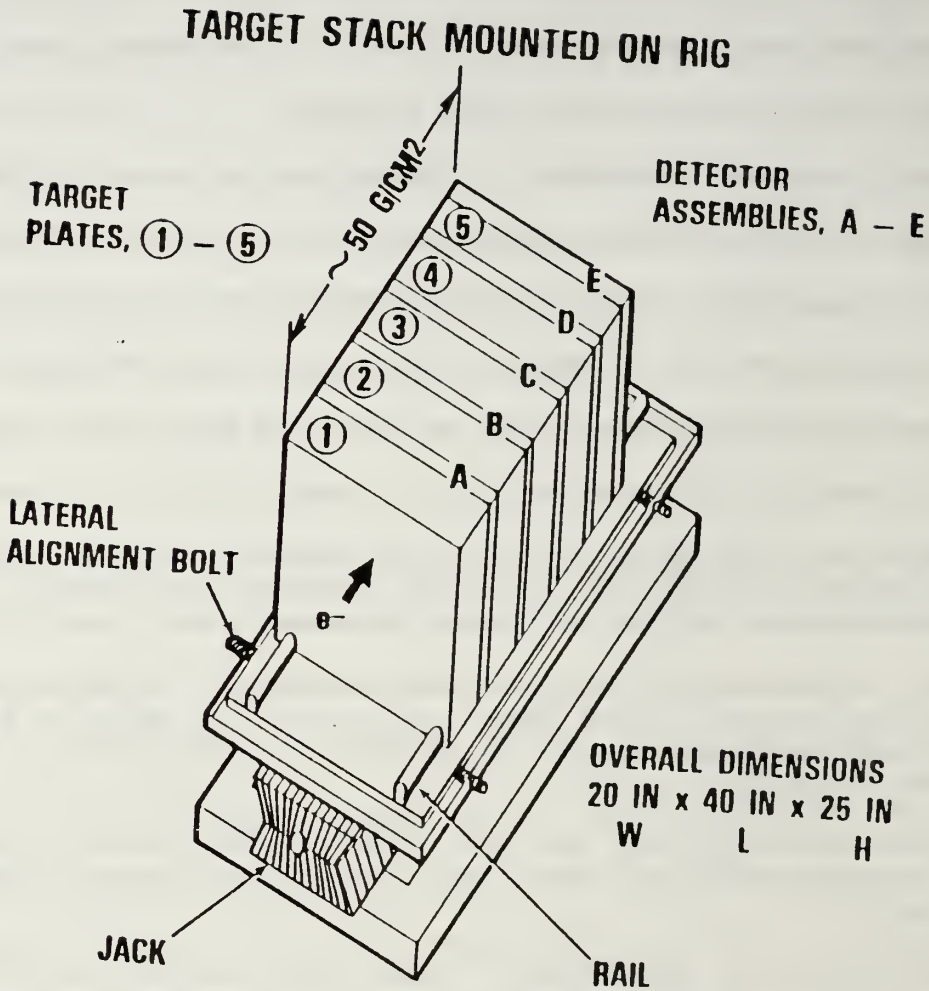

Figure 1. Schematic drawing of a target stack as configured for the NSWC measurements. [Ref. 1]

This conclusion was drawn from the results obtained by comparing the dose in a target with an air gap to that obtained when the air gap was replaced by a void, and finding that they were identical.

- A comparison of the NSWC 200 MeV data to CYLTRAN calculations was done. This was a new comparison since the NSWC work had not compared the data to a transport code at this energy. CYLTRAN produced results that agree very well with the data at 200 MeV except for on-axis measurements in two target configurations (PMMA and Lead followed by Aluminum). Analysis of these results indicates that the dosimeters used to take the data may have been saturated.

B. SOME CONSIDERATIONS IN ELECTRON TRANSPORT MODELING

1. Electron Step Size

The number of collisions undergone by an electron as it passes through a target are too numerous, except possibly at very low electron energies, to allow treatment of individual collisions even by the most powerful computers. Instead, the electron path through the material is divided into discreet segments in which a large number of collisions occur. The smaller pathlengths, or steps, allow the calculation of energy deposition by the sampling of net angular deflection and net energy loss using the appropriate multiple scattering approximation (the Goudsmit-Saunderson approximation for the ITS CYLTRAN code [Ref. 5]) and a "condensed history model" approach [Ref. 6].

Seltzer explains that the step size is chosen by the code user by weighing a set of conflicting requirements. The steps should be short enough that (1) most of the steps in the

electron history are completely inside the target so that the use of multiple-scattering theories for unbounded media are appropriate, (2) the average energy loss is small so that the use of one-velocity multiple-scattering distributions is justified, and (3) the net angular deflection is, on the average, small so that the spatial displacement for the step can be approximated closely by a straight line. The steps should be long enough that (1) there are a sufficient number of collisions per step to justify the use of multiple-scattering theories, and (2) the number of steps per history is not too large. [Ref. 7]

The portion of the ITS code package that generates cross-section data for the transport code to use in its calculations is called XGEN. The step size is determined during the execution of XGEN, in the cross-section generation process, so that it satisfies the relation

$$E_{i+1}=2^{-\frac{1}{k}}E_i. \qquad (1)$$

The value k=8 is chosen by default in XGEN, the ITS cross-section generating program, so that in passing through a given step, an electron will lose 8.3% of its energy [Ref. 8].

Translation of the percentage decrease in electron energy to an equivalent physical step length is done by assuming the electron slows down continuously over the step. The step size is given as

$$s_n = r_0(E_n) - r_0(E_{n+1}), \quad (2)$$

where r_0 is the electron range at the initial and final energies in the step as given by the continuous-slowing-down approximation.

2. Electron Radiation Length

It is convenient, in considering the passage of electromagnetic radiation through material, to measure the thickness of the material in terms of the radiation length. In most processes, some or all of the dependence on the medium is contained in the radiation length. The radiation length is defined as that distance L_R over which a high energy electron is slowed to a fraction equal to 1/e of its original energy. The values of radiation length for electrons for materials of interest in this work are given in Table I. The table gives values of radiation length in units of cm and g/cm^2, the latter being the product of the former and the density of the material.

Table I. RADIATION LENGTHS FOR SELECTED MATERIALS [Ref. 9]

Material	Rad. Length (cm)	Rad. Length (g/cm^2)
Aluminum	8.9	24.01
Lead	0.56	6.37
PMMA	34.4	40.55
Air	30420	36.66

3. Thin Film Scattering

The experimental work on which this work is based involved a target stack configuration with an air gap between two sections of solid material (Lucite). The possibility was explored in the present work that the ITS code might better predict doses in air if the air gap were treated as a thin film, due to the low density of air, and the long radiation length of an electron in air. Most electron/photon transport codes in current use, including the ITS series of codes, are subject to the constraint that they must be used in situations where the material depth exceeds the step size calculated for the electron as it traverses the material. The Goudsmit-Saunderson theory breaks down in the limit of small material thicknesses (thin films). Work in this area has produced the Jordan-Mack correction to the CYLTRAN code to correct the multiple scattering distribution in the code to give better agreement with measurements for thin film targets. [Ref.3, pp. 14-16] The effect of the Jordan-Mack correction, which can be applied to the CYLTRAN code by the user, was investigated in this case to determine if the same sort of thin film phenomenon might be involved in electron transport through an air gap.

C. OVERVIEW OF ITS

The Integrated Tiger Series of computer codes was developed over the last 20 years at the U.S. Department of

Energy's Sandia National Laboratory for use in the simulation of electron/photon transport through various materials. ITS is based primarily on ETRAN (for Electron TRANSport), which was developed by the National Bureau of Standards [Ref. 7, p. 249]. The codes forming the basis of ITS are TIGER, CYLTRAN, and ACCEPT. The three codes differ primarily in that (1) they treat problems in different dimensionalities and (2) they are designed to handle different problem geometries. The TIGER code is confined to the analysis of problems in one dimension. The three-dimensional codes, CYLTRAN and ACCEPT, have been applied in this work and will be explained in further detail below.

1. CYLTRAN

CYLTRAN, a fully three-dimensional transport code employing cylindrical geometry, is a natural choice for simulating problems involving electron beam sources. A complete description of the ITS-CYLTRAN code system is provided in Appendix A.

CYLTRAN enables the code user, relatively easily, to break a target with cylindrically symmetric geometry into an arbitrary number of zones and will determine the energy deposited in each zone by a beam of electrons (as in this case) or photons. The decision of the fineness of division of the target into zones must be balanced against the need for timely results, as the cost for more (or finer) zones is

longer run time in executing the CYLTRAN code. The CYLTRAN geometry allows the electron beam to be incident on the cylinder at any arbitrary point and from any direction. The CYLTRAN code has no ability to present results in a graphical form. The user must provide the resources to take the output from CYLTRAN (which by default is manageable, but can be quite lengthy) and manipulate it either manually or electronically into a form which can be analyzed graphically or in some other manner.

In this work, the CYLTRAN code was given an input file which gave geometry data defining the boundaries of the desired number of target zones. The ensuing code calculations produced a formatted output file containing the energy deposition distributions and other code results. This output file was read by an interactive program written in the Interactive Data Language (IDL), which manipulated the appropriate geometry data and energy deposition distributions into plottable formats for analysis.

2. ACCEPT

ACCEPT is a fully three-dimensional electron/photon transport code which is applicable to problems of any geometry using a combinatorial geometry scheme. While the combinatorial geometry system makes ACCEPT more complex to use, its basic computational algorithms are identical to those in CYLTRAN and

the two should give identical results, as long as the problem geometry allows the use of either code.

II. SIMULATION PROCEDURE

A. GENERAL PROCEDURAL APPROACH

As mentioned previously, references 1 through 3 reported the results of measurements taken by NSWC, and also reported the results of the comparison of measurements at 391 MeV beam energy with dosages predicted by two different Monte Carlo electron-photon transport simulation codes, EGS3 and ACCEPT. The measurements taken by NSWC, reported in reference 3, were not compared to any computer code calculations.

The NSWC results reported in references 1 through 3 were modeled in this work using the CYLTRAN member of the ITS code package. The CYLTRAN code was run on a DEC VAXStation 3200 minicomputer using VAX Fortran. The results of the CYLTRAN runs were read and plotted by a program written for this work using the Interactive Data Language (IDL), a commercially available graphics package marketed by Research Systems, Incorporated. A user's guide and the source code for the IDL program written for the manipulation and plotting of the calculations done in this work are attached as Appendix B.

Although the target stacks used in the NSWC experiment were actually rectangular, or box-shaped, the homogeneous nature of the target stack materials and the use of a normally incident, monoenergetic electron beam suggested that the

targets be modeled as a right circular cylinder with the electron beam (which is taken to be a "point" beam) traveling along the cylinder's longitudinal axis and incident on the face of the cylinder. This geometry allowed the natural use of the CYLTRAN member of the ITS code with its simpler input stream. Figure 2 is a schematic of the target model in the case of the NSWC target consisting of PMMA sandwiching an air gap located downstream of the first 10 g/cm^2 of target material.

The first runs of the CYLTRAN code were intended to determine whether CYLTRAN in fact produced the same results, within statistical expectations, as those obtained at NSWC using ACCEPT. The chief concern in these runs was the prediction of the dose in the TLDs interleaved between each target 'slab' along the length of the target, as opposed to later simulation runs, which would divide the target stack into many more zones, attempting to resolve in greater detail what was happening to the electron energies as the particles progress through the target. For reasons of distinguishing between the degree of fineness of the zones, these first target geometries were called "low resolution targets" and the corresponding CYLTRAN runs were called "low resolution" runs.

After the initial low resolution CYLTRAN runs had been completed, a series of runs was done to determine how the dose in the air gap and the layers of PMMA surrounding it responded to changes in various model characteristics. The

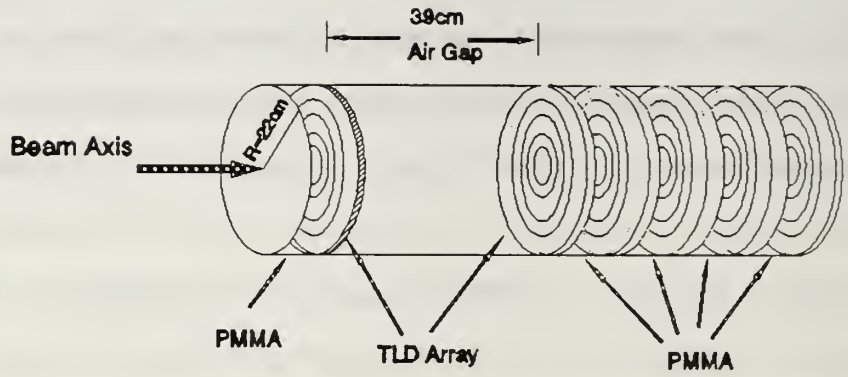

Figure 2. Low Resolution Target With a 39cm Air Gap Downstream of One PMMA Target Section. This target is called a low resolution target because the target material itself is not resolved into zones in which the dose is evaluated.

characteristics which were varied for comparison were the number of CYLTRAN input zones, the number of primary electron histories to be followed by CYLTRAN, the scattering angle approximation used in the code, and the location of the air gap.

CYLTRAN allows the user to determine the number and location of spatial zones to be monitored within the target cylinder. The user simply places into the input data file geometry data specifying the location of zone boundaries (in the terminology used by the ITS system, each zone is called an

"input zone"). One can treat the entire target cylinder as a single input zone or divide the target cylinder into hundreds of finely divided input zones and track the dose deposited in each zones, if so desired. In this series of runs, the CYLTRAN model cylinder and its target sections were divided into small, highly resolved "input zones". Each section of target material was divided longitudinally into 10 slices of equal thickness, and the 39cm air gap was divided into 13 slices, each having a thickness of 3cm. Each slice in all materials was itself divided into 12 radial zones to identically match the radial locations of the LiF TLD's used in the NSWC experiments. The resultant large number of input zones (828 in the case of PMMA sandwiching a 39cm air gap, 660 for all other configurations considered here) allowed CYLTRAN to track the energy deposition at a much finer scale, and a "high resolution" view was obtained of the energy dose in the target as a function of radius and depth. Figures 3 and 4 compare the zoning of the low resolution and high resolution cases.

The high resolution zoning approach to the CYLTRAN model was applied to all targets of concern in the NSWC experiment in order to better assess the performance of CYLTRAN in predicting the measured dose.

Some CYLTRAN runs were done to test the plausibility of the idea that the air gap could be treated as a thin film. The Jordan-Mack thin film scattering correction to the ITS codes was applied to CYLTRAN. Runs were conducted on one of the

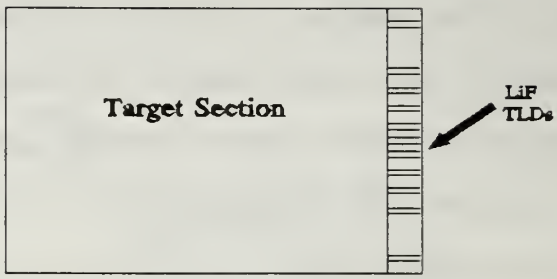

Figure 3. Low Resolution Target Section and Dosimeter Array

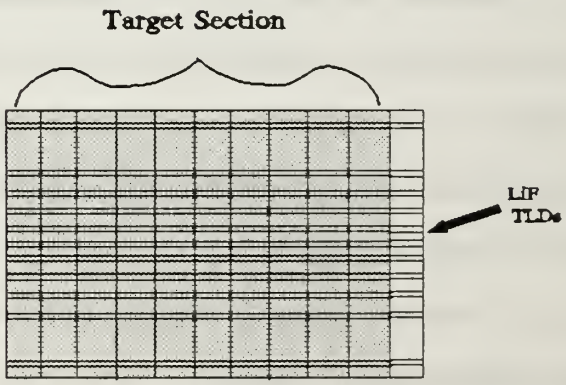

Figure 4. High Resolution Target Section and Dosimeter Array

targets of concern. The results of this run were compared to the results for the same target obtained from CYLTRAN without the correction applied to assess the correction's effect, if any, on the dose distribution in the air gap.

It was of some interest in this work to evaluate the statistical uncertainty involved in the CYLTRAN calculations, and to get some idea of how this uncertainty changed with the choice of input parameters. Of particular interest was the question of how the CYLTRAN-calculated dose in the target varies with a change in the number of primary electrons. To this end, it was necessary to consider how many electrons would be sufficient to statistically represent the real experiment. In the NSWC experiments, the targets were exposed for 10 to 20 seconds to a 0.1μA current. This translates to a total of from 1.6×10^{13} to 3.2×10^{13} electrons. Diagnostic CYLTRAN runs on the Digital VaxStation 3200 used in this work indicated that, with a baseline run time of about 2 hours for 10,000 primary electrons, increasing the number of primary electrons 10 fold to 100,000 would require a run time of about 24 hours, or a factor of 10 increase in computer run time. Changing the number of primary electrons from 10,000 to 100,000 causes a decrease in uncertainty from 20-50% in the former case to 10-20% in the latter (for all materials in this work except air). Due to relatively low value of uncertainty for 100,000 electrons, and to the fact that any further gains in the level of certainty would cost dearly in computer run

time, a CYLTRAN run with 100,000 electrons was decided to be sufficiently representative of the real beam. The CYLTRAN runs for the high resolution target were repeated using 100,000 electron histories and the impact of the gain in statistical certainty was assessed.

B. NEW ANALYSIS FOR 200 MEV ELECTRONS

Reference 3 listed the measurements obtained in experiments using 200 MeV electron beams. Data was reported by NSWC on the three target stacks consisting of only Aluminum, Lead followed by Aluminum, and PMMA. Computer simulations had not been done previously against this data. As part of this work, CYLTRAN runs were performed to see how well CYLTRAN would predict the dose distribution at this energy.

III. RESULTS AND DISCUSSIONS OF PREVIOUSLY ANALYZED DATA AT 391 MEV

A. RESULTS WITH CYLTRAN CORRECTED FOR THIN FILM SCATTERING

The Jordan-Mack correction for use in correcting the ITS code to accurately predict energy deposition in thin films, when applied to CYLTRAN in this work, has no effect on the dose distribution in any of the target configurations considered. This is an indication that, if the codes are inherently unable to treat an air gap at high energies, that inability is not related to any inability to handle thin film scattering phenomena.

B. GENERAL COMPARISON OF CYLTRAN TO ACCEPT AND NSWC DATA

Reference 1 reported dose distributions in the target stack as predicted by ACCEPT. ACCEPT calculations were reported for dose in the LiF dosimeters at 6 longitudinal points along the stack in the case of the 2 targets with PMMA sandwiching an air gap, and for 5 points along the stack in the cases of the other targets (PMMA, aluminum, and lead followed by aluminum). Figures 5 through 9 show the results of predictions calculated using CYLTRAN (it is important to note that figures 5 through 9 show points calculated at a few discreet points along the length of the cylinder corresponding to the longitudinal depths at which the NSWC data were taken.

Lines drawn between the points are shown only to help distinguish between sets of calculations/data). These calculations were done using the "low resolution" model detailed in Chapter II so that a fair comparison could be done between the two sets of calculations. Generally, agreement between the NSWC data and CYLTRAN calculations is good to very good. Discrepancies between the code and experiment seems to be greatest at a radius of 5 cm. In view of a statistical uncertainty at this radius of 20 - 40 percent, however, the discrepancy may not be significant. ITS calculations, in all target materials, agree very well for radii in the range from the axis to about 2 cm.

CYLTRAN scores a dose by whether it was deposited by a primary, knock-on, or gamma-secondary electron. Analysis of the CYLTRAN calculations shows that dose on axis is due almost totally to primary electrons. At a radius of 20 cm, the dose is due mostly to gamma-secondary electrons. The doses in between are due to various combinations of primary and gamma-secondary electrons. Knock-on electrons have only a minor contribution in all cases.

ACCEPT and CYLTRAN give results that vary by little in most cases. However, in some cases, especially as the radius approaches 20cm, the two codes seem to give widely varying answers. It has been noted previously that ACCEPT and CYLTRAN have the same transport physics as their basis, so their is no reason to believe the two codes should produce widely varying

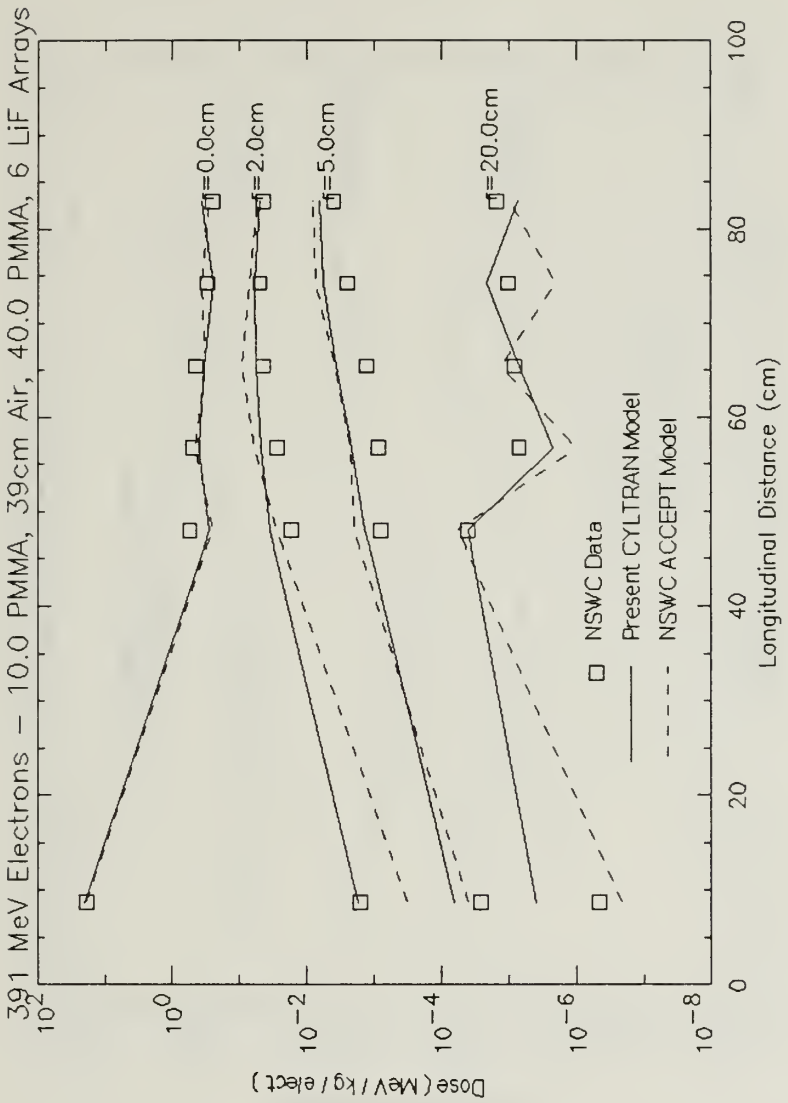

Figure 5. Low Resolution 391 MeV CYLTRAN Dose Distribution in PMMA with 39cm Air Gap Downstream of 1st PMMA Target Section, 10,000 primary electrons. Note close agreement of CYLTRAN and data. Compare with Figure 10.

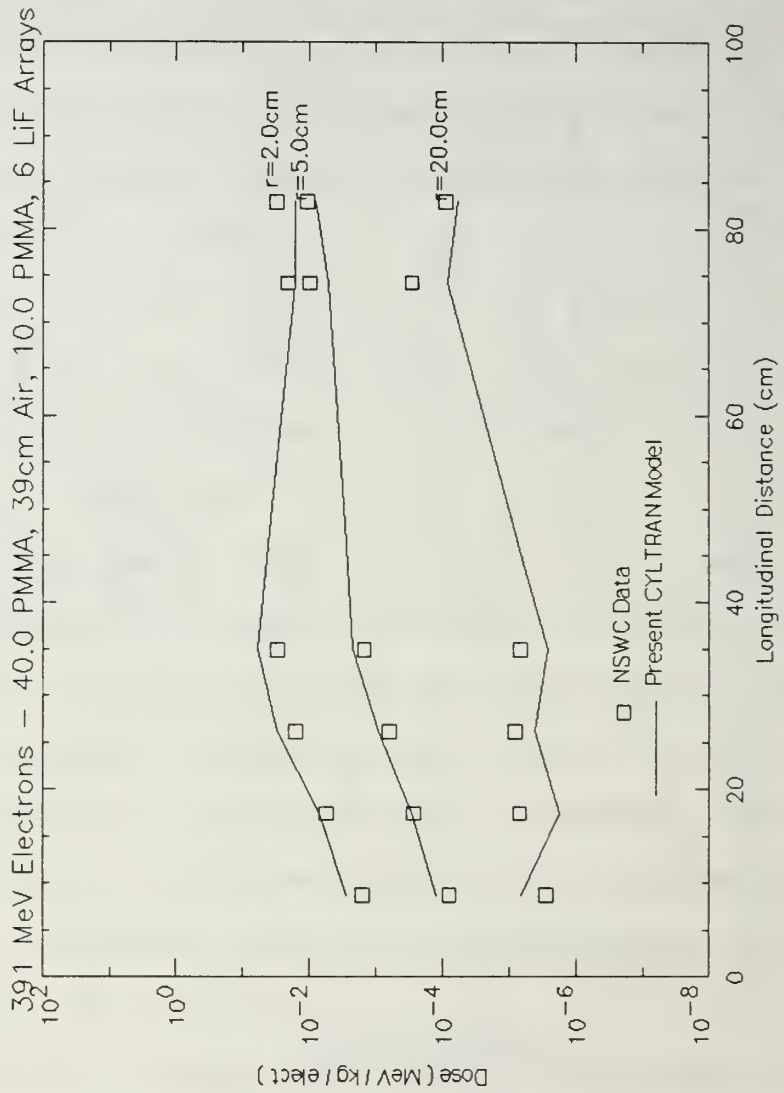

Figure 6. Low Resolution 391 MeV CYLTRAN Dose Distribution in PMMA with 39cm Air Gap Downstream of 4th PMMA Target Section, 10,000 primary electrons.

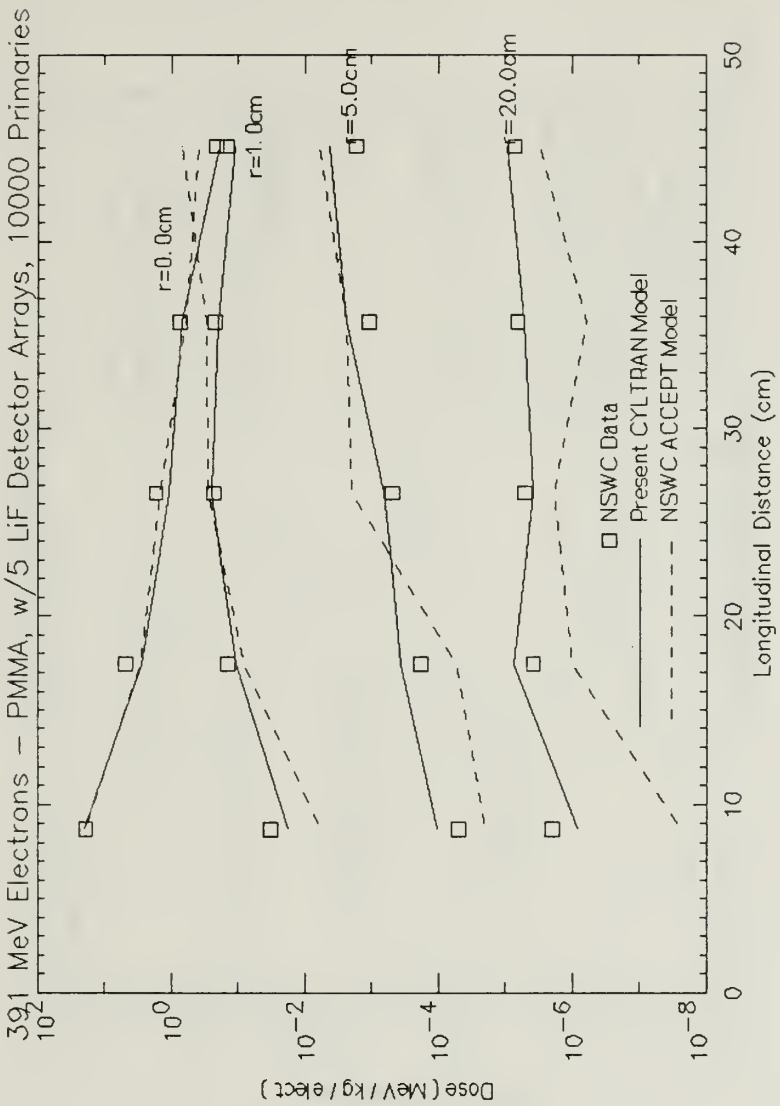

Figure 7. Low Resolution 391 MeV CYLTRAN Dose Distribution in PMMA Target with No Air Gap, 10,000 primary electrons.

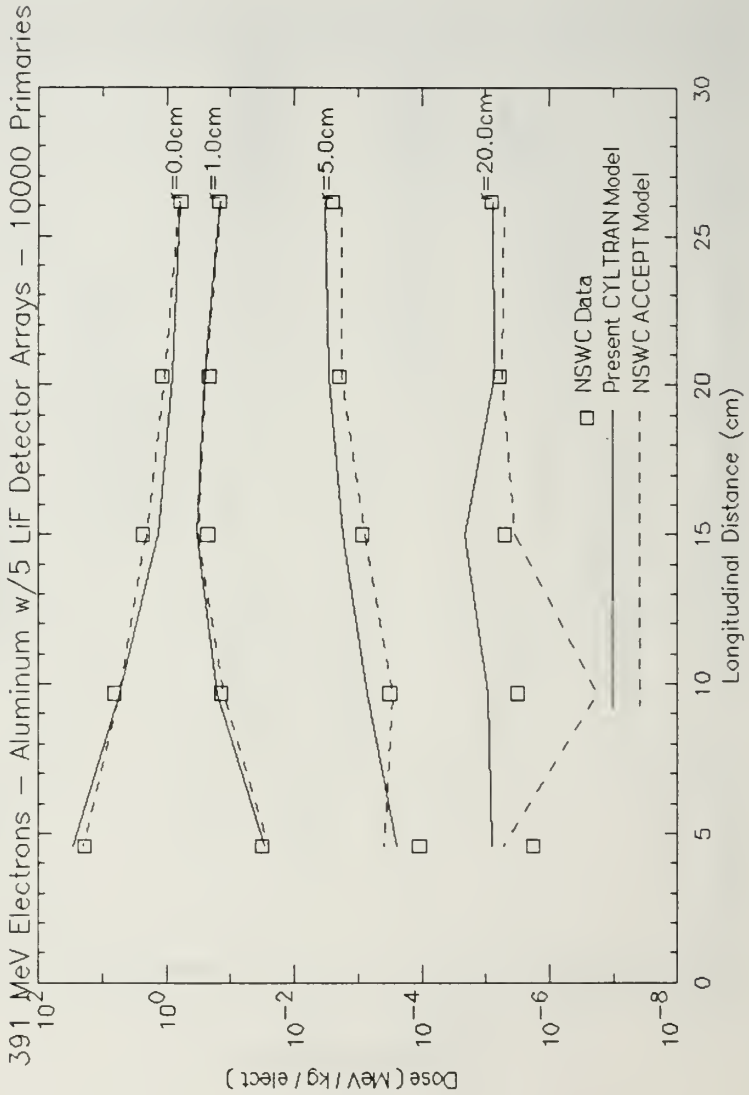

Figure 8. Low Resolution 391 MeV CYLTRAN Dose Distribution in Aluminum Target, 10,000 primary electrons.

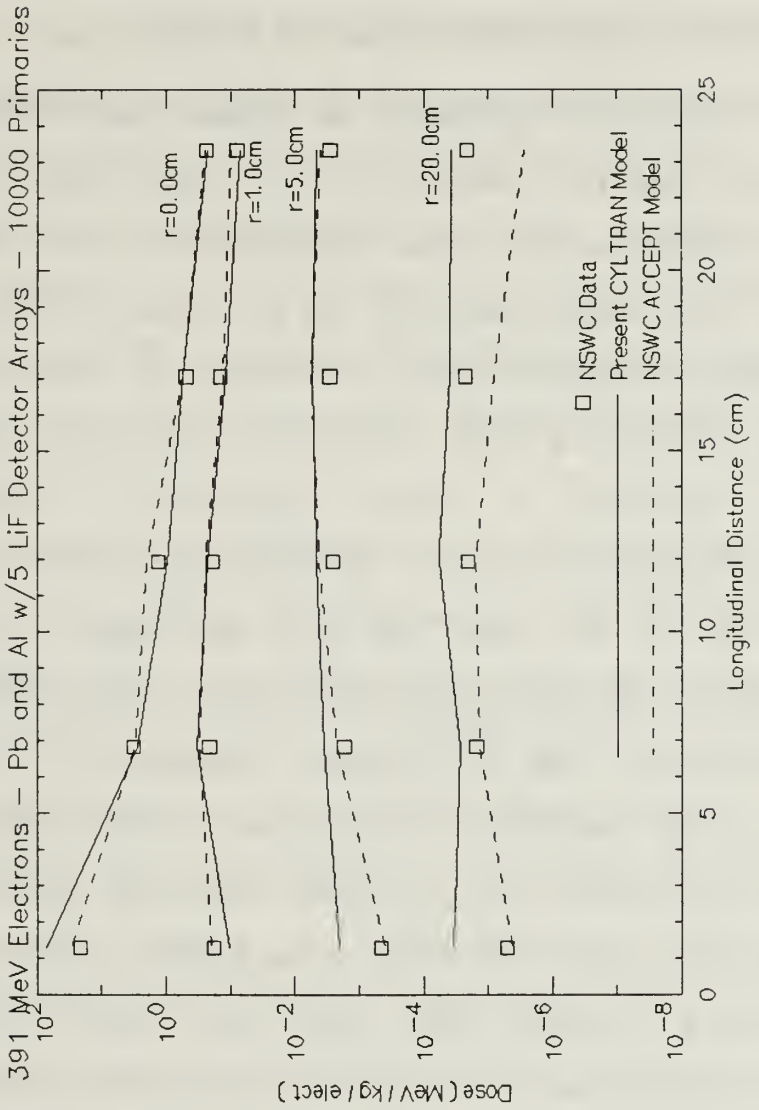

Figure 9. Low Resolution 391 MeV CYLTRAN Dose Distribution in Target of Lead followed by Aluminum, 10,000 primary electrons.

results. However, when consideration is given to the fact that, at 20cm radius the uncertainty in the calculations can be as high as 50%, the variation between the results is not that surprising. That is, ACCEPT and CYLTRAN seem to be within the statistical uncertainty of each other.

C. EFFECT OF AIR GAP LOCATION ON TARGET DOSE DISTRIBUTION

If an air gap is inserted in the target stack, there is a marked variation in the dose distribution. The dose in the portion of the target material on or close to the beam axis doesn't change significantly. However, as one looks at the results at distances away from the axis, the dose in any particular section of target material is significantly affected by whether or not it is preceded in the longitudinal direction by an air gap. As the air gap is moved to a different depth in the target stack, the dose in the material preceding the air gap is reduced. However, the section of target material immediately following the air gap receives a higher dose than that which would have been received if the air gap were not there. Both of these effects are increasingly pronounced as radius from the beam axis increases. A comparison of Figures 5, 6, and 7 illustrates this point.

CYLTRAN calculations agree very well with data in reference 1. That is, the changes in dose due to insertion of an air gap seem to be faithfully predicted within statistical uncertainty, which will be discussed later. Incidentally, in

those cases where there are noticeable discrepancies between CYLTRAN and data, the CYLTRAN dose distribution shows a tendency to overpredict. The only case in which the agreement between CYLTRAN and the data may be questionable is shown in Figure 5 at 5cm radius and, most remarkably, at 20cm radius. In this regard, it is well to note the large statistical uncertainty inherent in the CYLTRAN Monte Carlo algorithm, which runs from 25-50 percent at 20cm radius for 10,000 primary electrons in the target of Figure 5, as will be discussed later. In light of this uncertainty, the apparent disagreement in Figure 5 between CYLTRAN and data may not be significant.

The low resolution CYLTRAN calculations shown in figures 5 through 9 show only the doses in the dosimeter arrays located between the target sections and before and after the air gap. A high resolution CYLTRAN run, in which target sections are divided in much finer zones, sheds a great deal of light on how the dose distribution behaves in the target material itself. Figure 10 illustrates the high resolution dose distribution in the case of PMMA with the air gap located downstream of the first target section. Figure 11 shows the dose distribution for PMMA with the air gap downstream of the fourth target section. Figures 12, 13, and 14 show dose distributions for targets of solid PMMA, Aluminum, and Lead followed by Aluminum, respectively.

A comparison of Figure 10 with Figure 5 shows that the overall disagreement between the NSWC data and these CYLTRAN calculations is reduced by dividing the problem target geometry into smaller zones. The high resolution calculations verify the continuous nature of the dose distribution. Except for statistical fluctuations of the dose about a mean value, the dose is in fact smoothly distributed in the cylinder, even across the air gap. The most well-defined results are given on axis. This is what would be expected, as there the beam is most intense and the probability of an electron colliding with an "air molecule" would be the highest. In other words, the statistics are better on axis and get increasingly worse with increasing radius. This would explain the absence of plottable points at 5cm and 20cm radius in the air gap in Figure 10. At radii greater than about 5cm in the air gap with 10000 primary electrons the probability of a collision is extremely low. Thus, the dose in the air gap will be calculated by CYLTRAN to be zero in most cases. This is born out in Figure 10.

D. NUMBER OF PRIMARY ELECTRON HISTORIES

Since the Monte Carlo calculations which are the basis of the CYLTRAN code is statistical in nature, one might expect that increasing the number of primary electrons would cause a decrease in the statistical uncertainty of the CYLTRAN calculations. Results obtained in this work would indicate that this is so. A plot of dose per incident electron for the

target of Figure 10 using 100,000 incident electrons is shown as Figure 15. The better definition of the dose distribution at large radii in the air gap is a certain indication that statistics have improved significantly. Comparison of figures 10 and 15 reveals that, in the target material, the value of the dose calculated by CYLTRAN doesn't depend on the number of primary electron histories followed. The statistical benefit in raising the number of histories is shown in the comparison of Figures 16 and 17. A factor of 10 increase in the number of primary electrons produces a decrease in uncertainty of at least 50% at all radii. The most significant benefit derived by using more electrons is gained in the air gap and at large radii, where the collision probability is smallest.

E. DOSE BREAKDOWN BY ELECTRON TYPE

The dose deposited in a target zone by an electron can be classified by the type of electron that deposited the dose. The electron type is identified as either primary, gamma-secondary, or knock-on. A primary electron is an electron that was in the original electron beam incident on the target. A knock-on electron is one that has been knocked free of an atom through some collisional process. A gamma-secondary electron is an electron that has been emitted from an atom through any process involving a photon. An important part of this classification is that once a photon has knocked an electron from an atom, that electron is a gamma-secondary electron as

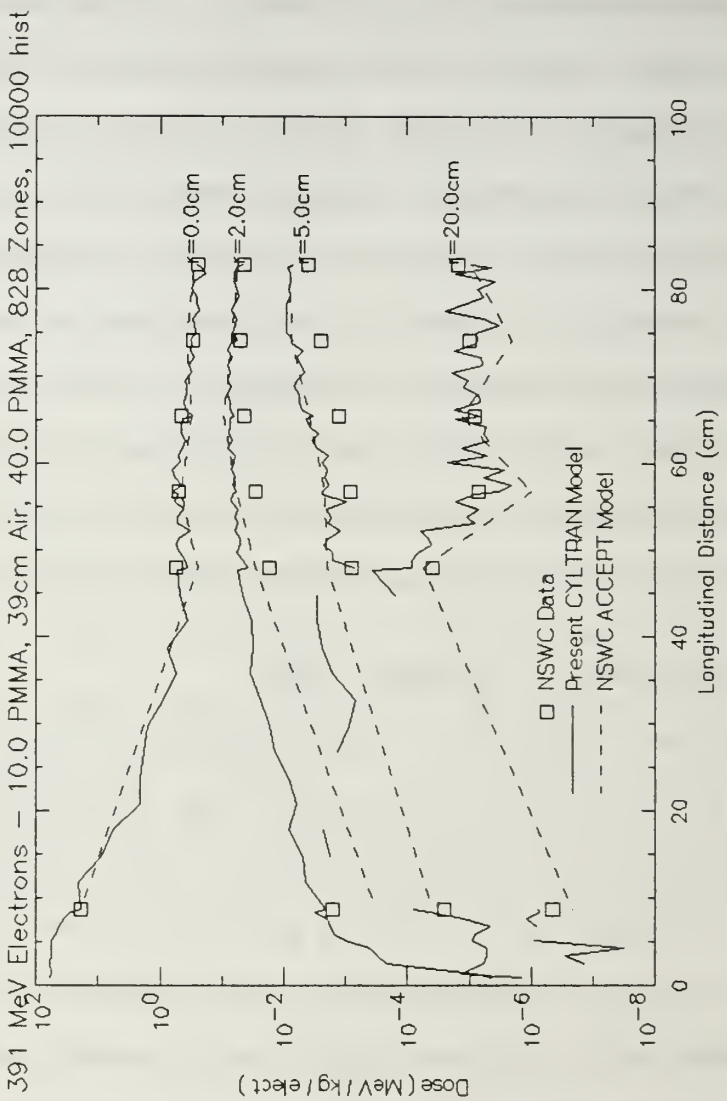

Figure 10. High Resolution 391 MeV CYLTRAN Dose Distribution in PMMA with 39cm Air Gap Downstream of 1st PMMA Target Section, 10,000 primary electrons. Compare to figure 5. Note reduced disagreement with data.

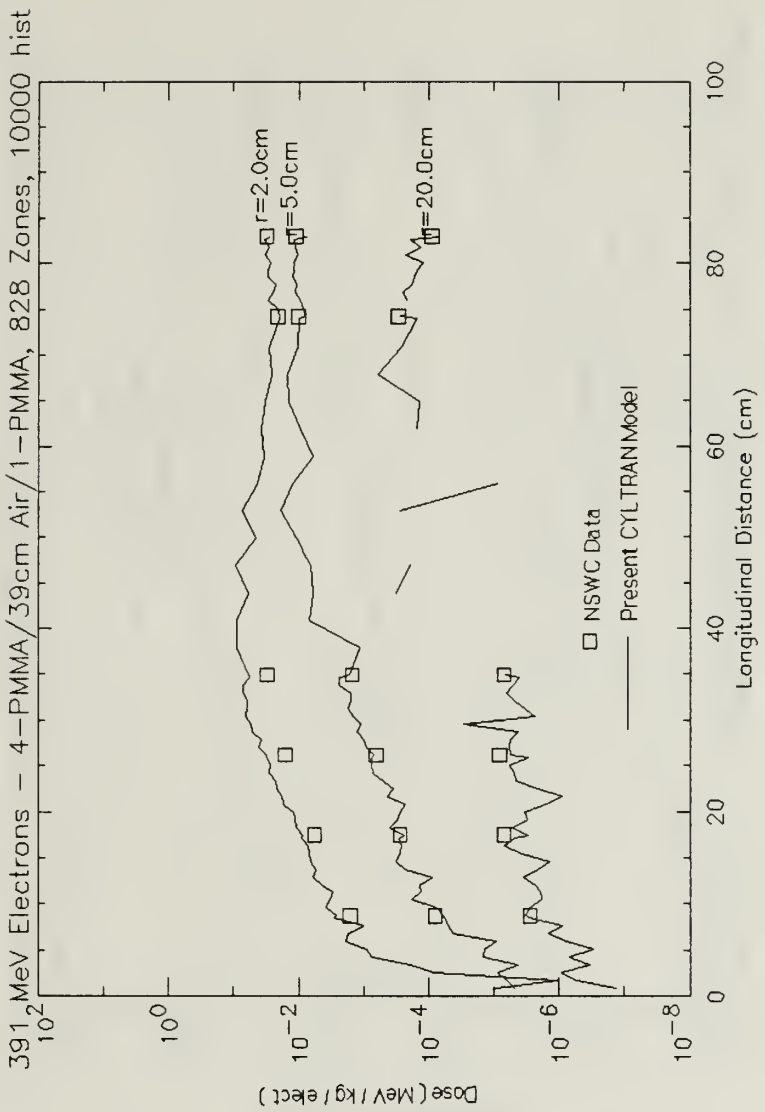

Figure 11. High Resolution 391 MeV CYLTRAN Dose Distribution for PMMA with 39cm Air Gap Downstream of 4th PMMA Target Section, 10,000 Primary Electrons. CYLTRAN agrees very well with data here.

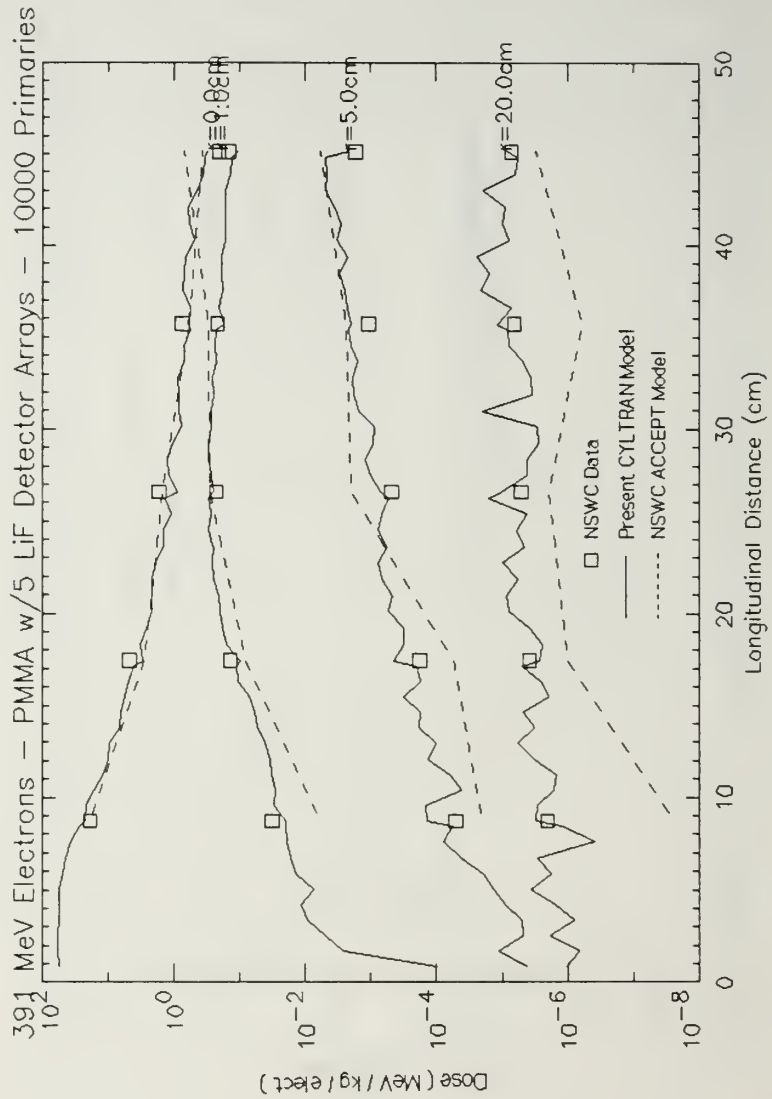

Figure 12. High Resolution 391 MeV CYLTRAN Dose Distribution for PMMA Target, 10,000 Primary Electrons. CYLTRAN agrees very well with data.

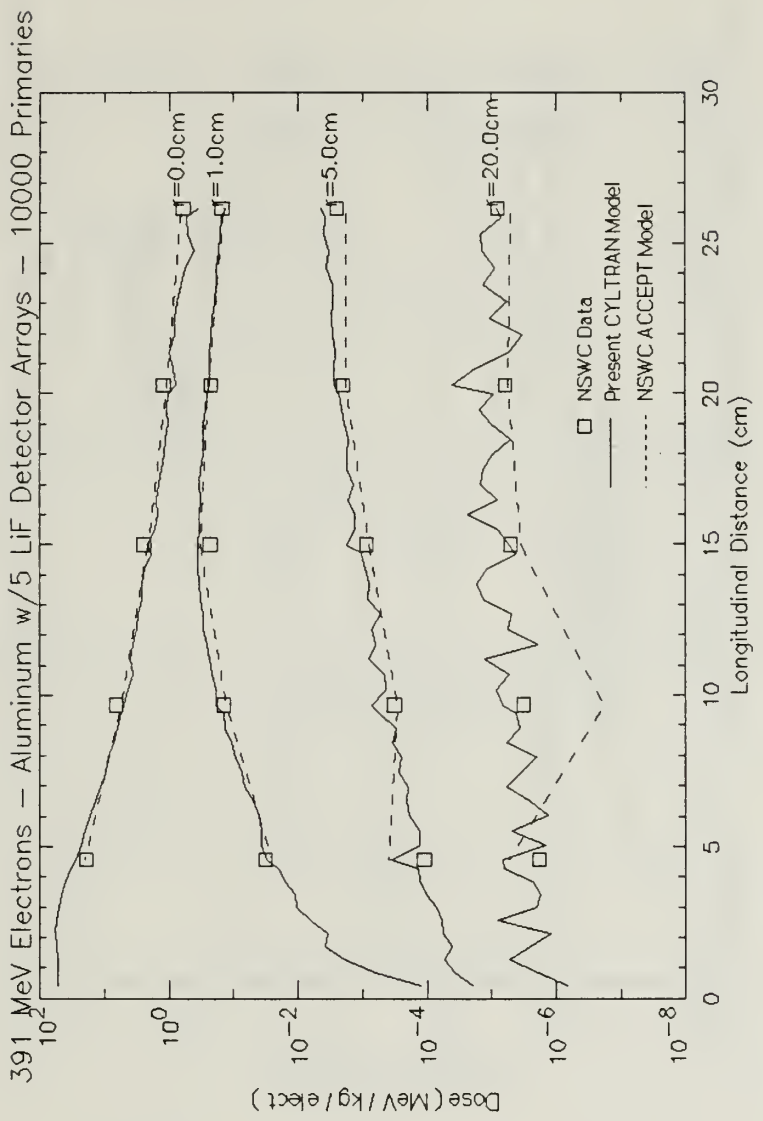

Figure 13. High Resolution 391 MeV CYLTRAN Dose Distribution for Aluminum Target, 10,000 Primary Electrons. CYLTRAN agrees very well with data.

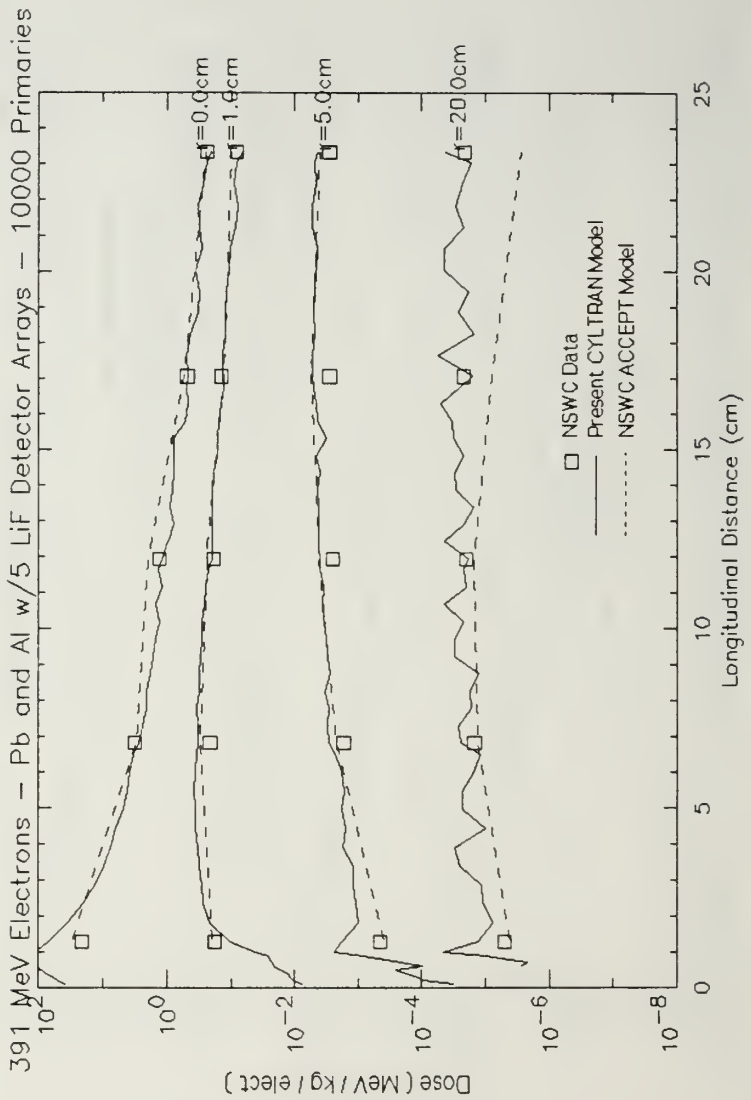

Figure 14. High Resolution 391 MeV CYLTRAN Dose Distribution for Target of Lead Followed by Aluminum, 10,000 Primary Electrons. CYLTRAN agrees very well with data.

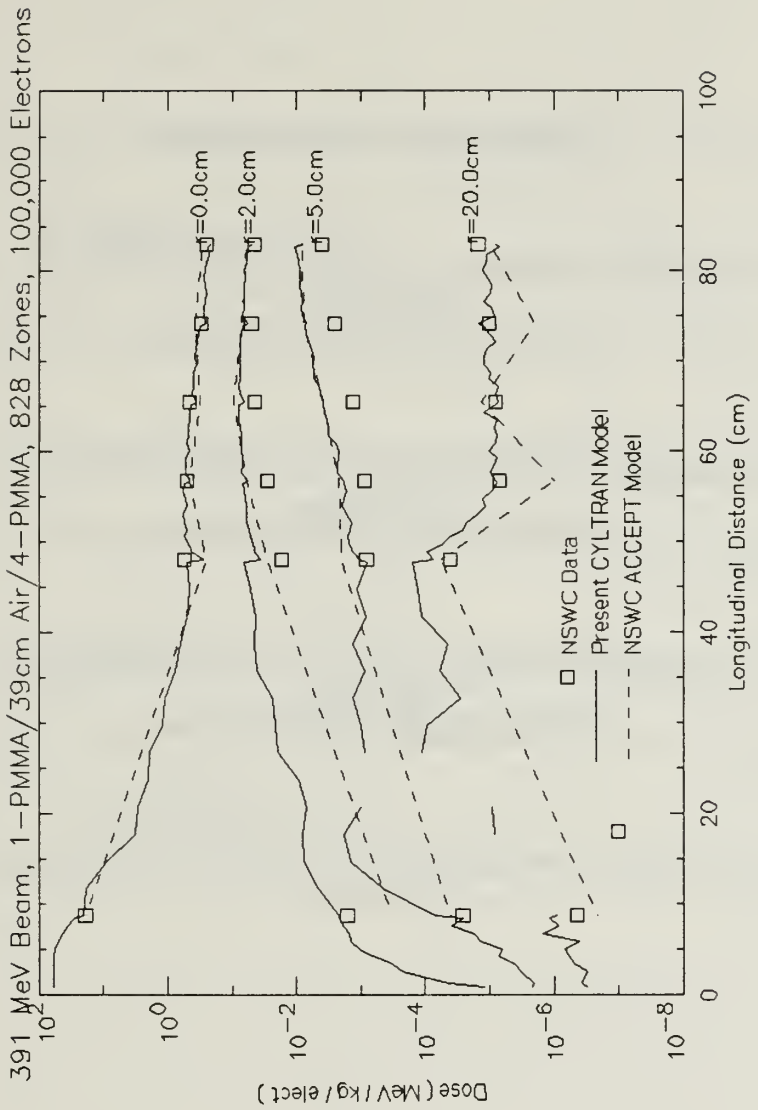

Figure 15. High Res. 391 MeV CYLTRAN Dose Distribution in PMMA with Air Gap Downstream of 1st PMMA Target Section, 100,000 primary electrons. Compare to previous figure to note drastic decrease in statistical uncertainty.

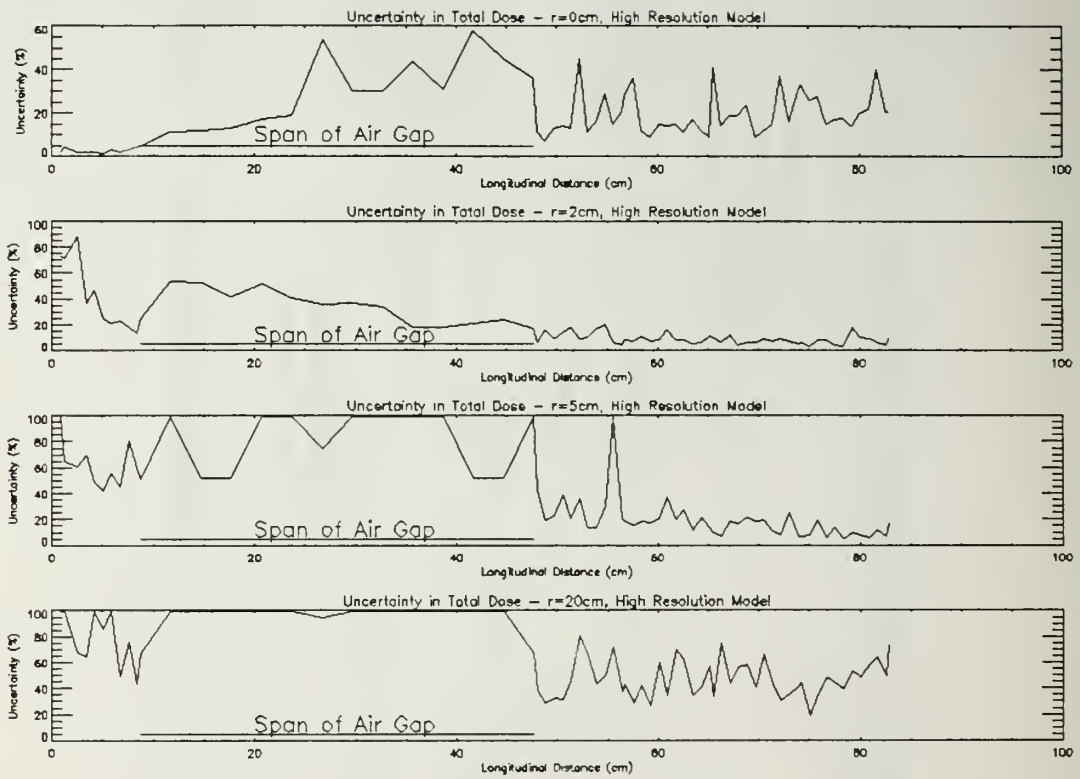
Uncertainty in Total Dose – r=0cm, High Resolution Model
Uncertainty (%)
Span of Air Gap
Longitudinal Distance (cm)
Uncertainty in Total Dose – r=2cm, High Resolution Model
Uncertainty (%)
Span of Air Gap
Longitudinal Distance (cm)
Uncertainty in Total Dose – r=5cm, High Resolution Model
Uncertainty (%)
Span of Air Gap
Longitudinal Distance (cm)
Uncertainty in Total Dose – r=20cm, High Resolution Model
Uncertainty (%)
Span of Air Gap
Longitudinal Distance (cm)

Figure 16. Uncertainty in Total Dose by Radius for 10,000 Primary Electrons in Target of Figure 9. Compare to following figure where 100,000 electrons are used. Note the improvement in statistics with a large number of electrons.

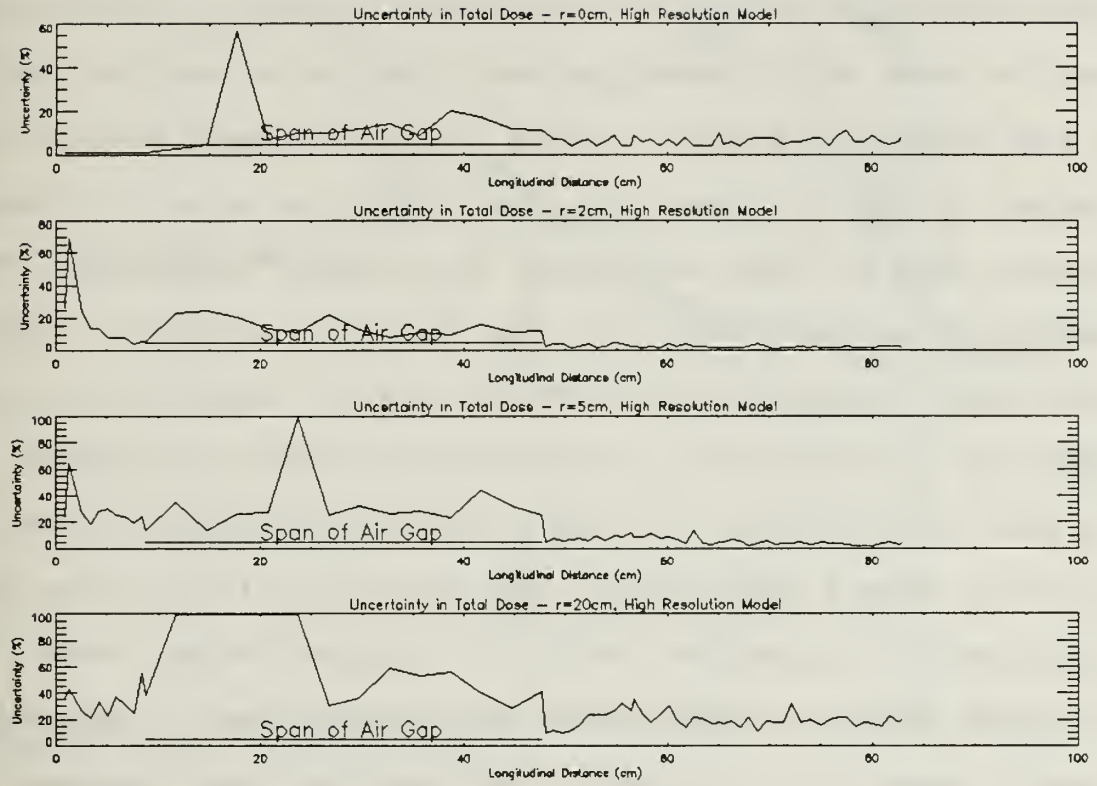
Uncertainty in Total Dose – r=0cm, High Resolution Model
Uncertainty (%)
Span of Air Gap
Longitudinal Distance (cm)
Uncertainty in Total Dose – r=2cm, High Resolution Model
Uncertainty (%)
Span of Air Gap
Longitudinal Distance (cm)
Uncertainty in Total Dose – r=5cm, High Resolution Model
Uncertainty (%)
Span of Air Gap
Longitudinal Distance (cm)
Uncertainty in Total Dose – r=20cm, High Resolution Model
Uncertainty (%)
Span of Air Gap
Longitudinal Distance (cm)

Figure 17. Uncertainty in Total Dose by Radius for 100,000 Primary Electrons in Target of Figure 10. Compare with the previous figure for 10,000 electrons. Note the improvement in statistics with a larger number of primary electrons.

well as all electrons on down the chain that the secondary electron might start. Figure 18 illustrates the classification of these dose deposition mechanisms.

The CYLTRAN output provides detailed analysis of whether the dose in any particular target zone comes from a primary, gamma-secondary, or knock-on electron. Figures 19 through 23 show the dose per incident primary electron at various radii on the target of Figure 10 with 100,000 primary electrons. Figures 19 and 20 show that, on axis, the dose is almost totally due to loss of energy by primary electrons. The negative dose contributed by the knock-on electrons simply says that a small portion of the energy deposited by the primaries is carried out of the zone by knock-ons created in the zone. Note that by the time the primary electrons traverse the first PMMA target section and enter the air gap, the on-axis dose is reduced to 25% of its original value. Once the electrons are one third of the way through the air gap, the on-axis dose due to primary electrons has been reduced to about 5% of its original value. Figure 20 shows that, although the dose on-axis through the end of the air gap is mostly from primaries, immediately downstream of the air gap the dose becomes dominated by gamma-secondary electrons. The small energy contribution from knock-ons does not play a significant role on-axis except in the first target section. We see from the off-axis CYLTRAN calculations in Figures 21 and 22 that, while there is very little dose away from the axis in the

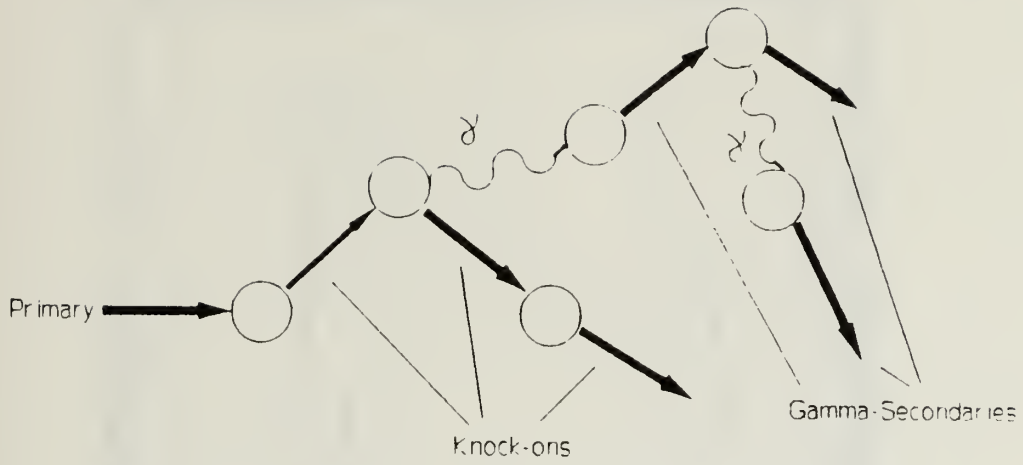

Figure 18. Classification of Dose Deposition by Type of Electron Depositing the Dose.

first target section, as the beam progresses down the cylinder the contribution from the primaries is increasingly overtaken by that from gamma-secondaries farther away from the beam axis. Finally, as shown in Figure 23, the dose at a radius of 20cm is almost totally due to gamma-secondary electrons. In fact, there is very little energy deposited in the cylinder at

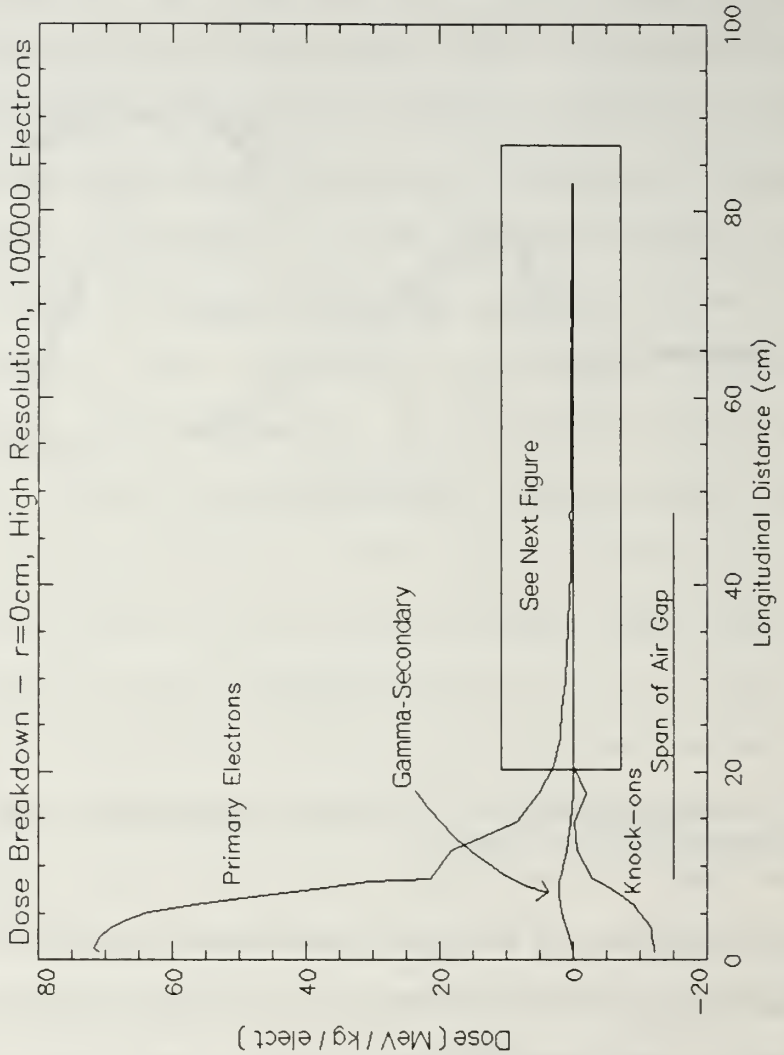

Figure 19. Dose Breakdown by Electron Type on Beam Axis for Target of Figure 10 with 100,000 Electrons, 391 MeV. Most of the dose is due to primary electrons in the first 15cm depth. The next figure expands the region beyond 20cm depth.

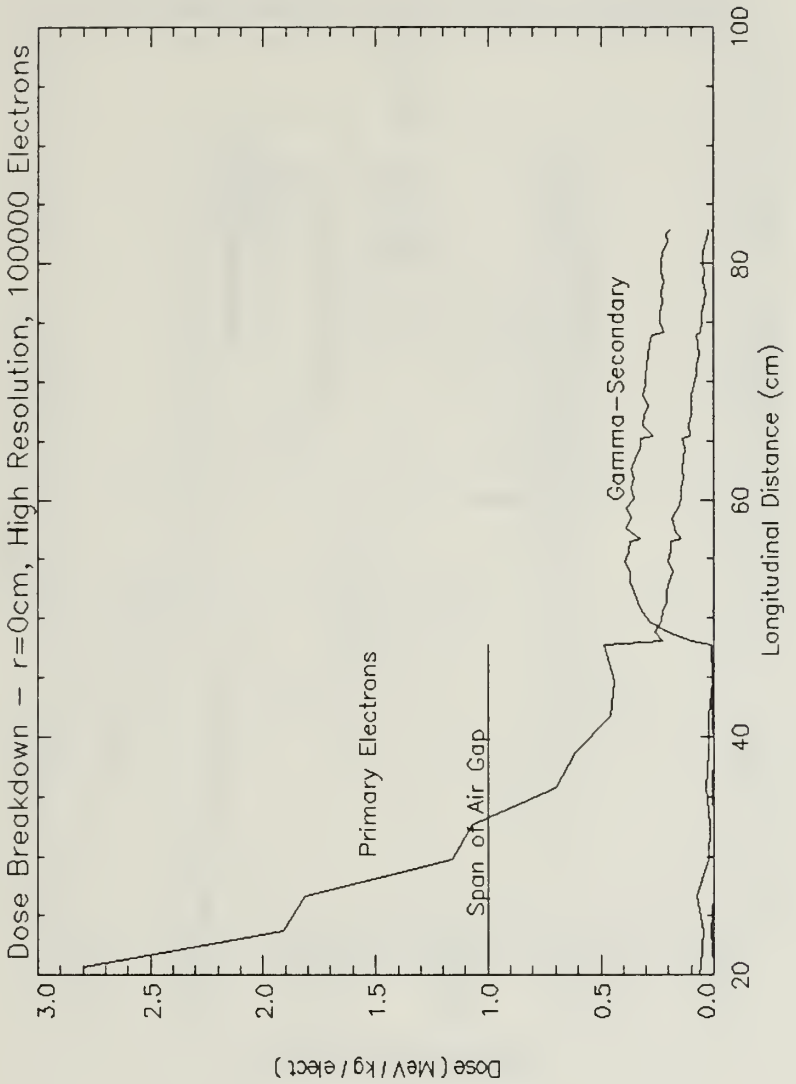

Figure 20. Dose Breakdown on Beam Axis (Expanded View Beyond 20cm Depth) for 100,000 Electrons at 391 MeV. Photon processes cause rapid increase in gamma-secondaries at air gap boundary, so beyond 48cm dose is mostly from low energy g-secondaries.

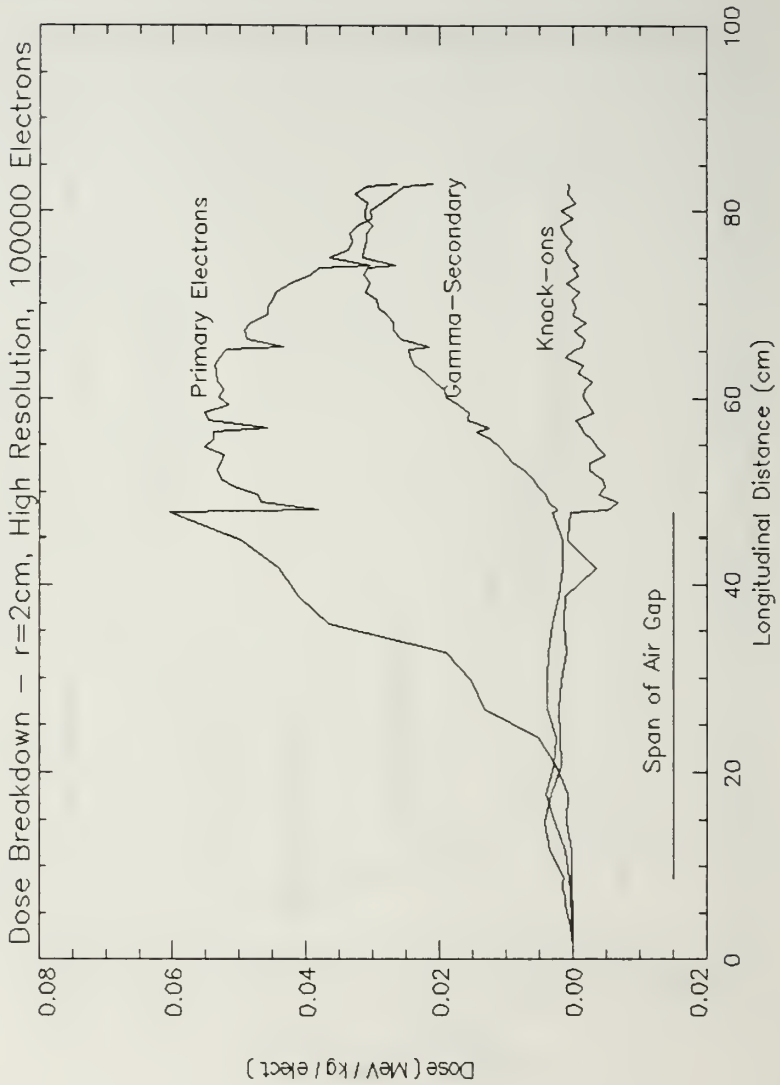

Figure 21. Dose Breakdown by Electron Type at 2cm Radius for Target of Figure 10 with 100,000 Electrons, 391 MeV. Dose at this radius is mostly from primaries and is highest at mid-depth after electrons have scattered to that radius.

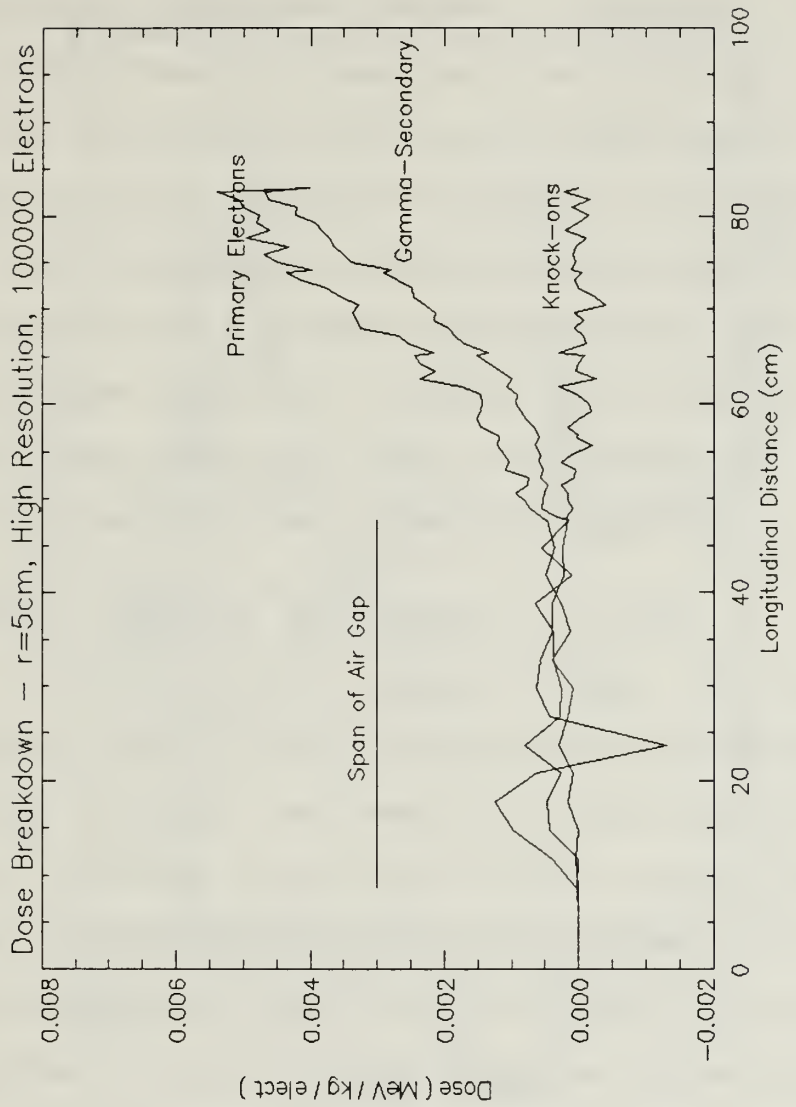

Figure 22. Dose Breakdown by Electron Type at 5cm Radius for Target of Figure 10 with 100,000 Electrons, 391 MeV. Statistics in the air gap begin to decrease because few electrons reach that radius inside the gap.

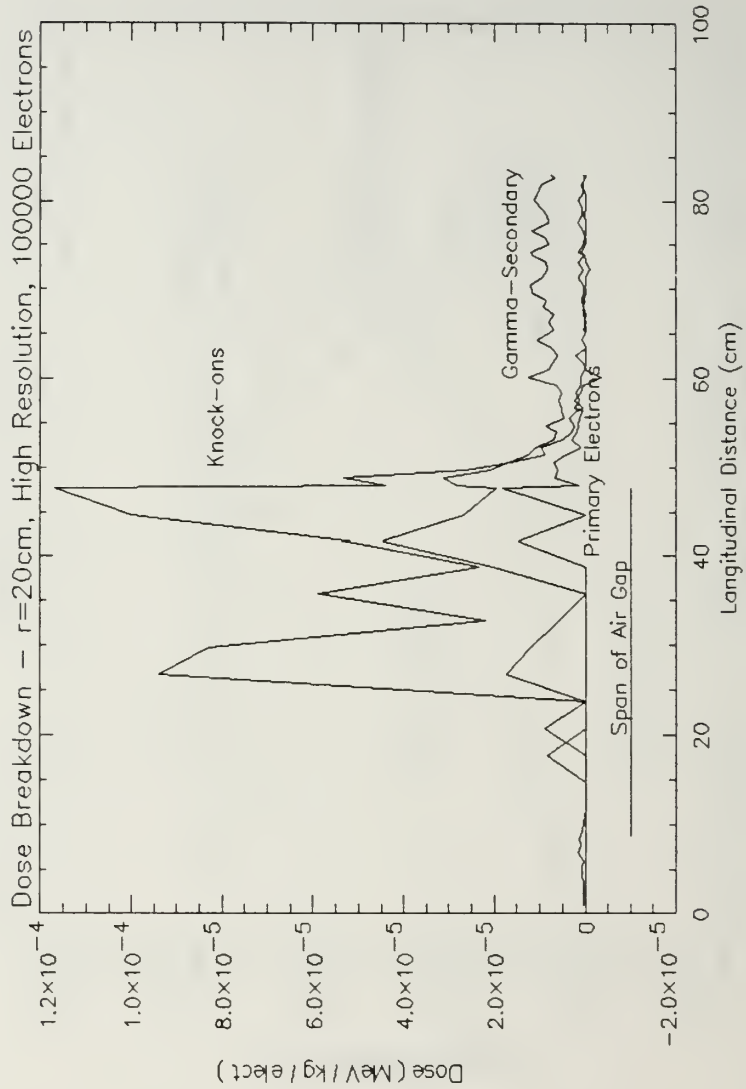

Figure 23. Dose Breakdown by Electron Type at 20cm Radius for Target of Figure 10 with 100,000 Electrons, 391 MeV. Dose from knock-ons overshadows others in the air gap. Uncertainty in the air gap is very high due to the few collisions occurring.

20cm until the air gap is passed, at which point the dose due to secondary and knock-on electrons rises dramatically, the knock-on dose falling slowly back to a very low level and the secondary dose falling and becoming a constant at a level slightly higher than the knock-on dose. This dose breakdown leads to the conclusion that the rise one sees in the dose after the air gap as indicated in Figure 10 is formed by an increase contribution from gamma-secondary electrons somehow built up in the beam's passage through the air gap.

Calculations identical to those above for the case of 10,000 electrons have been done, the results of which are attached in Appendix C as Figures C1 through C4.

F. EFFECT OF REPLACING THE AIR GAP BY A VOID

Some insight into the nature of the calculated dose distribution in the air gap was gained by substituting a void for the 39cm air gap. The result of doing this is shown as Figure 24. The dose in the void is, of course, zero. But, perhaps more significantly, there is no appreciable change in the dose distribution in the target material in this case from that reflected in Figure 10, the identical target with an air gap. These results would tend to suggest that the increased dose in the target material downstream of the air gap is not an artifact of the air itself, but rather one of the target geometry.

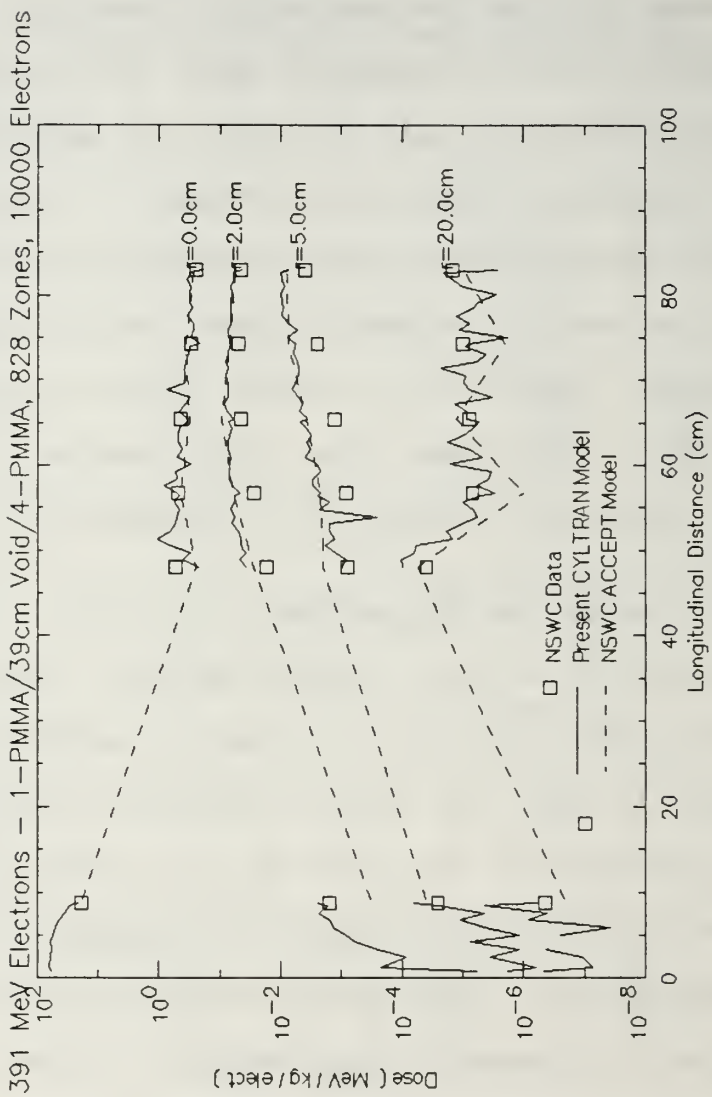

Figure 24. CYLTRAN Dose Distribution for Target of Figure 10 with a 39cm Void Replacing the Air Gap. This figure and figure 10 are very similar, showing that dose distribution dependence on air gap location is a geometry effect.

G. AIR GAP STEP SIZE EFFECTS

Work done by Bielajew and Rogers on calculations of the dose distributions in air due to high energy electrons has shown that if the default Monte Carlo step size is used, one could expect the dose to be overpredicted [Ref. 10]. In this work, it has not been possible to investigate the effect of changing the step size, as CYLTRAN does not have the capability of accomplishing this for only one material in a multi-material target. However, at an energy of 391 MeV, the step size required to obtain the optimum results, according to Biejalew and Rogers, would be about one target diameter, or 20cm. This step size would require the value of k in equation 1 to be equal to about 19,400.

H. RANDOM NUMBER EFFECTS

The dose in the material has a large dependence on the value of the initial random number seed used to start the ITS calculation. Obvious though this observation may be for a Monte Carlo-based algorithm, it is well to keep in mind that any result achieved using the code is subject to a calculable uncertainty. Figures C5 through C7 in Appendix C are given as examples of the effect of changing the random number seeds. When compared to their counterparts, they reflect noticeable variations. However, the variations are verifiably within that statistical uncertainty which is given by CYLTRAN along with

the dose values. The uncertainty in a dose in solid materials in this work typically runs about 20-50%.

IV. RESULTS FOR PREVIOUSLY UNANALYZED 200 MEV DATA

CYLTRAN calculations were done to check the validity of predictions at 200 MeV. Calculations were compared to measurements made at Bates and reported in Reference 1. Figures 25, 26, and 27 illustrate the results of the comparison for Aluminum, PMMA, and Lead followed by Aluminum targets, respectively.

The results of CYLTRAN runs compare very well with the measurements in all three targets, as was expected from the previous results (discussed in Chapter III) for the 391 MeV data. The sole notable deviation of CYLTRAN from the data is in the latter depths of the Pb/Al and PMMA targets. In both of these cases, the CYLTRAN calculations on the beam axis begin to provide results lower than the data in the third target section. The deviation on axis increases continuously through the end of the problem cylinder. Comparison of figures 25, 26, and 27 to figures 12, 13, and 14 in chapter III (which are the corresponding problems at 391 MeV), shows that general trends in the CYLTRAN calculations for the 391 MeV case have been repeated in the 200 MeV case, as one might expect. Also, examination of the NSWC data as shown in figures 25 and 27 (particularly for Pb/Al and PMMA targets) shows that the on-axis dose data begins to plateau after about two target sections depth. This seems suspect since, in all cases looked

at in this work, after a dose peak in the first few centimeters of target material, dose generally decreases continuously. Along with those facts, it is noteworthy that the CYLTRAN calculations have produced very good agreement in every other case examined in this work. There is no reason to expect such a significant difference in the results for the two energies, since the target configurations involved are identical. All this would tend to suggest that the TLD's used in the NSWC measurements for the target configurations of PMMA and Lead followed by Aluminum, on axis at least, had become saturated and did not provide accurate data.

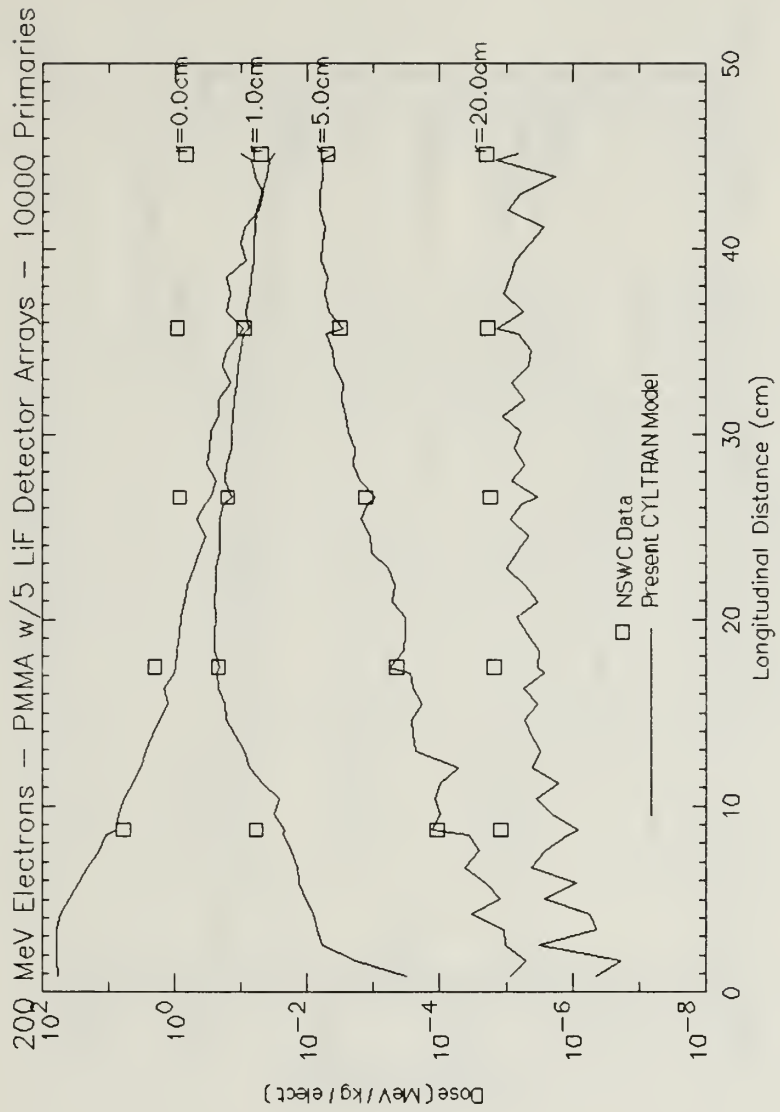

Figure 25. High Res. CYLTRAN Dose Dist. for 200 MeV Electrons in PMMA Target. CYLTRAN agrees well with data except on beam axis and large depth. Linearity of NSWC data past 25cm depth suggests saturation of TLD's on axis. Compare with figure 12.

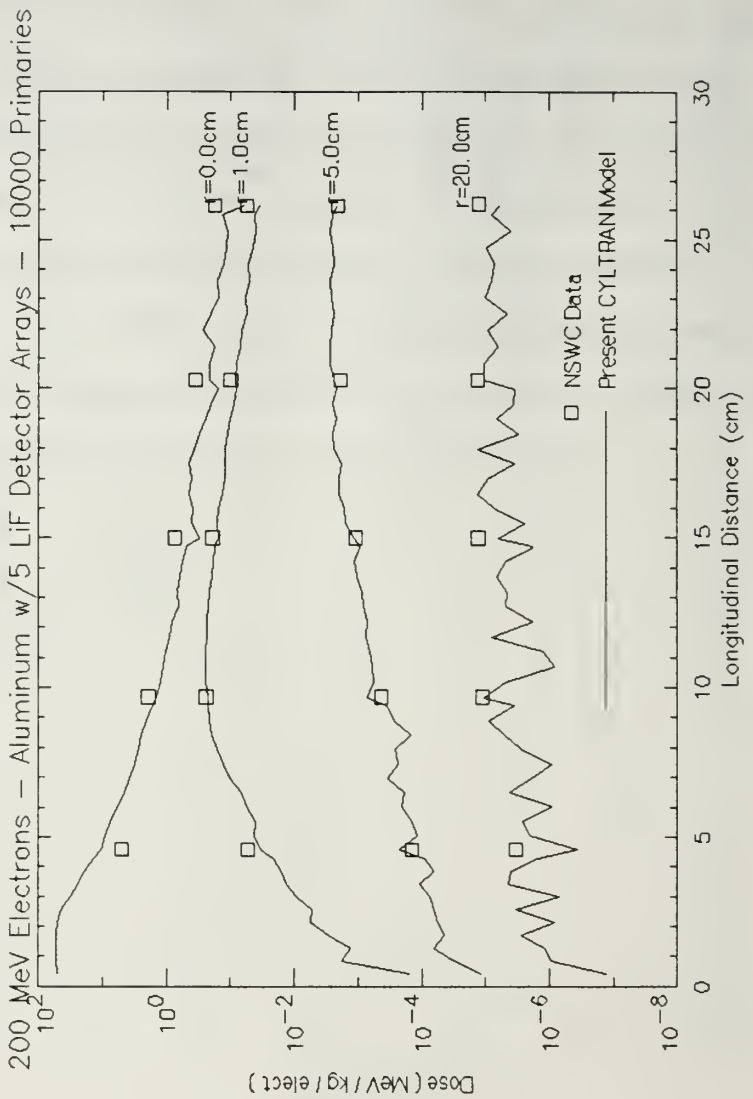

Figure 26. High Resolution CYLTRAN Dose Distribution for 200 MeV Electrons in Aluminum Target, 10,000 Primary Electrons. CYLTRAN agrees well with data for this case. Compare to figure 13 at 391 MeV.

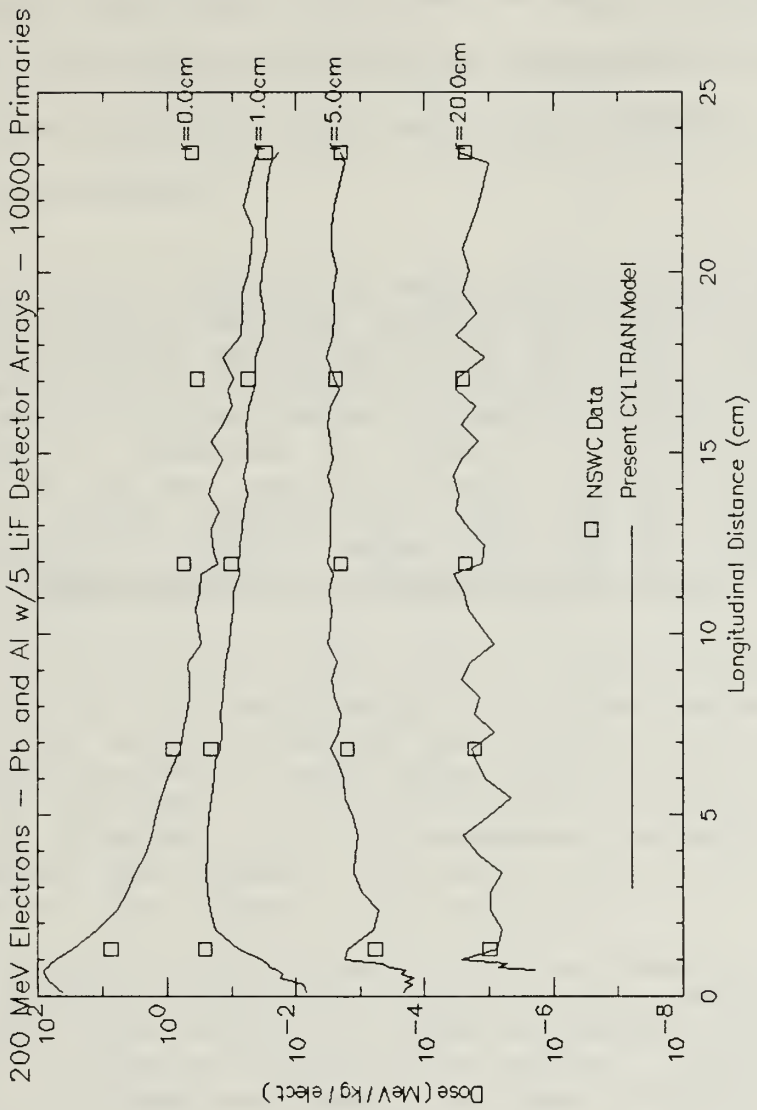

Figure 27. High Res. CYLTRAN Dose Distribution for 10,000 200 MeV Electrons in Target of Lead followed by Aluminum. CYLTRAN agrees with data except on axis at large depth. Again, TLD saturation is suggested. Compare to figure 14.

THIS PAGE INTENTIONALLY LEFT BLANK

V. CONCLUSIONS

In general the results obtained at Bates, as detailed in Reference 1, have been verified. A comparison of the Bates data to the calculations done here using CYLTRAN yields the following conclusions.

- The dose in any particular section of target material is significantly affected by whether or not it is preceded in the longitudinal direction by an air gap. However, this dependence is not a product of the air itself. Rather, it is an effect of the change in geometry produced when the air gap is inserted. We come to this conclusion by replacing the air gap by a void and getting identical results. A small angular deflection gives a small lateral displacement at short range, but gives a much larger lateral displacement at longer ranges. See Chapter III, Section C.

- Uncertainty in dose calculations in the air gap is very large due to the small number of collisions undergone by an electron as it traverses the air gap. The uncertainty is as much as 99% in some cases. This is not affected by changing the number of input zones (dividing the air more finely). However, it is decreased significantly by increasing the number of primary electrons used in the simulation. See Chapter III, Section D.

- In the PMMA/Air/PMMA target stack, the dose on axis is due almost totally to primary electrons. At a radius of 20 cm, the dose is due mostly to gamma-secondary electrons. The doses in between are due to various combinations of primary and gamma-secondary electrons. Knock-on electrons have only a minor contribution in all cases. See Chapter III, Section E.

- In constructing a model, the numerical results are not affected by the degree of fineness with which the target is divided into input zones. However, the added sense of continuity in the data provided when the problem geometry is more finely divided are tremendously beneficial. See Chapter III, Section C.

- Correcting the ITS code to treat the air gap as a thin film seems to have no affect on the dose distribution. See Chapter III, Section A.

- The final value of dose in the material depends greatly on the value of the initial random number seed used to start the ITS calculation. That is, any one ITS calculation is not absolute in its correctness. The value given for the energy deposited in a particular zone in this work could vary from 20-50%. However, the results obtained using different random seeds are statistically consistent, given that the statistical uncertainty in the calculations is also 20-50%. See Chapter III, Section H.

- CYLTRAN agrees well with data for all of the targets considered in this work. This is true for electron energies at both 200 MeV and 391 MeV. The 391 MeV data has been analyzed before by NSWC using ACCEPT. Our analysis shows the failure of the previous ACCEPT comparison to the data is probably due to lack of resolution and a small number of electron histories.

- The analysis of the 200 MeV data has not been done previously. This work shows that CYLTRAN is able to accurately calculate the measured dose. Beyond a radiation length, the dose on axis begins to deviate from the data. The trends in the data compared to the calculations suggest that the TLD's used in taking the 200 MeV measurements were saturated.

APPENDIX A. USING ITS ON THE DEC VAXStation 3200 COMPUTER

In this work, ITS was installed and executed on a dedicated DEC VAXStation 3200 computer. The work has not been completed without a significant amount of time spent in self-education in the DEC terminology and the use of the VAX VMS operating system used by the computer itself, and in learning the subtleties of properly using the ITS computer code. In the hope of saving future ITS code users some time at the front of the "learning curve", this appendix will attempt to explain rudimentary details of how to (1) turn on (boot) the computer, log on to a user account and to begin to work, and (2) how to execute a CYLTRAN run using the ITS system as currently installed on the VAXStation 3200.

A. BOOTING AND USING THE VAXSTATION 3200

1. Turning the Computer On

Turn on the Constant Voltage Conditioner with the red power switch. It will make an annoying constant humming noise, which is nothing to be alarmed about.

Turn on the computer by pressing the switch on the right of the little VAXStation 3200 logo on the front panel of the computer cabinet. The switch will glow orange after being pressed.

The system will go through diagnostics and booting procedures for a few minutes. The entire booting procedure should be complete in less than five minutes.

After the computer has completed booting, the monitor screen should show the DECWindows login screen with distinctive huge blocked letters spelling out DIGITAL and a small window below containing spaces to type in the username and password. At this time users are able to log on to the system, if a user account has been set up by accessing the computer's System Manager account. If a user account has not been previously established, it is recommended that it be done immediately by accessing the System Manager account as explained in Section 2 below and by following instructions in the computer's system management manual (a set of several volumes, usually kept on shelves next to the computer station). It is a dangerous habit (speaking from personal experience) to use the System Manager account for routine user tasks.

2. Logging on to the Computer

After the computer has completed the booting process, you are ready to log on to the computer and begin work. First, press any button. If it wasn't awake already, the monitor will "wake up" and display the DECWindows login screen (described in Section 1). Select USER by clicking the left mouse button on the space for the username and type your username. Then

select PASSWORD and type your password. Then press the ENTER key. The computer will begin to log in to your account and will put the DECWindows user screen on the monitor. This process takes a couple of minutes. After you log in, you can enter commands to the computer by using the pull-down menus (not a very fast way to do it) or by clicking on the DECterm window (which activates the window so you can enter a command) and type commands directly (much better).

If you wish to log in to SYSTEM (the System Manager account), type the username SYSTEM and the password ESMERALDA. You must log on to SYSTEM to establish any necessary user accounts. There will be times, since this is a machine essentially dedicated to one user, that the user will have to log on as SYSTEM to accomplish some task that can only be done by the System Manager, such as device allocation and memory management. After you log on to SYSTEM and the work screen appears on the monitor, click on the DECterm window to enter commands at the "$" prompt.

To log out, select SESSION on the Session Manager Window Menu Bar and click on QUIT. You will be asked to confirm that you want to quit and, if so, you will be logged out.

3. Turning the Computer Off

Log in to SYSTEM as described above. Click on the DECterminal window and type SHUTDOWN.

When the system goes completely through the shutdown sequence, which takes a minute or two, the message SYSTEM SHUTDOWN COMPLETE--USE CONSOLE TO HALT SYSTEM appears on the monitor. Shut off the computer with the orange switch and then turn off the Constant Voltage Conditioner with the red power switch.

4. Miscellaneous Comments on Operation of the Computer

Users accomplish tasks on the computer through the entering of user commands. Commands are entered to the VAXStation in a DEC language called DCL (Digital Command Language). Rather than try to explain a lot of commands here, it's best that you review the VAXStation User Manual volume titled "DCL Dictionary" to get a feel for the commands and what they can do. A few commands that apply directly to the use of ITS and IDL (Interactive Data Language) will be mentioned in this appendix and in Appendix B.

The VAXStation is currently connected to an ethernet accessing several computers in the Naval Postgraduate School Physics Department and other campus facilities, including the Physics Simulation Lab and the W.R. Church Computer Center. Access to this network is through a smaller network (the DECnet) of DEC VAXes (there are currently 4 VAXes on the DECnet) belonging to the Physics Department. To access another node on the network, the DCL command is

SET HOST nodename

You must know the nodename and it must be defined in the local database. If you have the right nodename the other computer will prompt you for a username and password.

There are two user-interface systems available on the VAXStation: DECWindows and VWS (VAX Window System). Currently the default on this machine is set to DECWindows due to the user friendliness of the interface. The VWS is a more barebones window system that runs faster but doesn't make things especially easy for the inexperienced user. The window system can be changed by making changes in the SYSTEM account file SYSTARTUP_V5.COM and going through a reboot procedure. Read the manual on the topic or seek help from a more experienced user.

Remember to do complete system backups on a regular basis. To backup the entire system:

- Set the Break Enable/Disable switch to Enable (in back of the computer above the LED number display). Point the switch toward the circle with a dot inside it.
- Shutdown the system.
- When you get the message SYSTEM SHUTDOWN COMPLETE--USE CONSOLE TO HALT SYSTEM appears on the monitor press the halt button on front of the computer twice. You should get the >>> prompt.
- Type the command: b/e0000000 (that's seven zeros).
- Write protect the hard disk by pressing the button on front of the computer.
- Perform the backup with the command (all on one line):
  "BACKUP/IMAGE/VERIFY/BUFFER_COUNT=5 (space)
  DUA0:MUA0:name.BCK/REWIND/LABEL=date

- Load a blank TK70 cartridge in the tape drive when prompted. When the backup is finished, unload the tape, write enable the hard disk and restart the computer.

B. ITS OVERVIEW

The Integrated Tiger Series of Electron/Photon transport codes (ITS) is the most widely used particle transport code in the world. The code package was developed to incorporate eight individual codes which were developed over the period from 1968 to 1981. All the codes are based on the original ETRAN model developed by M. Berger and S. Seltzer. The ITS code system consists of four primary code packages, which are listed in Table A1.

Table A1. FOUR PRIMARY ITS CODE PACKAGES.

XDATA:	The electron and photon cross section file.
XGEN:	The cross section generation program.
ITS:	The Monte Carlo program file.
UPEML:	A machine portable update emulator.

The heart of the ITS is the program library file ITS, which contains the eight Monte Carlo programs plus system directives for the CRAY, IBM, VAX, and CDC operating systems. The update emulator program UPEML creates the various Monte Carlo codes for a given system with any corrections to those codes that may be desired. The output fortran source code from UPEML is then compiled, linked, and stored as an executable module. Program XGEN generates the problem specific cross

section data tape using file XDATA for referenced inputs and a user defined input file. The Monte Carlo codes then read in the cross section tape and process the user defined problem.

One of the eight ITS codes is CYLTRAN, which simulates the transport of particle trajectories through a three-dimensional multimaterial right circular cylinder. For this project only the CYLTRAN code was used. As an ITS user the following steps were required to execute an ITS run.

1. Create the specific ITS code CYLTRAN with the required correction schemes.
2. Generate a cross section tape based on the different type of materials contained in the cylindrical geometry of a problem.
3. Create an input file which lists all the input parameters required to calculate desired outputs.
4. Submit the input file and the generated cross section tape to the ITS Monte Carlo codes to execute a run.

Table A2 is a sample input file to generate the cross section tape for the materials in a cylindrical geometry. Each material line represents a different medium in the cylinder. Percentages of each material in a compound and its density must be specified. Single element lines such as Cu, has its density stored in ITS and is automatically used for the simulation when needed.

Once a cross section tape is generated, an input file with the parameters designed for a particular simulation must be created. Section D below contains a sample input file to

Table A2. SAMPLE INPUT FILE TO CREATE A CROSS SECTION TAPE

```
Energy 16.0
Material Au
TITLE
    391 MeV Cross Section for Au Foil
```

execute a CYLTRAN run for one of the problems in this work.[Ref. 3, pp. 39-40]

C. RUNNING ITS ON THE VAXSTATION 3200

The VAXStation 3200 is currently set up to run ITS in either a batch mode or interactively. In the batch mode, the user can submit the code run to the computer as a job separate from any user interactive processes. This way, the user can continue to use the computer interactively while the ITS run is being processed in the background by the computer. In the interactive mode, the user cannot use the computer terminal while the run is in progress. The batch mode is by far the most efficient method to use when submitting ITS runs.

Before any ITS code may be run on the computer, an executable version of the code must be generated. Assume that you have generated, using the UPEML processor provided with the ITS package, an ITS specific fully compilable file with the name [.ITS]CYL0.FOR which you wish to run on the computer. Generate the executable file by following this procedure:

- Enter the command FOR [.ITS]CYL0.FOR. The computer's VAX Fortran compiler will compile the fortran file and save an object file in your default directory named CYL0.OBJ.

- Enter the command LINK CYL0.OBJ. The computer will link the program properly and will produce an executable file named CYL0.EXE and save it in your default directory.
- The executable file can then be executed under one of the procedures below.

The process to be followed in submitting an ITS run is given below. The example given is typical of a run done in this work. As ITS is currently configured on the VAXStation 3200, the process must be followed as given. In the example, it is assumed that a specific ITS code file, a cross section file, and a problem input file have been generated.

1. Batch Mode Submission of an ITS Run

Before an ITS job can be submitted in batch mode, two separate data files must be constructed using the VAX text editor. The first file contains 1) a command telling the computer where to look for input required in processing the batch job, and 2) a command telling the computer to run the executable file containing the ITS code. An example of the first file is the file BATCH.COM, which contains the following two lines.

```
DEFINE/USER_MODE SYS$INPUT '[YAW]BATCH_IN.DAT'
RUN [.ITS]CYL0_BATCH.EXE
```

The second data file contains the name of the XGEN-generated cross section file and the name of the file

containing the problem input parameters and geometry input. An example of the second data file for this work is the file BATCH_IN.DAT, which could contain the following two lines.

```
[YAW.PMMA]CYL10_39_40.INP
[YAW.ITS2]XTAPE.OUT
```

Once the two required files have been created, the batch job may be submitted. Submit the job by entering the DCL command

```
SUBMIT/NOTIFY/NOPRINTER BATCH.COM
```

where the filename BATCH.COM is the name of the file containing the name of the executable ITS file. The terms NOTIFY and NOPRINTER are keywords telling the computer to notify you when the batch is completed and to send the job log to a file in your login directory, but not to the print queue. See the DCL Dictionary for other keywords to use with the SUBMIT command.

After submitting the batch job, you may return to interactive use of the computer while the computer processes the job in the background. The nice thing about the batch process is that you may queue as many runs as you want and let the machine run overnight or over a weekend. However, before doing this, it's a smart idea to set the batch queue job limit to 1 by logging in to SYSTEM and entering the command

```
SET QUEUE/JOB_LIMIT=1 SYS$BATCH
```

Be sure to log out of SYSTEM and back in to your user account before submitting a job. If the job limit were higher than 1 (say 3, for instance) the computer would try to run all 3 jobs at the same time, and the run time for all 3 jobs would be significantly increased. Also, the computer's capabilities for running that many jobs at once are really limited, and it could bomb out altogether. With a job limit of 1, the jobs run one at a time, with an unlimited number of jobs held in the queue pending execution.

2. Running ITS Interactively on the VAXStation 3200

The interactive mode is the most user-friendly way to run ITS on the VAXStation 3200. To execute the ITS run, enter the command RUN followed by the filename of the ITS executable code you wish to run. A command to execute a run in this work would look like this:

```
RUN [.ITS]CYL0.EXE
```

where the file [.ITS]CYL0.EXE is an executable ITS problem specific code generated for this work.

The computer will then begin executing the code and interactive use of the computer will no longer be available. After the computer has begun execution of the code, the user will be prompted interactively for the names of the files containing the cross section input data and the problem input data. The user will enter the filenames at the keyboard and the computer will continue executing the program. Execution of

the program will be complete (usually after between 1 and 1.5 hours) when the message FORTRAN COMPLETE is shown on the screen and the "$" prompt returns.

D. SAMPLE CYLTRAN INPUT FILE

The input file to execute an ITS run consists primarily of order-independent keywords followed by keyword-specific parameter values. The following sample input file for a CYLTRAN run illustrates the use of the keywords and parameters.

```
ECHO 0
NO DUMP
TITLE
  391 MeV Electrons - 10.0 PMMA, 39cm Air, 40.0 PMMA, 6 LiF Arrays
******************GEOMETRY*******************************
GEOMETRY 78
* Zone 1 (PMMA)
0.00   8.42    0.00    22.0    1
* Zones 2 - 13 (LiF Detector Array)
8.42   8.72    0.00     0.1    3
8.42   8.72    0.1      0.95   0
8.42   8.72    0.95     1.05   3
8.42   8.72    1.05     1.95   0
8.42   8.72    1.95     2.05   3
8.42   8.72    2.05     4.95   0
8.42   8.72    4.95     5.05   3
8.42   8.72    5.05     9.95   0
8.42   8.72    9.95    10.05   3
8.42   8.72   10.05    19.95   0
8.42   8.72   19.95    20.05   3
8.42   8.72   20.05    22.0    0
* Zone 14 (Air)
8.72   47.72   0.00    22.0    2
* Zones 15 - 26 (LiF Detector Array)
47.72  48.02   0.00     0.1    3
47.72  48.02   0.1      0.95   0
47.72  48.02   0.95     1.05   3
47.72  48.02   1.05     1.95   0
47.72  48.02   1.95     2.05   3
47.72  48.02   2.05     4.95   0
47.72  48.02   4.95     5.05   3
```

```
47.72  48.02    5.05    9.95   0
47.72  48.02    9.95   10.05   3
47.72  48.02   10.05   19.95   0
47.72  48.02   19.95   20.05   3
47.72  48.02   20.05   22.0    0
* Zone 27  (PMMA)
48.02  56.44    0.00   22.0    1
* Zones 28 - 39 (LiF Detector Array)
56.44  56.74    0.00    0.1    3
56.44  56.74    0.1     0.95   0
56.44  56.74    0.95    1.05   3
56.44  56.74    1.05    1.95   0
56.44  56.74    1.95    2.05   3
56.44  56.74    2.05    4.95   0
56.44  56.74    4.95    5.05   3
56.44  56.74    5.05    9.95   0
56.44  56.74    9.95   10.05   3
56.44  56.74   10.05   19.95   0
56.44  56.74   19.95   20.05   3
56.44  56.74   20.05   22.0    0
* Zone 40 (PMMA)
56.74  65.16    0.00   22.0    1
* Zones 41 - 52 (LiF Detector Array)
65.16  65.46    0.00    0.1    3
65.16  65.46    0.1     0.95   0
65.16  65.46    0.95    1.05   3
65.16  65.46    1.05    1.95   0
65.16  65.46    1.95    2.05   3
65.16  65.46    2.05    4.95   0
65.16  65.46    4.95    5.05   3
65.16  65.46    5.05    9.95   0
65.16  65.46    9.95   10.05   3
65.16  65.46   10.05   19.95   0
65.16  65.46   19.95   20.05   3
65.16  65.46   20.05   22.0    0
* Zone 53 (PMMA)
65.46  73.86    0.00   22.0    1
* Zones 54 - 65 (LiF Detector Array)
73.88  74.18    0.00    0.1    3
73.88  74.18    0.1     0.95   0
73.88  74.18    0.95    1.05   3
73.88  74.18    1.05    1.95   0
73.88  74.18    1.95    2.05   3
73.88  74.18    2.05    4.95   0
73.88  74.18    4.95    5.05   3
73.88  74.18    5.05    9.95   0
73.88  74.18    9.95   10.05   3
73.88  74.18   10.05   19.95   0
73.88  74.18   19.95   20.05   3
73.88  74.18   20.05   22.0    0
* Zone 66 (PMMA)
```

```
74.16  82.6    0.00    22.0    1
* Zones 87 - 78 (LiF Detector Array)
82.6   82.9    0.00    0.1     3
82.6   82.9    0.1     0.95    0
82.6   82.9    0.95    1.05    3
82.6   82.9    1.05    1.95    0
82.6   82.9    1.95    2.05    3
82.6   82.9    2.05    4.95    0
82.6   82.9    4.95    5.05    3
82.6   82.9    5.05    9.95    0
82.6   82.9    9.95    10.05   3
82.6   82.9    10.05   19.95   0
82.6   82.9    19.95   20.05   3
82.6   82.9    20.05   22.0    0
**************************SOURCE************************
ELECTRONS
ENERGY 391.00
CUTOFFS 1.603 0.01
DIRECTION
**************************OTHER OPTIONS*****************
RANDOM-NUMBER
  10234
ELECTRON-ESCAPE
  NBINT 10 USER
    10.0 20.0 30.0 40.0 50.0 70.0 90.0 120.0 150.0 180.0
HISTORIES 10000
```

E. SAMPLE CYLTRAN OUTPUT FILE

The following sample CYLTRAN output file was generated using the sample input file given in section A.

```
 ****************************************
*                                      *
*   PROGRAM ITS - DECEMBER 8, 1987     *
*          VERSION 2.1                 *
*                                      *
*          JOHN A. HALBLEIB            *
*          THOMAS A. MEHLHORN          *
*          RONALD P. KENSEK            *
*                                      *
*   SANDIA NATIONAL LABORATORIES       *
*                                      *
****************************************
*        C Y L T R A N                 *
*        -------------           *
****************************************

****************************
*** DOUBLE PRECISION RUN ***
****************************

NUMBER OF MATERIALS
   3

************************************************************
* GAMMA RAY CROSS SECTION DATA FOR MATERIAL NUMBER   1 *
************************************************************

MPAIR  NTAB  MTAX
  25     1    48

ENERGIES (MEV)
1000.000000  800.000000  600.000000  500.000000  400.000000  300.000000
 200.000000  150.000000  100.000000   80.000000   60.000000   50.000000
  40.000000   30.000000   20.000000   15.000000   10.000000    8.000000
   6.000000    5.000000    4.000000    3.000000    2.000000    1.500000
   1.000000    0.800000    0.600000    0.500000    0.400000    0.300000
   0.200000    0.150000    0.100000    0.080000    0.060000    0.050000
   0.040000    0.030000    0.020000    0.015000    0.010000    0.008000
   0.006000    0.004000    0.003000    0.002000    0.001500    0.001000

TOTAL ATTENUATION COEFFICIENTS (CM2/G)
   0.017830    0.017643    0.017388    0.017172    0.016912    0.016553
   0.016008    0.015638    0.015055    0.014773    0.014717    0.014806
   0.015010    0.015428    0.016544    0.017969    0.020970    0.023126
   0.026530    0.029110    0.032786    0.038338    0.047873    0.055805
   0.068575    0.076285    0.086869    0.093930    0.102908    0.114920
   0.132288    0.144572    0.161630    0.171293    0.185668    0.197748
   0.219839    0.275480    0.507550    0.998802    3.178913    6.265552
  15.164587   52.254905  123.215628  399.982170  906.058528 2778.015825
```

RATIO OF SCATTERING PLUS PAIR PRODUCTION TO TOTAL ATTENUATION COEFFICIENTS

1.000000	1.000000	1.000000	1.000000	1.000000	1.000000
1.000000	1.000000	0.999999	0.999999	0.999999	0.999999
0.999999	0.999998	0.999997	0.999997	0.999998	0.999995
0.999994	0.999993	0.999992	0.999990	0.999985	0.999980
0.999965	0.999950	0.999915	0.999877	0.999798	0.999582
0.998737	0.997102	0.990193	0.980618	0.954018	0.921738
0.854502	0.784040	0.395241	0.204879	0.085454	0.033437
0.013920	0.004071	0.001733	0.000536	0.000237	0.000077

RATIO OF SCATTERING TO SCATTERING PLUS PAIR PRODUCTION ATTENUATION COEFFICIENTS

0.014854	0.018471	0.024920	0.030167	0.038126	0.051574
0.078908	0.108274	0.161482	0.202014	0.262870	0.308970
0.387431	0.455755	0.590550	0.680387	0.789872	0.841050
0.898388	0.924388	0.951209	0.975017	0.993018	0.998507
1.000000					

K SHELL IONIZATION DATA

BINDING ENERGY (MEV), PHOTOEFFECT EFFICIENCY AND FLUORESCENT EFFICIENCY

0.000533	0.482888	0.001849

K X-RAY ENERGIES (MEV)

0.000533	0.000533	0.000533	0.000533

K X-RAY ACCUMULATED RELATIVE INTENSITIES

1.000000	1.000000	1.000000	1.000000

AUGER ELECTRON ENERGIES (MEV)

0.000533	0.000533	0.000533

AUGER ELECTRON ACCUMULATED RELATIVE INTENSITIES

1.000000	1.000000	1.000000

****

* GAMMA RAY CROSS SECTION DATA FOR MATERIAL NUMBER 2 *

****

MPAIR	NTAB	MTAX
25	1	48

ENERGIES (MEV)

1000.000000	800.000000	600.000000	500.000000	400.000000	300.000000
200.000000	150.000000	100.000000	80.000000	60.000000	50.000000
40.000000	30.000000	20.000000	15.000000	10.000000	8.000000
6.000000	5.000000	4.000000	3.000000	2.000000	1.500000
1.000000	0.800000	0.600000	0.500000	0.400000	0.300000
0.200000	0.150000	0.100000	0.080000	0.060000	0.050000
0.040000	0.030000	0.020000	0.015000	0.010000	0.008000
0.006000	0.004000	0.003000	0.002000	0.001500	0.001000

TOTAL ATTENUATION COEFFICIENTS (CM2/G)

0.020823	0.020405	0.020092	0.019889	0.019568	0.019141
0.018454	0.017958	0.017127	0.016895	0.016413	0.016341
0.016331	0.016454	0.017138	0.018222	0.020649	0.022443
0.025348	0.027591	0.030818	0.035814	0.044488	0.051754
0.063568	0.070717	0.080538	0.087078	0.095409	0.100586
0.122757	0.134348	0.151081	0.101418	0.178903	0.195834
0.229234	0.319828	0.708959	1.526621	5.132228	10.201398
24.718980	84.768389	198.519335	835.034882	1419.555822	4244.419095

RATIO OF SCATTERING PLUS PAIR PRODUCTION TO TOTAL ATTENUATION COEFFICIENTS

1.000000	1.000000	1.000000	1.000000	1.000000	1.000000
1.000000	0.999999	0.999999	0.999999	0.999998	0.999998
0.999998	0.999997	0.999996	0.999995	0.999993	0.999991
0.999989	0.999987	0.999985	0.999981	0.999972	0.999962
0.999935	0.999908	0.999842	0.999770	0.999628	0.999222
0.997858	0.994834	0.981984	0.964821	0.917787	0.863849
0.759632	0.562098	0.282291	0.123980	0.037558	0.019038
0.007910	0.002320	0.000997	0.000313	0.000140	0.000047

RATIO OF SCATTERING TO SCATTERING PLUS PAIR PRODUCTION ATTENUATION COEFFICIENTS

0.011744	0.014805	0.019974	0.024188	0.030545	0.041343
0.063448	0.085828	0.131563	0.165703	0.218487	0.257625
0.313035	0.396082	0.528459	0.621934	0.743388	0.803349
0.869759	0.904074	0.937428	0.967509	0.990738	0.998039
1.000000					

K SHELL IONIZATION DATA

BINDING ENERGY (MEV), PHOTOEFFECT EFFICIENCY AND FLUORESCENT EFFICIENCY

0.000533	0.748013	0.001849

K X-RAY ENERGIES (MEV)

0.000533	0.000533	0.000533	0.000533

K X-RAY ACCUMULATED RELATIVE INTENSITIES

1.000000	1.000000	1.000000	1.000000

AUGER ELECTRON ENERGIES (MEV)

0.000533	0.000533	0.000533

AUGER ELECTRON ACCUMULATED RELATIVE INTENSITIES

1.000000	1.000000	1.000000

****

* GAMMA RAY CROSS SECTION DATA FOR MATERIAL NUMBER 3 *

****

MPAIR	NTAB	MTAX
25	1	48

ENERGIES (MEV)

1000.000000	800.000000	600.000000	500.000000	400.000000	300.000000
200.000000	150.000000	100.000000	80.000000	60.000000	50.000000
40.000000	30.000000	20.000000	15.000000	10.000000	8.000000
6.000000	5.000000	4.000000	3.000000	2.000000	1.500000
1.000000	0.800000	0.600000	0.500000	0.400000	0.300000
0.200000	0.150000	0.100000	0.080000	0.060000	0.050000
0.040000	0.030000	0.020000	0.015000	0.010000	0.008000
0.006000	0.004000	0.003000	0.002000	0.001500	0.001000

TOTAL ATTENUATION COEFFICIENTS (CM2/G)

0.018451	0.018274	0.018008	0.017805	0.017552	0.017182
0.016802	0.016173	0.015415	0.015114	0.014693	0.014824
0.014800	0.014928	0.015848	0.016701	0.018981	0.020852
0.023357	0.025451	0.028480	0.033109	0.041153	0.047892
0.058827	0.065443	0.074528	0.080589	0.088303	0.098841
0.113688	0.124538	0.140599	0.151021	0.169778	0.188650
0.227694	0.334742	0.794744	1.748197	5.865155	11.585241
27.658005	92.734359	213.500435	868.126321	1470.804487	4291.996621

RATIO OF SCATTERING PLUS PAIR PRODUCTION TO TOTAL ATTENUATION COEFFICIENTS

1.000000	1.000000	1.000000	1.000000	1.000000	1.000000
0.999999	0.999999	0.999999	0.999999	0.999998	0.999998
0.999997	0.999998	0.999994	0.999993	0.999990	0.999988
0.999988	0.999983	0.999980	0.999975	0.999964	0.999950
0.999914	0.999876	0.999789	0.999692	0.999491	0.998960
0.996895	0.992936	0.976452	0.954098	0.894974	0.828807
0.707716	0.496989	0.216524	0.100189	0.030413	0.015539
0.006547	0.001968	0.000858	0.000275	0.000125	0.000043

RATIO OF SCATTERING TO SCATTERING PLUS PAIR PRODUCTION ATTENUATION COEFFICIENTS

0.012147	0.015298	0.020832	0.024958	0.031513	0.042828
0.085284	0.088151	0.135287	0.169384	0.222823	0.283007
0.319538	0.403979	0.535888	0.627980	0.748387	0.807898
0.873404	0.906979	0.939409	0.968497	0.990933	0.998088
1.000000					

K SHELL IONIZATION DATA

BINDING ENERGY (MEV), PHOTOEFFECT EFFICIENCY AND FLUORESCENT EFFICIENCY

0.000687	0.927323	0.003376

K X-RAY ENERGIES (MEV)

0.000687	0.000687	0.000687	0.000687

K X-RAY ACCUMULATED RELATIVE INTENSITIES

1.000000	1.000000	1.000000	1.000000

AUGER ELECTRON ENERGIES (MEV)

0.000687	0.000687	0.000687

AUGER ELECTRON ACCUMULATED RELATIVE INTENSITIES

1.000000	1.000000	1.000000

```
**********************************************************
*    ELECTRON CROSS SECTION DATA FROM PROGRAM DATPAC     *
**********************************************************

NUMBER OF SETS ON DATAPAC TAPE =   3

******************** Cross Sections for 391 MeV Electrons in PMMA, Air Gap, LiF Detectors ********************


MATERIAL      DENSITY       DETOUR
      1  0.11880E+01  0.85500E+00
         Z            A            W
 0.10000E+01  0.10080E+01  0.80500E-01
 0.80000E+01  0.12011E+02  0.59990E+00
 0.80000E+01  0.15999E+02  0.31960E+00
 NSET  ITRM  IZIP  ISGN  ISUB  INAL  ICYC  NCYC  NMAX      EMAX          EMIN          RMAX       LMAT
    1     5     0     1     3     1     1     0    64  3.9100000E+02  1.5273440E+00  7.5139070E+01     3
 DATAPREP DATA FOR DATAPAC SET   1    64    33     3   121  7.513907E+01



MATERIAL      DENSITY       DETOUR
      2  0.11850E-02  0.83500E+00
         Z            A            W
 0.70000E+01  0.14007E+02  0.28340E+00
 0.80000E+01  0.15999E+02  0.73660E+00
 NSET  ITRM  IZIP  ISGN  ISUB  INAL  ICYC  NCYC  NMAX      EMAX          EMIN          RMAX       LMAT
    2     5     0     1     3     1     1     0    64  3.9100000E+02  1.5273440E+00  8.8428330E+01     2
 DATAPREP DATA FOR DATAPAC SET   2    64    33     3   121  8.842833E+01



MATERIAL      DENSITY       DETOUR
      3  0.26350E+01  0.83500E+00
         Z            A            W
 0.30000E+01  0.69390E+01  0.28750E+00
 0.90000E+01  0.18998E+02  0.71250E+00
 NSET  ITRM  IZIP  ISGN  ISUB  INAL  ICYC  NCYC  NMAX      EMAX          EMIN          RMAX       LMAT
    3     5     0     1     3     1     1     0    64  3.9100000E+02  1.5273440E+00  8.0237290E+01     2
 DATAPREP DATA FOR DATAPAC SET   3    64    33     3   121  8.023729E+01


 COLLISION / TOTAL DE/DX RATIOS FOR DATAPAC SET   3

 CUMULATIVE BREMSSTRAHLUNG CROSS SECTIONS FOR DATAPAC SET   3

 CUMULATIVE BREMSSTRAHLUNG ANGULAR DISTRIBUTIONS FOR DATAPAC SET   3

 LANGAUSS - EQUIPROBABLE ENDPOINTS FOR INTERPOLATION

 K X-RAY PRODUCTION FOR DATAPAC SET   3
```

PHOTOELECTRON ANGULAR DISTRIBUTIONS

PAIR ELECTRON ENERGY DIVISION DISTRIBUTION (LEAD)

```
**************************
*  BEGIN READING INPUT   *
**************************
```

```
************************************************************
*   COMPARISON OF STORAGE REQUIREMENTS VS ALLOCATIONS      *
************************************************************

NUMBER OF MATERIALS ON CROSS SECTION FILE                    / NMT    =    3 /   10
MAXIMUM NUMBER OF ELEMENTS IN A PROBLEM MATERIAL               / NEM    =    3 /    0
LENGTH OF ELECTRON CROSS SECTION ENERGY GRID                 / NMAX   =   64 /   64
ELECTRON ENERGY GRID LENGTH FOR SAMPLING BREMS. PHOTON ENERGY  / NMTOP  =   85 /   85
PHOTON ENERGY GRID LENGTH FOR SAMPLING BREMS. PHOTON ENERGY    / NKTOP  =   49 /   49
ELECTRON ANGLE GRID LENGTH FOR SAMPLING ELECTRON SCATTERING ANGLE / NMMAX  =   33 /   33
PHOTON ANGLE GRID LENGTH FOR SAMPLING BREMS. PHOTON ANGLE      / NPANG  =   21 /   21
PHOTON ENERGY GRID LENGTH FOR SAMPLING BREMS. PHOTON ANGLE     / NRANG  =   25 /   25
ELECTRON ENERGY GRID LENGTH FOR SAMPLING BREMS. PHOTON ANGLE   / NTANG  =    0 /    9
PHOTON ENERGY GRID LENGTH FOR SAMPLING PHOTO-ELECTRON DIRECTION / NEEL  =   13 /   17
ELECTRON ANGLE GRID LENGTH FOR SAMPLING PHOTO-ELECTRON DIRECTION / NPEL  =   21 /   21
PHOTON ENERGY GRID LENGTH FOR SAMPLING PAIR ELECTRON ENERGY    / NEPS   =    9 /   17
ELECTRON ENERGY GRID LENGTH FOR SAMPLING PAIR ELECTON ENERGY   / NPPS   =   21 /   21
GAUSSIAN FUNCTION GRID FOR SAMPLING ELECTRON ENEBGY LOSS STRAGGLING / NGAS  = 1000 / 1000
LANDAU FUNCTION GRID FOR SAMPLING ELECTRON ENEBGY LOSS STRAGGLING / NLAN  = 5000 / 5000
MAXIMUM NUMBER OF TABLES OF PHOTON CROSS SECTIONS              / NTAB   =    1 /   15
MAXIMUM LENGTH OF PHOTON CROSS SECTION TABLE                   / NTAX   =   48 /   48
NUMBER OF ELECTRON ESCAPE ENERGY BINS                        / IJMAX  =   10 /   50
NUMBER OF PHOTON ESCAPE ENERGY BINS                          / IJPMAX =    0 /   50
NUMBER OF ELECTRON ESCAPE POLAR ANGLE BINS                   / IKMAX  =   10 /   30
NUMBER OF PHOTON ESCAPE POLAR ANGLE BINS                     / IKPMAX =    0 /   30
LENGTH OF SOURCE SPECTRUM ENEBGY GRID                        / IJSPEC =    0 /   51
NUMBER OF PULSE HEIGHT ENERGY BINS                           / IJSMAX =    0 /   53
NUMBER OF ELECTRON FLUX ENERGY BINS                          / IJFMAX =    0 /   50
NUMBER OF PHOTON FLUX ENEBGY BINS                            / IJFMXP =    0 /   50
NUMBER OF ELECTRON FLUX ZONES                                / INLF   =    0 /  100
NUMBER OF PHOTON FLUX ZONES                                  / INLFP  =    0 /  100
NUMBER OF PBOBLEM ZONES                                      / INZON  =   78 /  100
SIZE OF DOUBLY DIFFERENTIAL BREMS DISTRIBUTION               / NCHANG = 4725 / 4725
SIZE OF SINGLY DIFFERENTIAL BREMS DISTRIBUTION               / NBOIS  = 3185 / 3185
SIZE OF GOUDSMIT-SAUNDERSON ANGULAR DISTRIBUTION             / NGG    = 2112 / 2112
NO. OF ELECTRON ESCAPE AZIMUTHAL ANGLE BINS                  / IKMAZ  =    1 /    1
NO. OF PHOTON ESCAPE AZIMUTHAL ANGLE BINS                    / IKPMAZ =    0 /    1
```

****
* GEOMETRY DEPENDENT INPUT *
****

NUMBER OF INPUT ZONES = 70

ZONE	MATERIAL	LEFT PLANE (CM)	RIGHT PLANE (CM)	INNER RADIUS (CM)	OUTER RADIUS (CM)	ELECTRON CUTOFF (MEV)	PHOTON FORCING FRACTION
1	1	0.00000E+00	0.42000E+00	0.00000E+00	2.20000E+01	1.803E+00	0.000E+00
2	3	0.42000E+00	0.72000E+00	0.00000E+00	1.00000E-01	1.803E+00	0.000E+00
3	0	0.42000E+00	0.72000E+00	1.00000E-01	9.50000E-01	1.803E+00	0.000E+00
4	3	0.42000E+00	0.72000E+00	9.50000E-01	1.05000E+00	1.803E+00	0.000E+00
5	0	0.42000E+00	0.72000E+00	1.05000E+00	1.95000E+00	1.803E+00	0.000E+00
6	3	0.42000E+00	0.72000E+00	1.95000E+00	2.05000E+00	1.803E+00	0.000E+00
7	0	0.42000E+00	0.72000E+00	2.05000E+00	4.95000E+00	1.803E+00	0.000E+00
8	3	0.42000E+00	0.72000E+00	4.95000E+00	5.05000E+00	1.803E+00	0.000E+00
9	0	0.42000E+00	0.72000E+00	5.05000E+00	9.95000E+00	1.803E+00	0.000E+00
10	3	0.42000E+00	0.72000E+00	9.95000E+00	1.00500E+01	1.803E+00	0.000E+00
11	0	0.42000E+00	0.72000E+00	1.00500E+01	1.99500E+01	1.803E+00	0.000E+00
12	3	0.42000E+00	0.72000E+00	1.99500E+01	2.00500E+01	1.803E+00	0.000E+00
13	0	0.42000E+00	0.72000E+00	2.00500E+01	2.20000E+01	1.803E+00	0.000E+00
14	2	0.72000E+00	4.77200E+01	0.00000E+00	2.20000E+01	1.803E+00	0.000E+00
15	3	4.77200E+01	4.80200E+01	0.00000E+00	1.00000E-01	1.803E+00	0.000E+00
16	0	4.77200E+01	4.80200E+01	1.00000E-01	9.50000E-01	1.803E+00	0.000E+00
17	3	4.77200E+01	4.80200E+01	9.50000E-01	1.05000E+00	1.803E+00	0.000E+00
18	0	4.77200E+01	4.80200E+01	1.05000E+00	1.95000E+00	1.803E+00	0.000E+00
19	3	4.77200E+01	4.80200E+01	1.95000E+00	2.05000E+00	1.803E+00	0.000E+00
20	0	4.77200E+01	4.80200E+01	2.05000E+00	4.95000E+00	1.803E+00	0.000E+00
21	3	4.77200E+01	4.80200E+01	4.95000E+00	5.05000E+00	1.803E+00	0.000E+00
22	0	4.77200E+01	4.80200E+01	5.05000E+00	9.95000E+00	1.803E+00	0.000E+00
23	3	4.77200E+01	4.80200E+01	9.95000E+00	1.00500E+01	1.803E+00	0.000E+00
24	0	4.77200E+01	4.80200E+01	1.00500E+01	1.99500E+01	1.803E+00	0.000E+00
25	3	4.77200E+01	4.80200E+01	1.99500E+01	2.00500E+01	1.803E+00	0.000E+00
26	0	4.77200E+01	4.80200E+01	2.00500E+01	2.20000E+01	1.803E+00	0.000E+00
27	1	4.80200E+01	5.84400E+01	0.00000E+00	2.20000E+01	1.803E+00	0.000E+00
28	3	5.84400E+01	5.87400E+01	0.00000E+00	1.00000E-01	1.803E+00	0.000E+00
29	0	5.84400E+01	5.87400E+01	1.00000E-01	9.50000E-01	1.803E+00	0.000E+00
30	3	5.84400E+01	5.87400E+01	9.50000E-01	1.05000E+00	1.803E+00	0.000E+00
31	0	5.84400E+01	5.87400E+01	1.05000E+00	1.95000E+00	1.803E+00	0.000E+00
32	3	5.84400E+01	5.87400E+01	1.95000E+00	2.05000E+00	1.803E+00	0.000E+00
33	0	5.84400E+01	5.87400E+01	2.05000E+00	4.95000E+00	1.803E+00	0.000E+00
34	3	5.84400E+01	5.87400E+01	4.95000E+00	5.05000E+00	1.803E+00	0.000E+00
35	0	5.84400E+01	5.87400E+01	5.05000E+00	9.95000E+00	1.803E+00	0.000E+00
36	3	5.84400E+01	5.87400E+01	9.95000E+00	1.00500E+01	1.803E+00	0.000E+00
37	0	5.84400E+01	5.87400E+01	1.00500E+01	1.99500E+01	1.803E+00	0.000E+00
38	3	5.84400E+01	5.87400E+01	1.99500E+01	2.00500E+01	1.803E+00	0.000E+00
39	0	5.84400E+01	5.87400E+01	2.00500E+01	2.20000E+01	1.803E+00	0.000E+00
40	1	5.87400E+01	8.51800E+01	0.00000E+00	2.20000E+01	1.803E+00	0.000E+00
41	3	8.51800E+01	8.54800E+01	0.00000E+00	1.00000E-01	1.803E+00	0.000E+00
42	0	8.51800E+01	8.54800E+01	1.00000E-01	9.50000E-01	1.803E+00	0.000E+00

43	3	8.51800E+01	8.54800E+01	9.50000E-01	1.95000E+00	1.803E+00	0.000E+00
44	0	8.51800E+01	8.54800E+01	1.95000E+00	1.95000E+00	1.803E+00	0.000E+00
45	3	8.51800E+01	8.54800E+01	1.95000E+00	2.95000E+00	1.803E+00	0.000E+00
46	0	8.51800E+01	8.54800E+01	2.95000E+00	4.95000E+00	1.803E+00	0.000E+00
47	3	8.51800E+01	8.54800E+01	4.95000E+00	5.95000E+00	1.803E+00	0.000E+00
48	0	8.51800E+01	8.54800E+01	5.95000E+00	9.95000E+00	1.803E+00	0.000E+00
49	3	8.51800E+01	8.54800E+01	9.95000E+00	1.00500E+01	1.803E+00	0.000E+00
50	0	8.51800E+01	8.54800E+01	1.00500E+01	1.99500E+01	1.803E+00	0.000E+00
51	3	8.51800E+01	8.54800E+01	1.99500E+01	2.00500E+01	1.803E+00	0.000E+00
52	0	8.51800E+01	8.54800E+01	2.00500E+01	2.20000E+01	1.803E+00	0.000E+00
53	1	8.54800E+01	7.38800E+01	0.00000E+00	2.20000E+01	1.803E+00	0.000E+00
54	3	7.38800E+01	7.41800E+01	0.00000E+00	1.00000E-01	1.803E+00	0.000E+00
55	0	7.38800E+01	7.41800E+01	1.00000E-01	9.50000E-01	1.803E+00	0.000E+00
56	3	7.38800E+01	7.41800E+01	9.50000E-01	1.95000E+00	1.803E+00	0.000E+00
57	0	7.38800E+01	7.41800E+01	1.95000E+00	1.95000E+00	1.803E+00	0.000E+00
58	3	7.38800E+01	7.41800E+01	1.95000E+00	2.95000E+00	1.803E+00	0.000E+00
59	0	7.38800E+01	7.41800E+01	2.95000E+00	4.95000E+00	1.803E+00	0.000E+00
60	3	7.38800E+01	7.41800E+01	4.95000E+00	5.95000E+00	1.803E+00	0.000E+00
01	0	7.38800E+01	7.41800E+01	5.95000E+00	9.95000E+00	1.803E+00	0.000E+00
02	3	7.38800E+01	7.41800E+01	9.95000E+00	1.00500E+01	1.803E+00	0.000E+00
03	0	7.38800E+01	7.41800E+01	1.00500E+01	1.00500E+01	1.803E+00	0.000E+00
04	3	7.38800E+01	7.41800E+01	1.99500E+01	2.00500E+01	1.803E+00	0.000E+00
05	0	7.38800E+01	7.41800E+01	2.00500E+01	2.20000E+01	1.803E+00	0.000E+00
08	1	7.41800E+01	8.28000E+01	0.00000E+00	2.20000E+01	1.803E+00	0.000E+00
07	3	8.28000E+01	8.29000E+01	0.00000E+00	1.00000E-01	1.803E+00	0.000E+00
08	0	8.28000E+01	8.29000E+01	1.00000E-01	0.50000E-01	1.803E+00	0.000E+00
09	3	8.28000E+01	8.29000E+01	0.50000E-01	1.05000E+00	1.803E+00	0.000E+00
70	0	8.28000E+01	8.29000E+01	1.05000E+00	1.95000E+00	1.803E+00	0.000E+00
71	3	8.28000E+01	8.29000E+01	1.95000E+00	2.05000E+00	1.803E+00	0.000E+00
72	0	8.28000E+01	8.29000E+01	2.05000E+00	4.95000E+00	1.803E+00	0.000E+00
73	3	8.28000E+01	8.29000E+01	4.95000E+00	5.05000E+00	1.803E+00	0.000E+00
74	0	8.28000E+01	8.29000E+01	5.05000E+00	9.95000E+00	1.803E+00	0.000E+00
75	3	8.28000E+01	8.29000E+01	9.95000E+00	1.00500E+01	1.803E+00	0.000E+00
76	0	8.28000E+01	8.29000E+01	1.00500E+01	1.99500E+01	1.803E+00	0.000E+00
77	3	8.28000E+01	8.29000E+01	1.99500E+01	2.00500E+01	1.803E+00	0.000E+00
78	0	8.28000E+01	8.29000E+01	2.00500E+01	2.20000E+01	1.803E+00	0.000E+00

```
************************
*  SOURCE INFORMATION  *
************************

SOURCE ELECTRONS

THE MAXIMUM SOURCE ENERGY IS    391.00000 MEV

THE GLOBAL ELECTRON CUTOFF ENERGY IS      1.80300 MEV

THE PHOTON CUTOFF ENERGY IS      0.01000 MEV

COORDINATES OF THE POINT SOURCE OR OF THE CENTER OF THE BEAM (DISK) SOURCE ARE
   X =  0.00000E+00 CM          Y =  0.00000E+00 CM          Z =  0.00000E+00 CM

THE RADIUS OF THE BEAM (DISK) SOURCE IS =   0.0000E+00 CM

REFERENCE DIRECTION FOR ANGULAR DISTRIBUTION IS DEFINED BY
   THETA =   0.0000 DEGREES          PHI =   0.0000 DEGREES

MONODIRECTIONAL SOURCE IN REFERENCE DIRECTION

THE STANDARD ERROR ESTIMATES ARE BASED ON   10 BATCHES OF    1000 HISTORIES EACH
```

```
**********
* OUTPUT OPTIONS *
**********

ELECTRON-ESCAPE ENERGY CLASSIFICATIONS (MEV)
  351.90000   312.80000   273.70000   234.60000   195.50000   156.40000
  117.30000    78.20000    39.10000     1.60300

ELECTRON-ESCAPE POLAR ANGLE CLASSIFICATIONS (DEGREES)
   10.00000    20.00000    30.00000    40.00000    50.00000    70.00000
   90.00000   120.00000   150.00000   180.00000

ELECTRON-ESCAPE AZIMUTH ANGLE CLASSIFICATIONS (DEGREES)
  180.00000
```

```
**********************
*  PHYSICAL OPTIONS  *
**********************

ELECTRON COLLISION AND RADIATION ENERGY LOSS STRAGGLING

KNOCK-ON ELECTRON PRODUCTION

NO COUPLED INELASTIC SCATTERING DEFLECTIONS

BREMSSTRAHLUNG AND CHARACTERISTIC X-RAY QUANTA FOLLOWED

BREMSSTRAHLUNG INTRINSIC ANGLE OF EMISSION FROM TABULATED DISTRIBUTION

PHOTON-PRODUCED ELECTRONS FOLLOWED

      MATERIAL NO.  1
ELECTRON RANGE AT MAXIMUM SOURCE ENERGY IS      0.75139E+02 (G/CM**2)
K X-RAY QUANTA NOT FOLLOWED
ELECTRON IMPACT IONIZATION NOT SAMPLED

      MATERIAL NO.  2
ELECTRON RANGE AT MAXIMUM SOURCE ENERGY IS      0.66426E+02 (G/CM**2)
K X-RAY QUANTA NOT FOLLOWED
ELECTRON IMPACT IONIZATION NOT SAMPLED

      MATERIAL NO.  3
ELECTRON RANGE AT MAXIMUM SOURCE ENERGY IS      0.80237E+02 (G/CM**2)
K X-RAY QUANTA NOT FOLLOWED
ELECTRON IMPACT IONIZATION NOT SAMPLED

ANNIHILATION QUANTA FOLLOWED

 THE VOLUME RATIO IS      0.10000000000000E+01
```

```
*******************************************************************************
*                                                                             *
*  391 MeV Electrons - 10.0 PMMA, 39cm Air, 40.0 PMMA, 0 LiF Arrays           *
*                                                                             *
*******************************************************************************

THE PROBLEM IS  100  PERCENT COMPLETE.  TIME TO FINISH IS        0.000 SECONDS. AVERAGE TIME PER BATCH IS      488.848

AVERAGE SOURCE ENERGY =  3.9100E+02  0 MEV

THE INITIAL RANDOM NUMBER OF THIS RUN IS                  0
THE INITIAL RANDOM NUMBER OF THE CURRENT BATCH IS         31411431531
THE  FINAL  RANDOM NUMBER OF THE CURRENT BATCH IS          8260170762

    ------------------------------------ HISTORIES ------------------------------------      REJ      REJ      --- STEPS ----
   PRIM      SEC    KNOCK      P E     PAIR      COM    AUGER      BREM      RAD     XRAY      LAND      PEAL      PRIM      SEC
  10000    85483    32594         0    18538    18333        0    138014    141424        0      5764         0    380732    883459

 NBLK =          0

                                ENERGY (MEV)     AVE ENERGY (MEV)     NUMBER/PRIMARY     NUMBER GENERATED
FIRST KNOCK (ABOVE TCUT)        1.5502E+01         8.7419E+00           2.2994E+00           22994
TOTAL KNOCK (ABOVE TCUT)        1.9350E+01         5.9388E+00           3.2594E+00           32594
PHOTO-ELECTRON                  1.0448E-01         3.8338E-02           2.7253E+00           27253
PAIR                            8.8541E+01         3.8458E+01           1.7822E+00           17822
COMPTON                         2.0269E+01         4.4750E-01           4.5294E+01           452938
AUGER                           0.0000E+00         0.0000E+00           0.0000E+00                0
FIRST BREMSSTRAHLUNG            2.2313E+02         2.4169E+01           9.2321E+00           92321
TOTAL BREMSSTRAHLUNG            2.4059E+02         1.7029E+01           1.4128E+01           141278
K X-RAY(P-IONIZATION)           0.0000E+00         0.0000E+00           0.0000E+00                0
K X-RAY(E-IONIZATION)           0.0000E+00         0.0000E+00           0.0000E+00                0
ANNIHILATION QUANTA             8.2881E-01         5.1098E-01           1.2308E+00           12308


NUMBER AND ENERGY (MEV PER SOURCE PARTICLE) OF SOURCE PARTICLES REJECTED FOR BEING BELOW THE GLOBAL CUTOFF
        0           0.00000E+00 99
```

NUMBER ESCAPE FRACTIONS --- KNOCK-ON AND PHOTON GENERATED ELECTRONS, ANNIHILATION RADIATION, K X-RAYS

TRANSMISSION

KNOCK	P-SEC	ANNIH
8.48E-02 4	8.81E-01 2	1.13E-01 1

K X-RAYS FROM MATERIAL NO. 1, K X-RAYS FROM MATERIAL NO. 2, ETC.

8.00E+00 99 8.00E+00 99 8.00E+00 99

REFLECTION

KNOCK	P-SEC	ANNIH
8.00E+00 99	8.00E+00 99	5.35E-03 8

K X-RAYS FROM MATERIAL NO. 1, K X-RAYS FROM MATERIAL NO. 2, ETC.

8.00E+00 99 8.00E+00 99 8.00E+00 99

LATERAL ESCAPE

KNOCK	P-SEC	ANNIH
3.30E-02 4	1.76E-02 8	9.24E-02 2

K X-RAYS FROM MATERIAL NO. 1, K X-RAYS FROM MATERIAL NO. 2, ETC.

8.00E+00 99 8.00E+00 99 8.00E+00 99

NUMBER AND ENERGY ESCAPE FRACTIONS

TRANSMISSION

ELECTRON			PHOTON		
NUMBER	ENERGY	COUNTS	NUMBER	ENERGY	COUNTS
1.48E+00 1	2.42E-01 1	14574	8.28E+00	3.88E-01 0	252142

REFLECTION

ELECTRON			PHOTON		
NUMBER	ENERGY	COUNTS	NUMBER	ENERGY	COUNTS
0.00E+00 99	0.00E+00 99	0	1.40E-01 2	6.11E-05 3	14268

LATERAL ESCAPE

ELECTRON			PHOTON		
NUMBER	ENERGY	COUNTS	NUMBER	ENERGY	COUNTS
5.40E-02 5	7.09E-04 4	548	3.05E+00	2.09E-03 1	338785

ENERGY DEPOSITION
(NORMALIZED TO ONE INCIDENT PARTICLE)

ZONE	MATERIAL	MASS(GM)	VOLUME(CC)	ENERGY DEPOSITION (MEV) PRIM	KNOCK	G-SEC	TOTAL
1	1	1.5210E+04	1.2803E+04	2.2143E+01 1	-1.8284E+00 5	1.0387E+00 3	2.1353E+01 1
2	3	2.4834E-02	9.4248E-03	5.1103E-01 2	-7.8790E-02 27	4.9484E-02 7	4.8973E-01 0
3	0	0.0000E+00	0.4116E-01	0.0000E+00 99	0.0000E+00 99	0.0000E+99 99	0.0000E+00 99
4	3	4.9669E-01	1.8850E-01	0.5848E-04 30	0.1804E-03 10	3.5877E-03 13	1.0427E-02 12
5	0	0.0000E+00	2.5447E+00	0.0000E+99 99	0.0000E+00 99	0.0000E+99 99	0.0000E+00 99
6	3	0.9337E-01	3.7699E-01	0.4915E-05 99	1.2443E-03 10	3.8779E-04 24	1.7270E-03 17
7	0	0.0000E+00	1.9132E+01	0.0000E+00 99	0.0000E+00 99	0.0000E+99 99	0.0000E+00 99
8	3	2.4834E+00	0.4248E-01	3.9429E-05 99	4.9515E-05 99	7.2100E-05 72	1.8104E-04 60
9	0	0.0000E+00	0.9272E+01	0.0000E+00 99	0.0000E+00 99	0.0000E+00 99	0.0000E+00 99
10	3	4.9669E+00	1.8850E+00	0.0000E+00 99	5.1664E-05 99	2.9165E-05 87	0.0329E-05 63
11	0	0.0000E+00	2.7992E+02	0.0000E+99 99	0.0000E+00 99	0.0000E+00 99	0.0000E+00 99
12	3	9.9337E+00	3.7699E+00	0.0000E+00 99	3.3943E-05 99	5.0904E-06 81	3.9034E-05 60
13	0	0.0000E+00	7.7281E+01	0.0000E+00 99	0.0000E+00 99	0.0000E+99 99	0.0000E+00 99
14	2	7.0271E+01	5.9301E+04	1.1616E-01 1	1.8912E-03 99	1.2189E-02 2	1.3004E-01 2
15	3	2.4834E-02	9.4248E-03	4.4335E-03 20	-2.5799E-04 99	2.7531E-03 23	0.9288E-03 12
16	0	0.0000E+00	0.4116E-01	0.0000E+00 99	0.0000E+00 99	0.0000E+00 99	0.0000E+00 99
17	3	4.9669E-01	1.8850E-01	7.8995E-02 5	-2.5069E-02 42	2.5129E-03 10	5.4436E-02 21
18	0	0.0000E+00	2.5447E+00	0.0000E+00 99	0.0000E+00 99	0.0000E+00 99	0.0000E+00 99
19	3	0.9337E-01	3.7699E-01	3.3707E-02 7	-0.0776E-04 00	1.7762E-03 37	3.4878E-02 7
20	0	0.0000E+00	1.9132E+01	0.0000E+00 99	0.0000E+00 99	0.0000E+00 99	0.0000E+00 99
21	3	2.4834E+00	0.4248E-01	1.5912E-03 54	7.4166E-04 39	1.0076E-03 32	3.3405E-03 31
22	0	0.0000E+00	0.9272E+01	0.0000E+00 99	0.0000E+00 99	0.0000E+99 99	0.0000E+00 99
23	3	4.9669E+00	1.8850E+00	1.3772E-04 85	0.5737E-04 52	5.0494E-04 28	1.3600E-03 30
24	0	0.0000E+00	2.7992E+02	0.0000E+00 99	0.0000E+00 99	0.0000E+00 99	0.0000E+00 99
25	3	0.9337E+00	3.7699E+00	0.0000E+00 99	2.7598E-04 47	1.1383E-04 53	3.0981E-04 30
26	0	0.0000E+00	7.7281E+01	0.0000E+00 99	0.0000E+00 99	0.0000E+99 99	0.0000E+00 99
27	1	1.5210E+04	1.2803E+04	2.1458E+01 0	-7.8998E-01 12	5.0807E+00 2	2.5749E+01 1
28	3	2.4834E-02	0.4248E-03	3.7857E-03 12	-2.1169E-03 30	0.4298E-03 13	1.0099E-02 10
29	0	0.0000E+00	0.4116E-01	0.0000E+00 99	0.0000E+00 99	0.0000E+00 99	0.0000E+00 99
30	3	4.9669E-01	1.8850E-01	5.4755E-02 7	-4.2342E-03 91	2.0843E-02 11	7.1184E-02 0
31	0	0.0000E+00	2.5447E+00	0.0000E+00 99	0.0000E+00 99	0.0000E+00 99	0.0000E+00 99
32	3	9.9337E-01	3.7699E-01	4.5100E-02 4	-1.0122E-02 99	1.1878E-02 12	4.8358E-02 23
33	0	0.0000E+00	1.9132E+01	0.0000E+00 99	0.0000E+00 99	0.0000E+00 99	0.0000E+00 99
34	3	2.4834E+00	0.4248E-01	3.8080E-03 14	5.4090E-04 33	0.5547E-04 17	5.2044E-03 10
35	0	0.0000E+00	0.9272E+01	0.0000E+00 99	0.0000E+00 99	0.0000E+00 99	0.0000E+00 99
36	3	4.9669E+00	1.8850E+00	3.1020E-04 84	5.6632E-05 99	3.9025E-04 50	7.5708E-04 38
37	0	0.0000E+00	2.7992E+02	0.0000E+00 99	0.0000E+00 99	0.0000E+00 99	0.0000E+00 99
38	3	0.9337E+00	3.7699E+00	0.0000E+00 99	0.0000E+00 99	2.1017E-05 54	2.1017E-05 54
39	0	0.0000E+00	7.7281E+01	0.0000E+00 99	0.0000E+00 99	0.0000E+00 99	0.0000E+00 99
40	1	1.5210E+04	1.2803E+04	2.0539E+01 1	-3.2898E-01 22	0.8930E+99 2	3.0110E+01 1
41	3	2.4834E-02	0.4248E-03	1.9321E-03 27	5.1593E-04 55	5.9257E-03 10	0.3737E-03 14
42	0	0.0000E+00	0.4116E-01	0.0000E+00 99	0.0000E+00 99	0.0000E+00 99	0.0000E+00 99
43	3	4.9669E-01	1.8850E-01	3.0378E-02 10	0.0805E-04 99	2.7760E-02 5	0.0827E-02 4
44	0	0.0000E+00	2.5447E+00	0.0000E+00 99	0.0000E+00 99	0.0000E+00 99	0.0000E+00 99
45	3	9.9337E-01	3.7699E-01	3.0074E-02 0	0.0992E-04 99	1.7434E-02 0	5.7178E-02 5
46	0	0.0000E+00	1.9132E+01	0.0000E+00 99	0.0000E+00 99	0.0000E+00 99	0.0000E+00 99
47	3	2.4834E+00	0.4248E-01	4.0069E-03 20	2.7722E-04 99	4.1097E-03 10	0.1939E-03 15

48	0	0.0000E+00	0.9272E+01	0.0000E+00 99	0.0000E+00 99	0.0000E+00 99	0.0000E+00 99
49	3	4.9689E+00	1.8850E+00	1.7435E-04 34	0.0000E+00 99	7.8772E-04 25	9.4207E-04 31
50	0	0.0000E+00	2.7992E+02	0.0000E+00 99	0.0000E+00 99	0.0000E+00 99	0.0000E+00 99

ENERGY DEPOSTION
(NORMALIZED TO ONE INCIDENT PARTICLE)

ZONE	MATERIAL	MASS(GM)	VOLUME(CC)	ENERGY DEPOSITION (MEV) PRIM	KNOCK	G-SEC	TOTAL
51	3	9.9337E+00	3.7699E+00	0.0000E+00 99	0.0000E+00 99	8.8818E-05 28	8.9918E-05 28
52	0	0.0000E+00	7.7281E+01	0.0000E+00 99	0.0000E+00 99	0.0000E+00 99	0.0000E+00 99
53	1	1.5210E+04	1.2803E+04	1.8879E+01 1	7.4848E-02 87	1.3800E+01 1	3.2754E+01 0
54	3	2.4834E-02	9.4248E-03	8.1309E-04 48	3.9800E-04 53	4.8587E-03 17	6.1618E-03 10
55	0	0.0000E+00	0.4116E-01	0.0000E+00 99	0.0000E+00 99	0.0000E+00 99	0.0000E+00 99
56	3	4.9689E-01	1.8850E-01	2.4305E-02 0	2.7405E-03 48	2.7595E-02 0	5.4841E-02 5
57	0	0.0000E+00	2.5447E+00	0.0000E+00 99	0.0000E+00 99	0.0000E+00 99	0.0000E+00 99
58	3	9.9337E-01	3.7699E-01	2.9979E-02 7	3.0575E-03 48	2.5037E-02 0	5.8074E-02 0
59	0	0.0000E+00	1.9132E+01	0.0000E+00 99	0.0000E+00 99	0.0000E+00 99	0.0000E+00 99
60	3	2.4834E+00	0.4248E-01	9.8568E-03 22	-3.2880E-03 95	7.9910E-03 11	1.4380E-02 30
61	0	0.0000E+00	0.9272E+01	0.0000E+00 99	0.0000E+00 99	0.0000E+00 99	0.0000E+00 99
62	3	4.9689E+00	1.8850E+00	1.7122E-04 58	8.8228E-05 99	4.9414E-04 26	7.5159E-04 25
63	0	0.0000E+00	2.7992E+02	0.0000E+00 99	0.0000E+00 99	0.0000E+00 99	0.0000E+00 99
64	3	9.9337E+00	3.7699E+00	5.7388E-05 99	0.0000E+00 99	1.5533E-04 38	2.1272E-04 41
65	0	0.0000E+00	7.7281E+01	0.0000E+00 99	0.0000E+00 99	0.0000E+00 99	0.0000E+00 99
66	1	1.5210E+04	1.2803E+04	1.8320E+01 1	1.8378E-01 31	1.0683E+01 1	3.3187E+01 1
67	3	2.4834E-02	9.4248E-03	1.0449E-03 50	-9.9077E-04 99	8.0582E-03 35	8.1103E-03 35
68	0	0.0000E+00	0.4116E-01	0.0000E+00 99	0.0000E+00 99	0.0000E+00 99	0.0000E+00 99
69	3	4.9689E-01	1.8850E-01	1.2975E-02 10	2.0852E-03 87	2.3038E-02 7	3.8095E-02 5
70	0	0.0000E+00	2.5447E+00	0.0000E+00 99	0.0000E+00 99	0.0000E+00 99	0.0000E+00 99
71	3	9.9337E-01	3.7699E-01	2.3282E-02 10	2.6730E-03 78	2.4487E-02 0	4.9842E-02 7
72	0	0.0000E+00	1.9132E+01	0.0000E+00 99	0.0000E+00 99	0.0000E+00 99	0.0000E+00 99
73	3	2.4834E+00	0.4248E-01	1.0478E-02 9	-2.1388E-03 85	7.5735E-03 17	1.5913E-02 11
74	0	0.0000E+00	0.9272E+01	0.0000E+00 99	0.0000E+00 99	0.0000E+00 99	0.0000E+00 99
75	3	4.9689E+00	1.8850E+00	8.7386E-04 32	1.5830E-04 87	8.7109E-04 38	1.7833E-03 23
76	0	0.0000E+00	2.7992E+02	0.0000E+00 99	0.0000E+00 99	0.0000E+00 99	0.0000E+00 99
77	3	9.9337E+00	3.7699E+00	0.0000E+00 99	4.4541E-05 99	2.7642E-05 51	7.2183E-05 81
78	0	0.0000E+00	7.7281E+01	0.0000E+00 99	0.0000E+00 99	0.0000E+00 99	0.0000E+00 99
			TOTAL	1.0039E+02 0	-2.7818E+00 3	4.6785E+01 1	1.4439E+02 0

THE ENERGY CONSERVATION FRACTION IS 0.1000237785204E+01 0

CHARGE DEPOSITION

(NORMALIZED TO ONE INCIDENT PARTICLE)

ZONE	MATERIAL	ZL	ZR	RI	RO	ELECTRONS PRIM	KNOCK	G-SEC	TOTAL
1	1	0.000E+00	0.420E+00	0.000E+00	2.200E+01	7.3000E-03	16-1.1770E-01	3-3.7800E-02	5-1.4800E-01 3
2	3	0.420E+00	0.720E+00	0.000E+00	1.000E-01	2.0000E-04	87-1.1800E-02	9-8.4000E-03	16-1.7200E-02 7
3	0	0.420E+00	0.720E+00	1.000E-01	9.500E-01	0.0000E+00	99 0.0000E+00	00 0.0000E+00	99 0.0000E+00 99
4	3	0.420E+00	0.720E+00	9.500E-01	1.050E+00	0.0000E+00	99 1.2000E-03	27 5.0000E-04	54 1.7000E-03 20
5	0	0.420E+00	0.720E+00	1.050E+00	1.950E+00	0.0000E+00	99 0.0000E+00	99 0.0000E+00	99 0.0000E+00 99
0	3	0.420E+00	0.720E+00	1.950E+00	2.050E+00	0.0000E+00	99 0.0000E+00	99 4.0000E-04	55 4.0000E-04 87
7	0	0.420E+00	0.720E+00	2.050E+00	4.950E+00	0.0000E+00	99 0.0000E+00	99 0.0000E+00	99 0.0000E+00 99
0	3	0.420E+00	0.720E+00	4.950E+00	5.050E+00	0.0000E+00	99 0.0000E+00	99 0.0000E+00	99 0.0000E+00 99
0	0	0.420E+00	0.720E+00	5.050E+00	9.950E+00	0.0000E+00	99 0.0000E+00	99 0.0000E+00	99 0.0000E+00 99
10	3	0.420E+00	0.720E+00	9.950E+00	1.005E+01	0.0000E+00	99 0.0000E+00	99 0.0000E+00	99 0.0000E+00 99
11	0	0.420E+00	0.720E+00	1.005E+01	1.995E+01	0.0000E+00	99 0.0000E+00	99 0.0000E+00	99 0.0000E+00 99
12	3	0.420E+00	0.720E+00	1.995E+01	2.005E+01	0.0000E+00	99 1.0000E-04	99 0.0000E+00	99 1.0000E-04 99
13	0	0.420E+00	0.720E+00	2.005E+01	2.200E+01	0.0000E+00	99 0.0000E+00	99 0.0000E+00	99 0.0000E+00 99
14	2	0.720E+00	4.772E+01	0.000E+00	2.200E+01	1.0000E-04	99-9.0000E-04	87 7.0000E-04	00-1.0000E-04 99
15	3	4.772E+01	4.802E+01	0.000E+00	1.000E-01	0.0000E+00	99-1.0000E-04	99-2.1000E-03	17-2.2000E-03 15
16	0	4.772E+01	4.802E+01	1.000E-01	9.500E-01	0.0000E+00	00 0.0000E+00	99 0.0000E+00	99 0.0000E+00 99
17	3	4.772E+01	4.802E+01	9.500E-01	1.050E+00	0.0000E+00	99-2.3000E-03	15-1.1000E-03	29-3.4000E-03 12
18	0	4.772E+01	4.802E+01	1.050E+00	1.950E+00	0.0000E+00	00 0.0000E+00	99 0.0000E+00	99 0.0000E+00 00
19	3	4.772E+01	4.802E+01	1.950E+00	2.050E+00	0.0000E+00	99-3.0000E-04	51-4.0000E-04	41-7.0000E-04 30
20	0	4.772E+01	4.802E+01	2.050E+00	4.950E+00	0.0000E+00	99 0.0000E+00	99 0.0000E+00	99 0.0000E+00 99
21	3	4.772E+01	4.802E+01	4.950E+00	5.050E+00	0.0000E+00	99 0.0000E+00	00 0.0000E+00	99 0.0000E+00 99
22	0	4.772E+01	4.802E+01	5.050E+00	9.950E+00	0.0000E+00	99 0.0000E+00	99 0.0000E+00	99 0.0000E+00 99
23	3	4.772E+01	4.802E+01	9.950E+00	1.005E+01	0.0000E+00	99 1.0000E-04	99 2.0000E-04	99 3.0000E-04 71
24	0	4.772E+01	4.802E+01	1.005E+01	1.995E+01	0.0000E+00	99 0.0000E+00	99 0.0000E+00	99 0.0000E+00 00
25	3	4.772E+01	4.802E+01	1.995E+01	2.005E+01	0.0000E+00	99 0.0000E+00	99 1.0000E-04	99 1.0000E-04 00
20	0	4.772E+01	4.802E+01	2.005E+01	2.200E+01	0.0000E+00	99 0.0000E+00	99 0.0000E+00	99 0.0000E+00 99
27	1	4.802E+01	5.844E+01	0.000E+00	2.200E+01	2.9100E-02	7-8.1400E-02	0-8.2900E-02	0-8.5200E-02 5
28	3	5.844E+01	5.874E+01	0.000E+00	1.000E-01	0.0000E+00	99-4.0000E-04	41-1.2000E-03	27-1.0000E-03 21
29	0	5.844E+01	5.874E+01	1.000E-01	9.500E-01	0.0000E+00	99 0.0000E+00	99 0.0000E+00	00 0.0000E+00 00
30	3	5.844E+01	5.874E+01	9.500E-01	1.050E+00	0.0000E+00	99-5.0000E-04	01 0.0000E+00	99-5.0000E-04 00
31	0	5.844E+01	5.874E+01	1.050E+00	1.950E+00	0.0000E+00	99 0.0000E+00	99 0.0000E+00	00 0.0000E+00 99
32	3	5.844E+01	5.874E+01	1.950E+00	2.050E+00	0.0000E+00	99-7.0000E-04	04-2.7105E-20	99-7.0000E-04 99
33	0	5.844E+01	5.874E+01	2.050E+00	4.950E+00	0.0000E+00	99 0.0000E+00	99 0.0000E+00	99 0.0000E+00 00
34	3	5.844E+01	5.874E+01	4.950E+00	5.050E+00	0.0000E+00	99 1.0000E-04	99-1.0000E-04	99-1.0842E-20 99
35	0	5.844E+01	5.874E+01	5.050E+00	9.950E+00	0.0000E+00	99 0.0000E+00	99 0.0000E+00	99 0.0000E+00 99
36	3	5.844E+01	5.874E+01	9.950E+00	1.005E+01	0.0000E+00	00 0.0000E+00	00 2.7105E-21	99 2.7105E-21 00
37	0	5.844E+01	5.874E+01	1.005E+01	1.995E+01	0.0000E+00	99 0.0000E+00	99 0.0000E+00	99 0.0000E+00 99
38	3	5.844E+01	5.874E+01	1.995E+01	2.005E+01	0.0000E+00	99 0.0000E+00	99-1.0000E-04	99-1.0000E-04 99
39	0	5.844E+01	5.874E+01	2.005E+01	2.200E+01	0.0000E+00	00 0.0000E+00	99 0.0000E+00	99 3.0000E+00 99
40	1	5.874E+01	8.518E+01	0.000E+00	2.200E+01	5.7500E-02	4-8.7000E-03	53-4.5800E-02	12 3.0000E-03 00
41	3	8.518E+01	8.548E+01	0.000E+00	1.000E-01	0.0000E+00	99-1.0000E-04	99-2.0000E-04	99-3.0000E-04 99
42	0	8.518E+01	8.548E+01	1.000E-01	9.500E-01	0.0000E+00	99 0.0000E+00	99 0.0000E+00	99 0.0000E+00 00
43	3	8.518E+01	8.548E+01	9.500E-01	1.950E+00	0.0000E+00	99 1.0000E-04	99-1.4000E-03	42-1.3000E-03 75
44	0	8.518E+01	8.548E+01	1.050E+00	1.950E+00	0.0000E+00	99 0.0000E+00	99 0.0000E+00	99 0.0000E+00 99
45	3	8.518E+01	8.548E+01	1.950E+00	2.050E+00	0.0000E+00	99-2.0000E-04	99-4.0000E-04	99-0.0000E-04 99
46	0	8.518E+01	8.548E+01	2.050E+00	4.950E+00	0.0000E+00	99 0.0000E+00	99 0.0000E+00	99 0.0000E+00 99
47	3	8.518E+01	8.548E+01	4.950E+00	5.050E+00	1.0000E-04	99 1.0000E-04	99-2.0000E-04	99-4.3368E-20 99

48	0	8.516E+01	8.548E+01	5.050E+00	9.950E+00	0.0000E+00	99	0.0000E+00	99	0.0000E+00	99	0.0000E+00	99		
49	3	8.516E+01	8.548E+01	9.950E+00	1.005E+01	0.0000E+00	99	0.0000E+00	99	-2.7105E-21	99	-2.7105E-21	99		
50	0	8.516E+01	8.548E+01	1.005E+01	1.005E+01	0.0000E+00	99	0.0000E+00	99	0.0000E+00	99	0.0000E+00	99		

CHARGE DEPOSITION
(NORMALIZED TO ONE INCIDENT PARTICLE)

						ELECTRONS			
ZONE	MATERIAL	ZL	ZR	RI	RO	PRIM	KNOCK	G-SEC	TOTAL
51	3	8.518E+01	8.548E+01	1.995E+01	2.005E+01	0.0000E+00 99	0.0000E+00 99	-3.0000E-04 51	-3.0000E-04 51
52	0	8.518E+01	8.548E+01	2.005E+01	2.200E+01	0.0000E+00 99	0.0000E+00 99	0.0000E+00 99	0.0000E+00 99
53	1	8.548E+01	7.388E+01	0.000E+00	2.200E+01	3.2800E-02 2	1.0400E-02 43	-4.1100E-02 25	8.2100E-02 20
54	3	7.388E+01	7.418E+01	0.000E+00	1.000E-01	0.0000E+00 99	0.0000E+00 99	-3.0000E-04 31	-3.0000E-04 31
55	0	7.388E+01	7.418E+01	1.000E-01	9.500E-01	0.0000E+00 99	0.0000E+00 99	0.0000E+00 00	0.0000E+00 99
56	3	7.388E+01	7.418E+01	9.500E-01	1.050E+00	2.0000E-04 67	-0.0000E-04 99	5.0000E-04 00	4.0000E-04 99
57	0	7.388E+01	7.418E+01	1.050E+00	1.950E+00	0.0000E+00 99	0.0000E+00 99	0.0000E+00 99	0.0000E+00 99
58	3	7.388E+01	7.418E+01	1.950E+00	2.050E+00	1.0000E-04 99	-5.0000E-04 54	-3.2528E-20 99	-4.0000E-04 99
59	0	7.388E+01	7.418E+01	2.050E+00	4.950E+00	0.0000E+00 99	0.0000E+00 99	0.0000E+00 99	0.0000E+00 99
60	3	7.388E+01	7.418E+01	4.950E+00	5.050E+00	0.0000E-04 51	-4.0000E-04 76	1.0000E-04 99	-1.8342E-20 99
61	0	7.388E+01	7.418E+01	5.050E+00	8.950E+00	0.0000E+00 99	0.0000E+00 99	0.0000E+00 00	0.0000E+00 99
62	3	7.388E+01	7.418E+01	8.950E+00	1.005E+01	0.0000E+00 99	1.0000E-04 99	-1.8263E-20 99	1.0000E-04 99
63	0	7.388E+01	7.418E+01	1.005E+01	1.995E+01	0.0000E+00 99	0.0000E+00 99	0.0000E+00 99	0.0000E+00 99
64	3	7.388E+01	7.418E+01	1.995E+01	2.005E+01	0.0000E+00 99	0.0000E+00 99	-5.4210E-21 99	-5.4210E-21 99
65	0	7.388E+01	7.418E+01	2.005E+01	2.200E+01	0.0000E+00 99	0.0000E+00 99	0.0000E+00 99	0.0000E+00 99
66	1	7.418E+01	8.280E+01	0.000E+00	2.200E+01	1.2240E-01 2	1.5300E-02 25	-2.8700E-02 28	1.0900E-01 0
67	3	8.280E+01	8.290E+01	0.000E+00	1.000E-01	0.0000E+00 99	0.0000E+00 99	-2.0000E-04 99	-2.0000E-04 99
68	0	8.280E+01	8.290E+01	1.000E-01	9.500E-01	0.0000E+00 99	0.0000E+00 99	0.0000E+00 99	0.0000E+00 99
69	3	8.280E+01	8.290E+01	9.500E-01	1.050E+00	1.0000E-04 99	0.0000E-04 99	-0.0000E-04 75	1.0000E-04 99
70	0	8.280E+01	8.290E+01	1.050E+00	1.950E+00	0.0000E+00 99	0.0000E+00 99	0.0000E+00 99	0.0000E+00 99
71	3	8.280E+01	8.290E+01	1.950E+00	2.050E+00	0.0000E+00 99	2.0000E-04 99	4.0000E-04 99	8.0000E-04 99
72	0	8.280E+01	8.290E+01	2.050E+00	4.950E+00	0.0000E+00 99	0.0000E+00 99	0.0000E+00 99	0.0000E+00 99
73	3	8.280E+01	8.290E+01	4.950E+00	5.050E+00	0.0000E+00 99	-5.0000E-04 81	3.0000E-04 99	-2.0000E-04 99
74	0	8.280E+01	8.290E+01	5.050E+00	8.950E+00	0.0000E+00 99	0.0000E+00 99	0.0000E+00 99	0.0000E+00 99
75	3	8.280E+01	8.290E+01	8.950E+00	1.005E+01	0.0000E+00 99	0.0000E+00 99	-3.0000E-04 87	-3.0000E-04 87
76	0	8.280E+01	8.290E+01	1.005E+01	1.995E+01	0.0000E+00 99	0.0000E+00 99	0.0000E+00 99	0.0000E+00 99
77	3	8.280E+01	8.290E+01	1.995E+01	2.005E+01	0.0000E+00 99	0.0000E+00 99	-2.0000E-04 99	-2.0000E-04 99
78	0	8.280E+01	8.290E+01	2.005E+01	2.280E+01	0.0000E+00 99	0.0000E+00 99	0.0000E+00 99	0.0000E+00 99
TOTAL						3.1020E-01 1	-1.7770E-01 3	-2.2890E-01 3	-9.6400E-02 12

ENERGY SPECTRA OF TRANSMITTED ELECTRONS
(NUMBER/MEV, NORMALIZED TO ONE INCIDENT PARTICLE)

E (MEV)			
391.0000	351.9000	0.00E+00	99
351.9000	312.8000	7.67E-06	51
312.8000	273.7000	1.10E-04	14
273.7000	234.9000	8.31E-04	5
234.8000	195.5000	1.53E-03	5
195.5000	156.4000	2.20E-03	3
156.4000	117.3000	2.93E-03	3
117.3000	78.2000	4.14E-03	3
78.2000	39.1000	8.89E-03	1
39.1000	1.8030	1.94E-02	1

ENERGY SPECTRA OF REFLECTED ELECTRONS
(NUMBER/MEV, NORMALIZED TO ONE INCIDENT PARTICLE)

E (MEV)			
391.0000	351.9000	0.00E+00	99
351.9000	312.8000	0.00E+00	99
312.8000	273.7000	0.00E+00	99
273.7000	234.8000	0.00E+00	99
234.8000	195.5000	0.00E+00	99
195.5000	156.4000	0.00E+00	99
156.4000	117.3000	0.00E+00	99
117.3000	78.2000	0.00E+00	99
78.2000	39.1000	0.00E+00	99
39.1000	1.8030	0.00E+00	99

ENERGY SPECTRA OF LATERALLY ESCAPING ELECTRONS
(NUMBER/MEV, NORMALIZED TO ONE INCIDENT PARTICLE)

E (MEV)			
391.0000	351.9000	0.00E+00	99
351.9000	312.8000	0.00E+00	99
312.8000	273.7000	0.00E+00	99
273.7000	234.8000	0.00E+00	99
234.8000	195.5000	0.00E+00	99
195.5000	156.4000	0.00E+00	99
156.4000	117.3000	0.00E+00	99
117.3000	78.2000	0.00E+00	99
78.2000	39.1000	7.87E-06	51
39.1000	1.8030	1.43E-03	5

ANGULAR DISTRIBUTIONS OF TRANSMITTED AND REFLECTED ELECTRONS
(NUMBER/SR, NORMALIZED TO ONE INCIDENT PARTICLE)

PHI(DEG) = 0.000
THETA (DEG) 180.000

0.0000 - 10.0000	8.04E+00	1
10.0000 - 20.0000	1.32E+00	2
20.0000 - 30.0000	3.33E-01	4
30.0000 - 40.0000	1.38E-01	4
40.0000 - 50.0000	5.28E-02	5
50.0000 - 70.0000	1.84E-02	8
70.0000 - 90.0000	1.91E-03	14
90.0000 - 120.0000	0.00E+00	99
120.0000 - 150.0000	0.00E+00	99
150.0000 - 180.0000	0.00E+00	99

ANGULAR DISTRIBUTIONS OF LATERALLY ESCAPING ELECTRONS
(NUMBER/SR, NORMALIZED TO ONE INCIDENT PARTICLE)

PHI(DEG) = 0.000
THETA (DEG) 180.000

0.0000 - 10.0000	0.00E+00	99
10.0000 - 20.0000	1.78E-03	45
20.0000 - 30.0000	1.82E-02	12
30.0000 - 40.0000	3.04E-02	7
40.0000 - 50.0000	1.54E-02	11
50.0000 - 70.0000	0.77E-03	8
70.0000 - 90.0000	0.84E-04	15
90.0000 - 120.0000	0.55E-05	71
120.0000 - 150.0000	0.00E+00	99
150.0000 - 180.0000	0.00E+00	99

ENERGY SPECTRA AND ANGULAR DISTRIBUTIONS OF ELECTRONS TRANSMITTED AND REFLECTED
AZIMUTHAL INTERVAL IS 0.00000 TO 180.00000 DEGREES
(NUMBER/(MEV*SR), NORMALIZED TO ONE PARTICLE)

THETA =	0.000	10.000	20.000	30.000	40.000	50.000	70.000	90.000	120.000
E (MEV)	10.000	20.000	30.000	40.000	50.000	70.000	90.000	120.000	150.000
391.000-351.900	0.00E+00 99	0.00E+00 99	0.00E+00 99	0.00E+00 99	0.00E+00 99	0.00E+00 99	0.00E+00 99	0.00E+00 99	0.00E+00 99
351.900-312.800	0.04E-05 51	0.00E+00 99	0.00E+00 99	0.00E+00 99	0.00E+00 99	0.00E+00 99	0.00E+00 99	0.00E+00 99	0.00E+00 99
312.800-273.700	1.15E-03 14	0.00E+00 99	0.00E+00 99	0.00E+00 99	0.00E+00 99	0.00E+00 99	0.00E+00 99	0.00E+00 99	0.00E+00 99
273.700-234.800	0.38E-03 5	1.17E-04 38	0.00E+00 99	0.00E+00 99	0.00E+00 99	0.00E+00 99	0.00E+00 99	0.00E+00 99	0.00E+00 99
234.800-195.500	1.52E-02 5	2.80E-04 13	0.00E+00 99	0.00E+00 99	0.00E+00 99	0.00E+00 99	0.00E+00 99	0.00E+00 99	0.00E+00 99
195.500-156.400	2.15E-02 3	5.05E-04 14	0.00E+00 99	0.00E+00 99	0.00E+00 99	0.00E+00 99	0.00E+00 99	0.00E+00 99	0.00E+00 99
156.400-117.300	2.79E-02 3	9.20E-04 8	1.86E-05 51	0.00E+00 99	0.00E+00 99	0.00E+00 99	0.00E+00 99	0.00E+00 99	0.00E+00 99
117.300-78.200	3.49E-02 3	2.72E-03 7	7.18E-05 39	4.07E-00 99	0.00E+00 99	0.00E+00 99	0.00E+00 99	0.00E+00 99	0.00E+00 99
78.200-39.100	4.87E-02 2	7.53E-03 3	5.75E-04 8	3.28E-05 17	0.00E-00 87	1.35E-06 99	0.00E+00 99	0.00E+00 99	0.00E+00 99

39.100-1.603 5.19E-02 2 2.27E-02 2 8.19E-03 4 3.42E-03 4 1.39E-03 5 4.88E-04 6 5.09E-05 14 0.00E+00 99 0.00E+00 99

ENERGY SPECTRA AND ANGULAR DISTRIBUTIONS OF ELECTRONS TRANSMITTED AND REFLECTED
AZIMUTHAL INTERVAL IS 0.00000 TO 180.00000 DEGREES
(NUMBER/(MEV*SR), NORMALIZED TO ONE PARTICLE)

E (MEV)	THETA = 158.000 180.000
391.0000 - 351.9000	0.00E+00 99
351.9000 - 312.8000	0.00E+00 99
312.8000 - 273.7000	0.00E+00 99
273.7000 - 234.6000	0.00E+00 99
234.6000 - 195.5000	0.00E+00 99
195.5000 - 156.4000	0.00E+00 99
156.4000 - 117.3000	0.00E+00 99
117.3000 - 78.2000	0.00E+00 99
78.2000 - 39.1000	0.00E+00 99
39.1000 - 1.8030	0.00E+00 99

ENERGY SPECTRA AND ANGULAR DISTRIBUTIONS OF ELECTRONS LATERALLY ESCAPING
AZIMUTHAL INTERVAL IS 0.00000 TO 180.00000 DEGREES
(NUMBER/(MEV*SR), NORMALIZED TO ONE PARTICLE)

E (MEV)	THETA = 0.000 10.000	10.000 20.000	20.000 30.000	30.000 40.000	40.000 50.000	50.000 70.000	70.000 90.000	90.000 120.000	120.000 150.000
391.000-351.900	0.00E+00 99	0.00E+00 99	0.00E+00 99	0.00E+00 99	0.00E+00 99	0.00E+00 99	0.00E+00 99	0.00E+00 99	0.00E+00 99
351.900-312.800	0.00E+00 99	0.00E+00 99	0.00E+00 99	0.00E+00 99	0.00E+00 99	0.00E+00 99	0.00E+00 99	0.00E+00 99	0.00E+00 99
312.800-273.700	0.00E+00 99	0.00E+00 99	0.00E+00 99	0.00E+00 99	0.00E+00 99	0.00E+00 99	0.00E+00 99	0.00E+00 99	0.00E+00 99
273.700-234.600	0.00E+00 99	0.00E+00 99	0.00E+00 99	0.00E+00 99	0.00E+00 99	0.00E+00 99	0.00E+00 99	0.00E+00 99	0.00E+00 99
234.600-195.500	0.00E+00 99	0.00E+00 99	0.00E+00 99	0.00E+00 99	0.00E+00 99	0.00E+00 99	0.00E+00 99	0.00E+00 99	0.00E+00 99
195.500-156.400	0.00E+00 99	0.00E+00 99	0.00E+00 99	0.00E+00 99	0.00E+00 99	0.00E+00 99	0.00E+00 99	0.00E+00 99	0.00E+00 99
156.400-117.300	0.00E+00 99	0.00E+00 99	0.00E+00 99	0.00E+00 99	0.00E+00 99	0.00E+00 99	0.00E+00 99	0.00E+00 99	0.00E+00 99
117.300- 78.200	0.00E+00 99	0.00E+00 99	0.00E+00 99	0.00E+00 99	0.00E+00 99	0.00E+00 99	0.00E+00 99	0.00E+00 99	0.00E+00 99
78.200- 39.100	0.00E+00 99	0.00E+00 99	0.00E+00 99	0.00E+00 99	3.30E-00 99	1.35E-00 99	1.19E-00 99	0.00E+00 99	0.00E+00 99
39.100- 1.803	0.00E+00 99	4.70E-05 45	4.32E-04 12	8.11E-04 7	4.08E-04 11	1.79E-04 8	2.23E-05 14	2.55E-06 71	0.00E+00 99

ENERGY SPECTRA AND ANGULAR DISTRIBUTIONS OF ELECTRONS LATERALLY ESCAPING
AZIMUTHAL INTERVAL IS 0.00000 TO 180.00000 DEGREES
(NUMBER/(MEV*SR), NORMALIZED TO ONE PARTICLE)

E (MEV)	THETA = 150.000 180.000
391.8000 - 351.8000	0.00E+00 99
351.8000 - 312.8000	0.00E+00 99
312.8000 - 273.7000	0.00E+00 99
273.7000 - 234.6000	0.00E+00 99
234.6000 - 195.5000	0.00E+00 99
195.5000 - 156.4000	0.00E+00 99
156.4000 - 117.3000	0.00E+00 99
117.3000 - 78.2000	0.00E+00 99
78.2000 - 39.1000	0.00E+00 99
39.1000 - 1.8030	0.00E+00 99

APPENDIX B. INTERACTIVE DATA LANGUAGE (IDL) DATA MANIPULATION AND PLOTTING PROGRAM

IDL is a programming language commercially available from Research Systems Incorporated that is capable of being used in a wide variety of computing and graphics applications. In this work the IDL language was used to write a relatively user-friendly program that performs basic functions necessary to extract data from the standard ITS/CYLTRAN formatted output files, rearrange the data into proper data structures for plotting, and plot the data on a selected device. There is no substitute for reading the IDL user manuals as an education in how to use the language, however, the following is a user's guide to using the analysis and plotting program written for this work.

A. RUNNING IDL AND EXECUTING PROGRAMS

The IDL compiler is an interactive program that is installed on the VAXStation 3200 in the directory IDL.DIR. All IDL commands are compiled as they are entered, whether they are entered directly into the compiler from the terminal or as a batch stream from a command file, or program. In this respect, then, IDL runs in a mode very similar to PC Basic. To invoke the IDL compiler after logging on to a user account, type "IDL". Some licensing

information will be printed on the screen and the prompt "IDL>" will appear. At this point, IDL commands may be entered and compiled directly from the terminal. The point of entering commands this way is that the powerful capabilities of the language (which can be appreciated by reviewing the commands and what they can do) can be used without a lot of programming effort.

A complicated series of IDL commands, such as the ones necessary to manipulate the large CYLTRAN output files, should be typed into a command file. The format of the commands is the same as if they were entered interactively, but they are put in a text file using the text editor available with the VAXStation 3200 (called EVE). After constructing the command file, save it with a name ending in the file extension ".PRO", for example MY_PROGRAM.PRO.

To run an IDL program saved in a text file, type the IDL executive command ".run MY_PROGRAM.PRO". The IDL compiler will compile and execute the program.

Output from the program can be displayed on one of several devices with great ease. To display a plot on the monitor, the command "SET_PLOT, 'X' " should be entered prior to the PLOT command, which generates the plot itself. X (for X-windows) is the default output device. To plot a drawing on a Hewlett-Packard plotter which uses the HPGL language, enter " SET_PLOT, 'HP' " prior to the PLOT command.

B. RUNNING PLOT.PRO TO ANALYZE CYLTRAN OUTPUT

The name of the IDL program written to analyze the formatted output generated by CYLTRAN in this work is PLOT.PRO. The main program calls the three procedures (which is the IDL name for a subroutine) called READ.PRO, PLOTDATA.PRO, and REFDOSE.PRO. The IDL command code for these four command procedures are located each in separate text files of the same names. To run the program, all four of these files must be in the user's directory (they don't actually have to be in the user's directory, per se, but the user must be able to tell the IDL compiler where to look for them, and the IDL compiler must be able to access them).

To execute the program PLOT.PRO, at the IDL> prompt, type the command " .run PLOT.PRO ". This assumes that all four of the program files are in the user's root directory. IDL will compile and execute the plotting program.

As the program is executing, it will prompt the user, either through the terminal command window or by a mouse menu window, for input or choices. If the user knows the name of the CYLTRAN output file, the answers to some elementary questions about the problem geometry and CYLTRAN input zones, what kind of output he wants, and what device he wants it on, the use of the program should be self-explanatory.

The data reading portion of the program is generally applicable. That is, the PLOT.PRO procedure should be able

to read most of the data usually of interest from any CYLTRAN output file, regardless of the problem material, geometry, of number of input zones. This capability is a tremendous asset in itself, because the user has the ability to halt the program after it reads the data and to enter commands interactively to plot or manipulate the data in any manner desired. However, if the program is used for graphics output on any CYLTRAN problem that deviates even in a small way from the geometry of this work (cylindrical with annular arrays of TLD's radially dispersed at regular longitudinal intervals) the results cannot be guaranteed. Proceed with caution.

More comments on the specific use and purpose of each portion of the program are included in the source code documentation for the program itself. The user is encouraged to read through the source code briefly before running the program.

```
;*********************************************************************
;begin main program
;*********************************************************************
COMMON PLOT,
   modules,zones,radius,zfact,aigap,series,series1,series2,series3,$
   series4,series5,series6,struc2,elect_energy,target,ref,ref1,ref2,$
   ref3,ref4,refpts,acceptx1,accepty1,acceptx2,accepty2,$
   acceptx3,accepty3,acceptx4,accepty4,zstart,geochoice,choice,$
   plotchoice,radnum,maxval,minval,file,cmd,choice2,struc1,$
   flag,title,filename,card,tempstruc,zonetemp,temp1,lowmult,temp2,$
   eflag,i,j,k,zone
  zones=0 &title=''
  choice=0
  struc1={zone,number:0,mat:0,zleft:0.0,zright:0.0,rin:0.0,rout:0.0,$
          elcut:0.0,photcut:0.0,mass:0.0,volume:0.0,energy:fltarr(8)}
  struc2={annzone,number:0,mat:0,zleft:0.0,zright:0.0,rin:0.0,rout:0.0,$
      elcut:0.0,photcut:0.0,mass:0.0,volume:0.0,energy:fltarr(8), $
```

```
        radius:0.0,Z:0.0,zfact:0.0,dose:fltarr(8)}
;This is the main menu section
   flag=0
   while flag EQ 0 do begin
        choice=wmenu(['ITS GRAPHICS ROUTINE','Process a set of data',$
            'Produce a standard plot','Exit'],Title=0)
        case choice of
           1: readdata
           2: plotdata
           3: flag=1
        endcase
   endwhile
print,'Type .continue to halt the program '
print,' or enter interactive IDL commands.'
stop
end
PRO readdata
;
;This procedure should be able to read any output file produced by the
;CYLTRAN ITS code. It may even be able to read ACCEPT output files,
;but its ability to do so has not been tested.
;
COMMON PLOT,
    modules,zones,radius,zfact,aigap,series,series1,series2,series3,$
    series4,series5,series6,struc2,elect_energy,target,ref,ref1,ref2,$
    ref3,ref4,refpts,acceptx1,accepty1,acceptx2,accepty2,$
    acceptx3,accepty3,acceptx4,accepty4,zstart,geochoice,choice,$
    plotchoice,radnum,maxval,minval,file,cmd,choice2,struc1,$
    flag,title,filename,card,tempstruc,zonetemp,temp1,lowmult,temp2,$
    eflag,i,j,k,zone
    filename='' &title='' &zones=0 &i=0 &j=0 &k=0 &eflag=0
    card=''
    print, 'Type the name of the ITS output file '
    print, format= '("  e.g. [jones.directory]cyl50.out;1 ",$) '
    read, filename
    openr, 1, filename
    for i=0,14 do readf,1,card
    WHILE NOT EOF(1) DO BEGIN
        readf, 1, card    ;begin reading data
        ;look for key headings
        if strmid(card,0,5) eq '1****' then begin
           readf, 1, card
           ;find the number of zones and the zone geometry data
           ;and read them
           if strmid(card,5,24) eq 'GEOMETRY DEPENDENT INPUT' $
           then begin
              readf, 1, card
              ;read the number of zones
              readf, 1, format='(24x,I5)', zones
              zone=replicate(struc1,zones)
              ;create a structure for each input zone
```

```
        tempstruc={zonetemp,number:0.0,mat:0.0,zleft:0.0,$
            zright:0.0,rin:0.0,rout:0.0,elcut:0.0,photcut:0.0 }
            zonetemp=replicate(tempstruc,zones)
;This section reads in zone geometry data for any number of zones.
;The number of zones is read from the ITS output file.
            for i=0,2 do readf,1,card
            readf,1,zonetemp
            zone.number=zonetemp.number
            zone.mat=zonetemp.mat
            zone.zleft=zonetemp.zleft
            zone.zright=zonetemp.zright
            zone.rin=zonetemp.rin
            zone.rout=zonetemp.rout
            zone.elcut=zonetemp.elcut
            zone.photcut=zonetemp.photcut
          endif
;find the title
          if strmid(card,0,5) eq ' *   ' then begin
            readf,1,card
            if strmid(card,0,5) eq ' *   ' then $
              title=strmid(card,5,74)
          endif
        endif
;find the energy data and read it into the structure
        if (strtrim(strmid(card,1,69),1) eq 'ENERGY DEPOSITION') $
          and (eflag EQ 0) then begin
;This section reads in energy deposition data for 800-849 zones.
;To read for more or fewer zones, you must change the size of
;the structure accordingly, i.e. to read 659 zones, set the value
;of "lowmult" to 650 or ,in general, it should be x, the nearest
;lower multiple of 50. Also, the upper limit on j is automatically
;set equal to that number divided by 50 minus 1, e.g. 650/50-1,
;so j=0,12
      tempstruc1={zonetemp1,number:0.0,mat:0.0,mass:0.0,volume:0.0, $
                        energy:fltarr(8)}
      temp1=replicate(tempstruc1,50)
      print,'*********************************************'
      print,' The parameter "lowmult" should be set to the '
      print,' nearest lower multiple of 50 to the number of '
      print,' input zones in the problem. '
      print,' '
      print, format= '(" Type the value of lowmult:",$)'
      read, lowmult
      temp2=replicate(tempstruc1,zones-lowmult)
      for i=0,2 do readf,1,card
      for j=0,fix(lowmult/50.0-1.0) do begin
            readf,1,temp1
            zone(j*50:j*50+49).number=temp1.number
            zone(j*50:j*50+49).mat=temp1.mat
            zone(j*50:j*50+49).mass=temp1.mass
            zone(j*50:j*50+49).volume=temp1.volume
```

```
            zone(j*50:j*50+48).energy=temp1.energy
            for i=0,3 do readf,1,card
        endfor
        readf,1,temp2
        zone(lowmult:zones-1).number=temp2.number
        zone(lowmult:zones-1).mat=temp2.mat
        zone(lowmult:zones-1).mass=temp2.mass
        zone(lowmult:zones-1).volume=temp2.volume
        zone(lowmult:zones-1).energy=temp2.energy
        eflag=1
      endif
    ENDWHILE
    print, 'End of data file reached'
    return
end

PRO plotdata
;
;This procedure is written to produce plots for the specific
;CYLTRAN geometry being studied in the thesis by RN Yaw. It will
;probably not produce meaningful graphics for any other
;configuration, although any other program for plotting
;ITS output will probably be similar to this.
;
COMMON PLOT
   modules,zones,radius,zfact,airgap,series,series1,series2,series3,$
   series4,series5,series6,struc2,elect_energy,target,ref,ref1,ref2,$
   ref3,ref4,refpts,acceptx1,accepty1,acceptx2,accepty2,$
   acceptx3,accepty3,acceptx4,accepty4,zstart,geochoice,choice,$
   plotchoice,radnum,maxval,minval,file,cmd,choice2,struc1,$
   flag,title,filename,card,tempstruc,zonetemp,temp1,lowmult,temp2,$
   eflag,i,j,k,zone
;The parameter modules must be set to describe the number of sets
;of annular rings used in the problem, i.e. 6 (78 zones),
;63 (756 zones), 69 (828 zones), 55 (660 zones), etc
      &i=0 &j=0 &choice=0 &choice1=0
      print, '************************************************'
      print, format= '(" Type the number of detector $
            modules present:",$)'
      read, modules
      Z=fltarr(zones)
      radius=0.0
      zfact=0.0
      airgap=0.0
      series=replicate(struc2,modules)
      series1=series &series2=series &series3=series &series4=series
      series5=series &series6=series
      print, '************************************************'
      print, format= '(" What is the average electron energy in$
            MeV?",$)'
      read, elect_energy
```

```
      print, '*********************************************'
;
;This section takes note of the target materials being used and
;assigns values to the doses obtained by experiment at Bates-MIT
;so that a reference line can be plotted against ITS calculations
;
      target=0

      zstart=0.0
      ref_dose
;*****************************************************************************;The following loop assigns zone data to 6
separate structures;
;one for each radius at which dose is measured. The index i counts
;through the number of input zones present at each radius. This is
;different for each geometry. The upper limit of i is
;(zones-unmeasured zones)/#annular rings - 1
;For series of 6 LiF detectors with no intermediate target zones i=0,5
;For 756 input zones, no LiF detectors, i=0,62
;For 828 input zones, with 6 LiF detectors, i=0,68
;For 660 input zones, with 5 LiF detectors, i=0,54
;In any case, the upper limit on i is modules-1
;*****************************************************************************
      geochoice=" "
      print, '*********************************************************************'
      print, ' Are there any target sections between detector$
          rings for which'
      print, format= '("  the dose will not be plotted? y or n:",$) '
      read, geochoice
      print,'*****************************************************'
      for i=0,modules-1 do begin
        for j=0,N_TAGS(zone)-1 do begin
          if (geochoice eq "y") then begin
            series1(i).(j)=zone(1+i*13).(j)
            series2(i).(j)=zone(3+i*13).(j)
            series3(i).(j)=zone(5+i*13).(j)
            series4(i).(j)=zone(7+i*13).(j)
            series5(i).(j)=zone(9+i*13).(j)
            series6(i).(j)=zone(11+i*13).(j)
            series1(i).Z=Z(1+i*13)
            series2(i).Z=Z(3+i*13)
            series3(i).Z=Z(5+i*13)
            series4(i).Z=Z(7+i*13)
            series5(i).Z=Z(9+i*13)
            series6(i).Z=Z(11+i*13)
          endif else begin
            series1(i).(j)=zone(i*12).(j)
            series2(i).(j)=zone(2+i*12).(j)
            series3(i).(j)=zone(4+i*12).(j)
            series4(i).(j)=zone(6+i*12).(j)
            series5(i).(j)=zone(8+i*12).(j)
            series6(i).(j)=zone(10+i*12).(j)
```

```
            series2(i).z=z(2+i*12)
            series3(i).z=z(4+i*12)
            series4(i).z=z(6+i*12)
            series5(i).z=z(8+i*12)
            series6(i).z=z(10+i*12)
          endelse
          series1(i).zfact=(series1(i).mass/series1(i).volume)* $
              (series1(i).zright-series1(i).zleft)
          series1(i).dose=series1(i).energy/series1(i).mass
          series2(i).zfact=(series2(i).mass/series2(i).volume)* $
              (series2(i).zright-series2(i).zleft)
          series2(i).dose=series2(i).energy/series2(i).mass
          series3(i).zfact=(series3(i).mass/series3(i).volume)* $
              (series3(i).zright-series3(i).zleft)
          series3(i).dose=series3(i).energy/series3(i).mass
          series4(i).zfact=(series4(i).mass/series4(i).volume)* $
              (series4(i).zright-series4(i).zleft)
          series4(i).dose=series4(i).energy/series4(i).mass
          series5(i).zfact=(series5(i).mass/series5(i).volume)* $
              (series5(i).zright-series5(i).zleft)
          series5(i).dose=series5(i).energy/series5(i).mass
          series6(i).zfact=(series6(i).mass/series6(i).volume)* $
              (series6(i).zright-series6(i).zleft)
          series6(i).dose=series6(i).energy/series6(i).mass
        endfor
      endfor
      series1(0).z=series1(0).zfact
      series2(0).z=series2(0).zfact
      series3(0).z=series3(0).zfact
      series4(0).z=series4(0).zfact
      series5(0).z=series5(0).zfact
      series6(0).z=series6(0).zfact
      for i=1,modules-1 do begin
        series1(i).z=series1(i-1).z+series1(i).zfact
        series2(i).z=series2(i-1).z+series2(i).zfact
        series3(i).z=series3(i-1).z+series3(i).zfact
        series4(i).z=series4(i-1).z+series4(i).zfact
        series5(i).z=series5(i-1).z+series5(i).zfact
        series6(i).z=series6(i-1).z+series6(i).zfact
        endfor
      series1.radius=0.0
      series2.radius=1.0
      series3.radius=2.0
      series4.radius=5.0
      series5.radius=10.0
      series6.radius=20.0
loop: choice=wmenu(['Select a plot -',$
        'Total dose - all radii, Z in g/cm2', $
        'Total dose - all radii, Z in cm',$
        'Breakdown by electron type - one radius',$
        'Stop and Make a Custom Plot','Exit'], Title=0)
```

```
      case choice of
        1: begin
; This section does a plot of energy deposition versus Z for all
; radii with Z given in grams per square centimeter
; allow a choice of output graphics devices
             plotchoice=wmenu($
               ['Choose a graphics device -','X-windows', $
                'HPGL','PCL','Postscript'],Title=0)
             case plotchoice of
               1: set_plot,'X'
               2: set_plot,'HP'
               3: set_plot,'PCL'
               4: set_plot,'PS'
             endcase
; plot the Bates data for reference
             if (target eq 5) then begin
               ;there are only 3 reference lines
               ; given in data for this target
               plot_io,ref2.z,ref2.dose,title=strtrim(title),$
                   ytitle='Dose (MeV/kg)',$
                   xtitle='Longitudinal Distance (g/cm2)',$
                   yrange=[1.0e-08,1.0e+02], $
                   xrange=[0,max(ref2.z+10)],psym=8
               oplot,ref2.z,ref2.dose,color=3
               xyouts,ref2.z(refpts-1)+1.5,$
                     ref2.dose(refpts-1),'r=2.0cm'
             endif else begin
               plot_io,ref1.z,ref1.dose,title=strtrim(title),$
                   ytitle='Dose (MeV/kg)',$
                   xtitle='Longitudinal Distance (g/cm2)',$
                   yrange=[.0000001,max(ref1.dose)], $
                   xrange=[0,max(ref1.z+10)],psym=8
               oplot,ref1.z,ref1.dose,color=3
               xyouts,ref1.z(refpts-1)+1.5,$
                     ref1.dose(refpts-1),'r=0.0cm'
               oplot,ref2.z,ref2.dose,psym=8
               oplot,ref2.z,ref2.dose,color=3
               if (target eq 4) then $
                 xyouts,ref2.z(refpts-1)+1.5,$
                       ref2.dose(refpts-1),'r=2.0cm' $
               else $
                 xyouts,ref1.z(refpts-1)+1.5,$
                       ref1.dose(refpts-1),'r=1.0cm'
             endelse
             oplot,ref3.z,ref3.dose,psym=8
             oplot,ref3.z,ref3.dose,color=3
             xyouts,ref3.z(refpts-1)+1.5,$
                   ref3.dose(refpts-1),'r=5.0cm'
             oplot,ref4.z,ref4.dose,psym=8
             oplot,ref4.z,ref4.dose,color=3
             xyouts,ref4.z(refpts-1)+1.5,$
```

```
                ref4.dose(refpts-1),'r=20.0cm'
            x=[10,18]
            y=[6.0e-08,6.0e-08]
            if (target eq 5) then y=[2.0e-07,2.0e-07]
            xyouts,x(1)+1,0.9*y(1),'Bates data'
            oplot,x,y,color=3
;plot the calculated doses
;if target is 4-PMMA/air/1-PMMA,there are only 3 reference lines
;given in the data for the target, so don't plot series1
            if (target ne 5) then $
               oplot,series1.z,series1.dose(6),psym=1
            if (target eq 4) or (target eq 5) then $
               oplot,series3.z,series3.dose(6),psym=2 $
            else oplot,series2.z,series2.dose(6),psym=2
            oplot,series4.z,series4.dose(6),psym=4
            oplot,series8.z,series8.dose(6),psym=5
           end
        2: begin
;This section does a plot of energy deposition versus Z for all radii
;with Z given in centimeters
;
;allow a choice of output graphics devices
           plotchoice=wmenu($
              ['Choose a graphics device -','X-windows', $
              'HPGL','PCL','Postscript'],Title=0)
           case plotchoice of
              1: set_plot,'X'
              2: set_plot,'HP'
              3: set_plot,'PCL'
              4: set_plot,'PS'
           endcase
;plot the Bates data for reference
            if (target eq 5) then begin
              ;there are only 3 reference lines
              ;given in data for this target
               plot_io,ref2.zright,ref2.dose,title=strtrim(title),$
                 ytitle='Dose (MeV/kg)',$
                 xtitle='Longitudinal Distance (cm)',$
                 yrange=[1.0e-08,1.0e+02], $
                 xrange=[0,max(ref2.zright)],psym=6
               xyouts,ref2.zright(refpts-1)+1.5,$
                     ref2.dose(refpts-1),'r=2.0cm'
            endif else begin
              plot_io,ref1.zright,ref1.dose,title=strtrim(title),$
                ytitle='Dose (MeV/kg)',$
                xtitle='Longitudinal Distance (cm)',$
                yrange=[.0000001,max(ref1.dose)], $
                xrange=[0,max(ref1.zright)],psym=6
              xyouts,ref1.zright(refpts-1)+.05,$
                     ref1.dose(refpts-1),'r=0.0cm'
              oplot,ref2.zright,ref2.dose,psym=6
```

```
            if (elect_energy eq 391.0) then begin
              oplot,acceptx1,accepty1,linestyle=2
              oplot,acceptx2,accepty2,linestyle=2
            endif
            if (target eq 4) or (target eq 5) then $
              xyouts,ref2.zright(refpts-1)+.05,$
                    ref2.dose(refpts-1),'r=2.0cm'  $
            else $
              xyouts,ref2.zright(refpts-1)+.05,$
                    ref2.dose(refpts-1),'r=1.0cm'
          endelse
          oplot,ref3.zright,ref3.dose,psym=6
          xyouts,ref3.zright(refpts-1)+.05,ref3.dose(refpts-1),$
                'r=5.0cm'
          oplot,ref4.zright,ref4.dose,psym=6
          xyouts,ref4.zright(refpts-1)+.05,ref4.dose(refpts-1),$
                'r=20.0cm'
          x=[16,16]
          y=[1.0e-07,1.0e-07]
          if (target eq 5) then y=[2.0e-07,2.0e-07]
          xyouts,x(1)+2,0.6*y(1),'Bates data'
          oplot,x,y,psym=6 ;,color=3
          oplot,[x(1)-10,x(1)],[0.5*y(1),0.5*y(1)]
          xyouts,x(1)+2,0.45*y(1),'Present CYLTRAN Model'
          if (target ne 5) and (elect_energy eq 391.0) then begin
            oplot,acceptx3,accepty3,linestyle=2
            oplot,acceptx4,accepty4,linestyle=2
            oplot,[x(1)-10,x(1)],[0.25*y(1),0.25*y(1)],$
                  linestyle=2
            xyouts,x(1)+2,0.2*y(1),'Bates ACCEPT Model'
          endif
;plot the calculated doses
;if target is 4-PMMA/air/1-PMMA,there are only 3 reference lines
;given in the data for the target, so don't plot series1
          if (target ne 5) then $
            oplot,series1.zright,series1.dose(6) ;,psym=1
          if (target eq 4) or (target eq 5) then $
            oplot,series3.zright,series3.dose(6)  $
          else oplot,series2.zright,series2.dose(6)
          oplot,series4.zright,series4.dose(6)
          oplot,series6.zright,series6.dose(6)
        end
      3: begin
;
;This section does a plot of the energy deposition calculated at a
;chosen radius. The total energy deposited is plotted over the values
;for deposition by each type of electron (i.e. primary, secondary,
;and knockons)
;
          choice1=wmenu(['What radius will you plot?','0.0cm', $
            '1.0cm','2.0cm','5.0cm','10.0cm','20.0cm',$
```

```
            'Exit'],Title=0)
          case choice1 of
           1: begin &series=series1 &radius=0.0 &end
           2: begin &series=series2 &radius=1.0 &end
           3: begin &series=series3 &radius=2.0 &end
           4: begin &series=series4 &radius=5.0 &end
           5: begin &series=series5 &radius=10.0 &end
           6: begin &series=series6 &radius=20.0 &end
          endcase
;allow a choice of output graphics devices
          plotchoice=wmenu($
            ['Choose a graphics device -','X-windows', $
            'HPGL','PCL','Postscript'],Title=0)
          case plotchoice of
            1: set_plot,'X'
            2: set_plot,'HP'
            3: set_plot,'PCL'
            4: set_plot,'PS'
          endcase
          radnum=string(radius)
          maxval=max(series.dose) &minval=min(series.dose)
          plot_io,series.z,series.dose(0),$
        title=strtrim(title)+'!CRadius='+strmid(radnum,4,5)+$
              'cm',$
            ytitle='Dose (MeV/kg)',$
            xtitle='Longitudinal Distance (g/cm2)',$
            yrange=[minval,maxval],$
            xrange=[0,60],ymargin=[4,4]
          xyouts,series(5).z+2,series(5).dose(0),'Primary'
          oplot,series.z,series.dose(2)
          xyouts,series(5).z+2,series(5).dose(2),'Knock-ons'
          oplot,series.z,series.dose(4)
          xyouts,series(5).z+2,series(5).dose(4),'G-sec'
          oplot,series.z,series.dose(6)
          xyouts,series(5).z+2,series(5).dose(6),'Total'
        end
      4: begin
;allow a choice of output graphics devices
          plotchoice=wmenu($
            ['Choose a graphics device -','X-windows', $
            'HPGL','PCL','Postscript'],Title=0)
          case plotchoice of
            1: set_plot,'X'
            2: set_plot,'HP'
            3: set_plot,'PCL'
            4: set_plot,'PS'
          endcase
          ;allow user to make a custom plot with processed
          ;data file
          stop
        end
```

```
      endcase
      if (plotchoice eq 1) then i=1
;if the device is a hardcopy device, give the option of producing
;hardcopy
      if (plotchoice eq 2) or (plotchoice eq 3) or $
        (plotchoice eq 4) then $
         i=2
      case i of
        1: print,'CONTINUING IN X-WINDOWS MODE'
        2: begin
hard:       set_plot,'x'
           hardcopy=wmenu(['Hardcopy Options',$
              'Produce a Hardcopy on the Plotter',$
              'Make an addition to the plot','No Hardcopy'],$
            title=0)
           case hardcopy of
             1: begin
                set_plot,'hp'
                device,/close
                file='idl.' + strlowcase(!d.name)
                cmd = 'copy ' + file + ' csa0:'
                spawn, cmd
                set_plot,'x'
                end
             2: begin
           print, '*** Enter any additional plot annotations$
                  interactively.*'
           print, '*** Type .continue to continue the program. ***'
                stop
                goto, hard
                end
             3: begin
                set_plot,'hp'
                device,/close
                end
           endcase
         end
      endcase
   print,'**** Type .continue to halt the program   ****'
   print,'****    or enter interactive IDL commands.****'

   stop
   set_plot,'X'
   choice2=wmenu(['Make a choice!',$
        'Make another plot with current data', $
        'Return to main menu','Exit'],Title=0)
   case choice2 of
       1: goto, loop
       2: return
   endcase
end
```

```
PRO ref_dose
;
  COMMON PLOT
    modules,zones,radius,zfact,aigap,series,series1,series2,series3,$
    series4,series5,series6,struc2,elect_energy,target,ref,ref1,ref2,$
    ref3,ref4,refpts,acceptx1,accepty1,acceptx2,accepty2,$
    acceptx3,accepty3,acceptx4,accepty4,zstart,geochoice,choice,$
    plotchoice,radnum,maxval,minval,file,cmd,choice2,struc1,$
    flag,title,filename,card,tempstruc,zonetemp,temp1,lowmult,temp2,$
    eflag,i,j,k,zone
  target=wmenu(['What is the Target? ', $
       'Aluminum', 'Lead Followed by Aluminum' ,$
       'PMMA (Lucite)',$
       '1-PMMA, Air Gap, 4-PMMA','4-PMMA, Air Gap, 1-PMMA'], Title=0)
  case target of
      1: begin                    ;for Aluminum target
           ref={reference,z:fltarr(5),zright:fltarr(5),radius:0.0,$
                dose:fltarr(5) }
           ref1=ref &ref2=ref &ref3=ref &ref4=ref
           refpts=5
           acceptx1=fltarr(refpts)  &accepty1=fltarr(refpts)
           acceptx2=fltarr(refpts)  &accepty2=fltarr(refpts)
           acceptx3=fltarr(refpts)  &accepty3=fltarr(refpts)
           acceptx4=fltarr(refpts)  &accepty4=fltarr(refpts)
           ref1.z=[11.50,24.50,38.00,51.50,66.50]
           ref1.radius=0.0
           ref1.zright=[4.56,9.68,14.88,20.28,26.14]
           ref2.z=ref1.z
           ref2.zright=ref1.zright
           ref2.radius=1.0
           ref3.z=ref1.z
           ref3.zright=ref1.zright
           ref3.radius=5.0
           ref4.z=ref1.z
           ref4.zright=ref1.zright
           ref4.radius=20.0
           if (elect_energy eq 391.0) then begin
                ref1.dose=[19.0,6.5,2.4,1.2,0.6]
                acceptx1=ref1.zright
                accepty1=[20.0,5.4,2.1,1.1,0.65]
                ref2.dose=[3.2e-02,1.4e-01,2.3e-01,2.2e-01,1.5e-01]
                acceptx2=ref2.zright
                accepty2=[2.5e-02,.13,.32,0.25,0.14]
                ref3.dose=[1.1e-04,3.2e-04,8.5e-04,2.0e-03,2.5e-03]
                acceptx3=ref3.zright
                accepty3=[4.0e-04,2.9e-04,8.0e-04,1.8e-03,1.8e-03]
                ref4.dose=[1.8e-06,3.2e-06,5.0e-06,6.0e-06,8.0e-06]
                acceptx4=ref4.zright
                accepty4=[5.4e-06,1.8e-07,3.5e-06,5.5e-06,5.0e-06]
           endif
           if (elect_energy eq 200.0) then begin
```

```
        ref1.dose=[5.0,1.9,0.75,0.35,0.18]
        ref2.dose=[0.58,0.24,0.19,0.1,0.055]
        ref3.dose=[1.4e-04,4.3e-04,1.1e-03,1.9e-03,2.05e-03]
        ref4.dose=[3.3e-06,1.1e-05,1.3e-05,1.35e-05]
    endif
  end
2: begin      ;for Lead followed by Aluminum
    ref={reference,z:fltarr(5),zright:fltarr(5),radius:0.0,$
        dose:fltarr(5) }
    ref1=ref &ref2=ref &ref3=ref &ref4=ref
    refpts=5
    acceptx1=fltarr(refpts)  &accepty1=fltarr(refpts)
    acceptx2=fltarr(refpts)  &accepty2=fltarr(refpts)
    acceptx3=fltarr(refpts)  &accepty3=fltarr(refpts)
    acceptx4=fltarr(refpts)  &accepty4=fltarr(refpts)
    ref1.z=[10.9,25.0,38.0,51.0,67.1]
    ref1.zright=[1.29,6.81,11.93,17.05,23.32]
    ref1.radius=0.0
    ref2.z=ref1.z
    ref2.zright=ref1.zright
    ref2.radius=1.0
    ref3.z=ref1.z
    ref3.zright=ref1.zright
    ref3.radius=5.0
    ref4.z=ref1.z
    ref4.zright=ref1.zright
    ref4.radius=20.0
    if (elect_energy eq 391.0) then begin
      ref1.dose=[21.0,3.2,1.3,0.48,0.24]
      acceptx1=ref1.zright
      accepty1=[30.0,2.95,2.0,0.55,0.25]
      ref2.dose=[0.18,0.21,0.19,0.14,8.0e-02]
      acceptx2=ref2.zright
      accepty2=[0.2,0.3,0.24,0.13,0.1]
      ref3.dose=[4.5e-04,1.7e-03,2.5e-03,2.8e-03,2.8e-03]
      acceptx3=ref3.zright
      accepty3=[3.8e-04,2.2e-03,4.1e-03,5.5e-03,3.8e-03]
      ref4.dose=[5.0e-06,1.5e-05,2.0e-05,2.2e-05,2.1e-05]
      acceptx4=ref4.zright
      accepty4=[4.2e-06,1.3e-05,1.5e-05,7.8e-06,2.8e-06]
    endif
    if (elect_energy eq 200.0) then begin
      ref1.dose=[7.5,.80,.54,.34,.41]
      ref2.dose=[.26,.21,.10,.055,.03]
      ref3.dose=[5.8e-04,1.6e-03,2.0e-03,2.4e-03,2.0e-03]
      ref4.dose=[9.9e-06,1.7e-05,2.3e-05,2.5e-05,2.3e-05]
    endif
  end
  3: begin      ;for PMMA only
    ref={reference,z:fltarr(5),zright:fltarr(5),radius:0.0,$
        dose:fltarr(5) }
```

```
      ref1=ref &ref2=ref &ref3=ref &ref4=ref
      refpts=5
      acceptx1=fltarr(refpts)  &accepty1=fltarr(refpts)
      acceptx2=fltarr(refpts)  &accepty2=fltarr(refpts)
      acceptx3=fltarr(refpts)  &accepty3=fltarr(refpts)
      acceptx4=fltarr(refpts)  &accepty4=fltarr(refpts)
      ref1.z=[10.0,20.0,30.5,41.0,51.8]
      ref1.zright=[8.72,17.44,26.57,35.71,45.10]
      ref1.radius=0.0
      ref2.z=ref1.z
      ref2.zright=ref1.zright
      ref2.radius=1.0
      ref3.z=ref1.z
      ref3.zright=ref1.zright
      ref3.radius=5.0
      ref4.z=ref1.z
      ref4.zright=ref1.zright
      ref4.radius=20.0
      if (elect_energy eq 391.0) then begin
         ref1.dose=[19.0,4.8,1.7,0.75,0.21]
         acceptx1=ref1.zright
         accepty1=[19.0,2.9,1.5,0.6,.38]
         ref2.dose=[3.2e-02,1.4e-01,2.3e-01,2.2e-01,1.5e-01]
         acceptx2=ref2.zright
         accepty2=[5.8e-03,8.0e-02,0.29,0.30,0.70]
         ref3.dose=[5.0e-05,1.8e-04,4.9e-04,1.1e-03,1.7e-03]
         acceptx3=ref3.zright
         accepty3=[2.0e-05,5.4e-05,2.0e-03,2.4e-03,6.0e-03]
         ref4.dose=[2.0e-06,3.8e-06,5.1e-06,6.5e-06,7.1e-06]
         acceptx4=ref4.zright
         accepty4=[2.4e-08,1.0e-06,1.9e-06,6.0e-07,3.1e-06]
      endif
      if (elect_energy eq 200.0) then begin
         ref1.dose=[6.0,2.0,.85,.92,.68]
         ref2.dose=[.059,.22,.16,.09,.05]
         ref3.dose=[1.1e-04,4.4e-04,1.3e-03,3.2e-03,4.9e-03]
         ref4.dose=[1.2e-05,1.5e-05,1.7e-05,1.9e-05,2.0e-05]
      endif
   end
4: begin    ;1-PMMA followed by an air gap, followed by
            ;4-PMMA
      ref={reference,z:fltarr(6),zright:fltarr(6),radius:0.0,$
           dose:fltarr(6) }
      ref1=ref &ref2=ref &ref3=ref &ref4=ref
      refpts=6
      acceptx1=fltarr(refpts)  &accepty1=fltarr(refpts)
      acceptx2=fltarr(refpts)  &accepty2=fltarr(refpts)
      acceptx3=fltarr(refpts)  &accepty3=fltarr(refpts)
      acceptx4=fltarr(refpts)  &accepty4=fltarr(refpts)
      print,format='("Enter the length of the air gap in $
               cm -",$)'
```

```
      read, airgap
      ref1.z=[10.35,10.40,20.90,31.60,42.30,53.10]
      ref1.zright=[8.72,48.02,58.74,65.46,74.18,82.90]
      ref1.radius=0.0
      ref1.dose=[19.0,0.55,0.50,0.45,0.30,0.25]
      acceptx1=ref1.zright
      accepty1=[19.0,.25,.45,.32,.37,.28]
      ref2.z=ref1.z
      ref2.zright=ref1.zright
      ref2.radius=2.0
 ref2.dose=[1.6e-03,1.7e-02,2.6e-02,4.5e-02,5.0e-02,4.5e-02]
      acceptx2=ref2.zright
 accepty2=[3.2e-04,2.6e-02,6.0e-02,9.5e-02,7.0e-02,5.5e-02]
      ref3.z=ref1.z
      ref3.zright=ref1.zright
      ref3.radius=5.0
 ref3.dose=[2.6e-05,8.0e-04,8.5e-04,1.3e-03,2.5e-03,4.0e-03]
      acceptx3=ref3.zright
 accepty3=[4.0e-05,2.0e-03,2.2e-03,3.8e-03,7.5e-03,8.0e-03]
      ref4.z=ref1.z
      ref4.zright=ref1.zright
      ref4.radius=20.0
 ref4.dose=[4.5e-07,4.0e-05,7.0e-06,8.0e-06,1.0e-05,1.5e-05]
      acceptx4=ref4.zright
 accepty4=[2.1e-07,5.5e-05,1.0e-06,1.3e-05,2.0e-06,9.5e-06]
    end
5: begin   ;4-PMMA followed by an air gap, followed by 1-PMMA
      ref={reference,z:fltarr(6),zright:fltarr(6),radius:0.0,$
           dose:fltarr(6) }
      ref1=ref &ref2=ref &ref3=ref &ref4=ref
      refpts=6
      print,format='("Enter the length of the air gap in $
                cm -",$)'
      read, airgap
      ref1.z=[10.0,20.0,31.0,41.5,43.1,53.1]
      ref1.zright=[8.72,17.44,26.16,34.88,74.18,82.90]
      ref1.radius=0.0
      ref1.dose=[0.00,0.00,0.00,0.00,0.00,0.00]
      ref2.z=ref1.z
      ref2.zright=ref1.zright
      ref2.radius=2.0
ref2.dose=[1.6e-03,5.6e-03,1.6e-02,3.0e-02,2.1e-02,3.1e-02]
      ref3.z=ref1.z
      ref3.zright=ref1.zright
      ref3.radius=5.0
ref3.dose=[8.0e-05,2.7e-04,6.4e-04,1.5e-03,1.0e-02,1.1e-02]
      ref4.z=ref1.z
      ref4.zright=ref1.zright
      ref4.radius=20.0
ref4.dose=[2.8e-06,7.0e-06,8.1e-06,6.9e-06,2.9e-04,8.9e-05]
      end
```

```
    endcase
  return
end
```

APPENDIX C. SUPPLEMENTARY FIGURES

The supplementary figures are intended to enhance the discussion in chapter 3, but are not essential to understanding the results of this work. The figures begin on the following page.

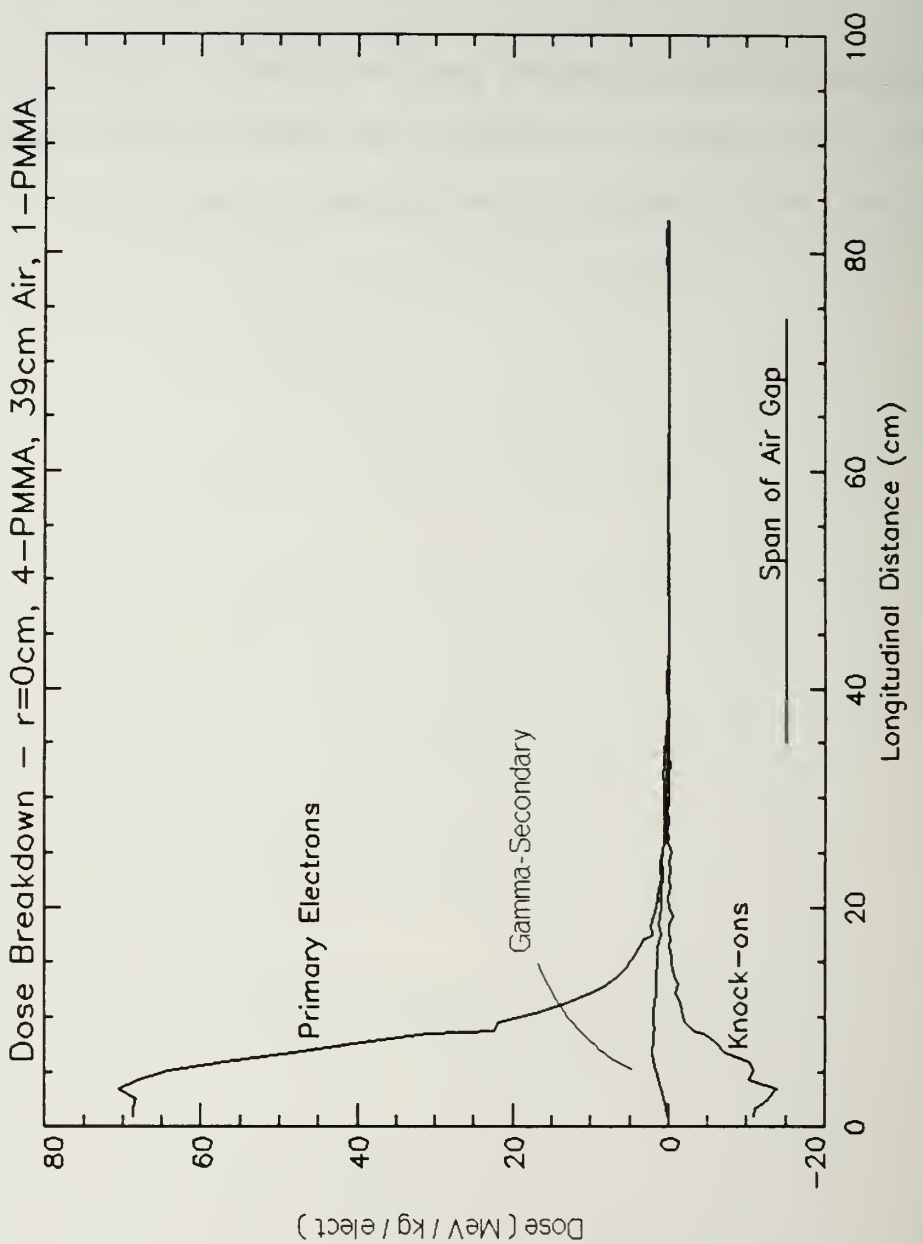

Figure C1. Dose Breakdown on Beam Axis for Target of Figure 11 w
10000 Electrons. On the centerline the dose is almost completely due
primary electrons. Note the lack of dose after a radiation length, wh
is 34.4 cm in PMMA.

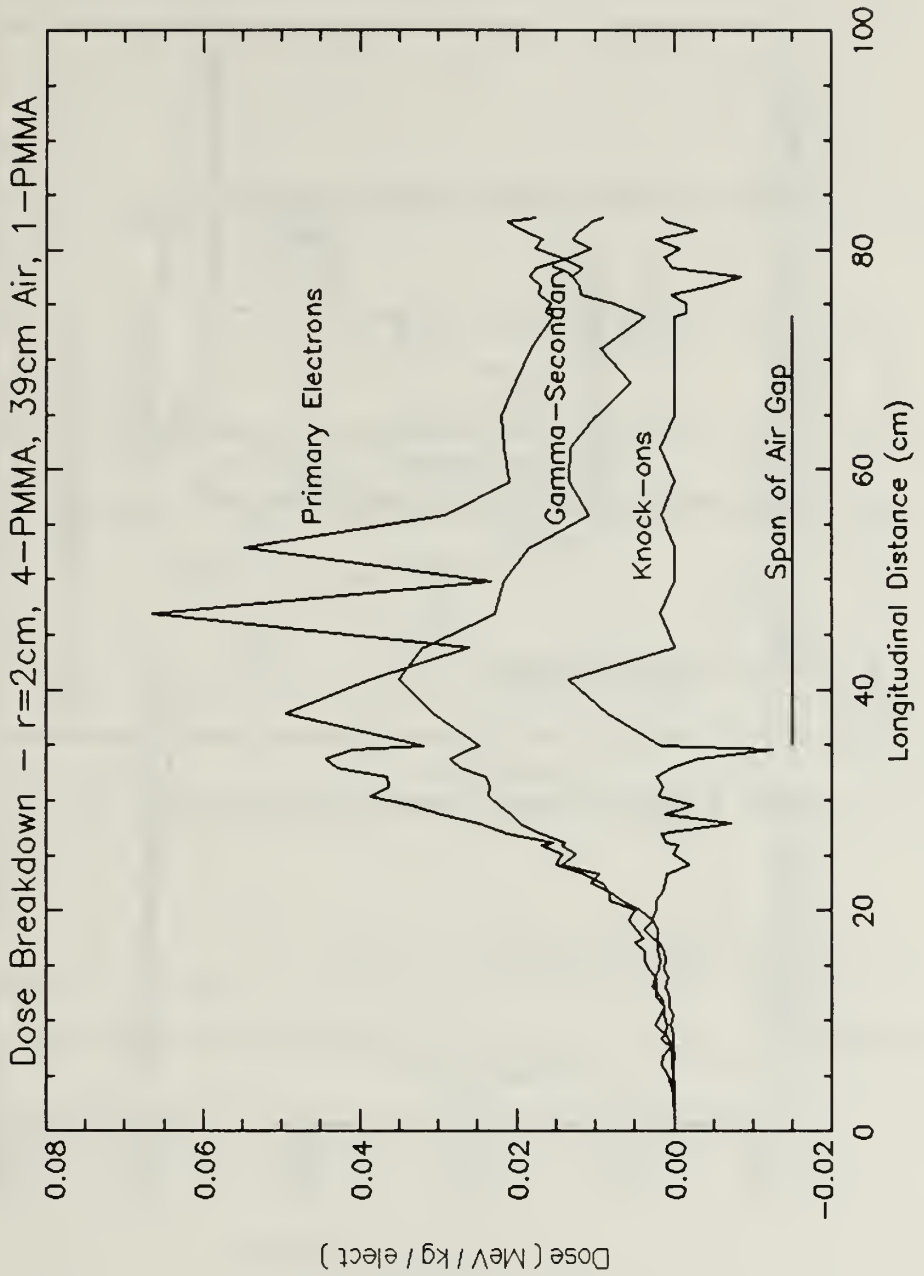

Figure C2. Dose Breakdown at 2cm Radius for Target of Figure 11 with 10,000 Electrons. There is very little energy deposited in the first 20cm. Note the reduction in scale from the previous figure, i.e the dose is reduced quickly off-axis.

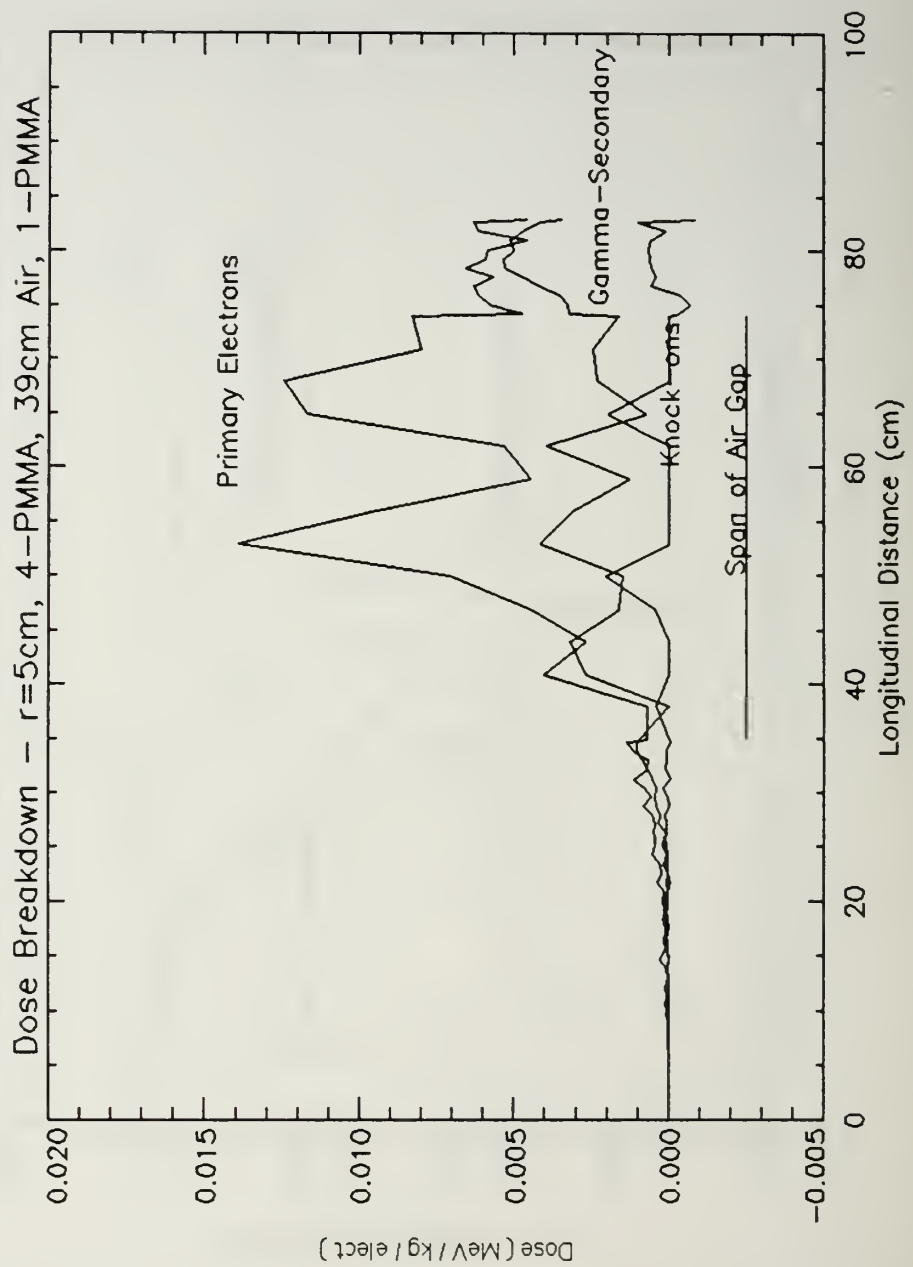

Figure C3. Dose Breakdown at 5cm Radius for Target of Figure 11 w
10,000 Electrons. Dose is negligible until electrons reach the air g
Photon processes obviously play a more important role off-axis.

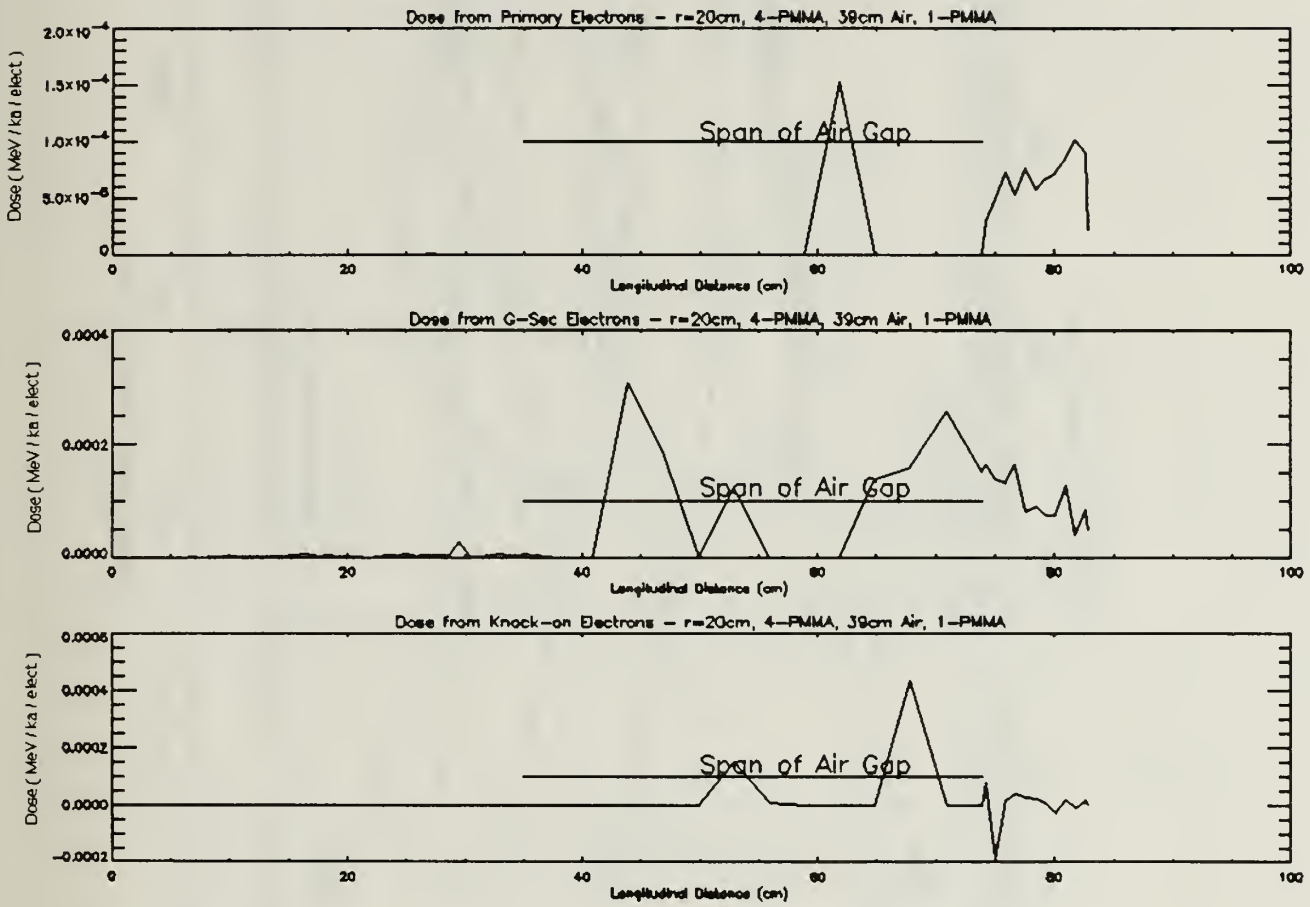
Dose from Primary Electrons – r=20cm, 4–PMMA, 39cm Air, 1–PMMA
Dose (MeV / kg / elect)
Span of Air Gap
Longitudinal Distance (cm)
Dose from G–Sec Electrons – r=20cm, 4–PMMA, 39cm Air, 1–PMMA
Dose (MeV / kg / elect)
Span of Air Gap
Longitudinal Distance (cm)
Dose from Knock–on Electrons – r=20cm, 4–PMMA, 39cm Air, 1–PMMA
Dose (MeV / kg / elect)
Span of Air Gap
Longitudinal Distance (cm)

Figure C4. Dose Breakdown at 20cm Radius for Target of Figure 11 with 10,000 Electrons. Note reduction in scale from previous figures. Also note that the dose from primary, gamma-secondary, and knock-on electrons is roughly equal.

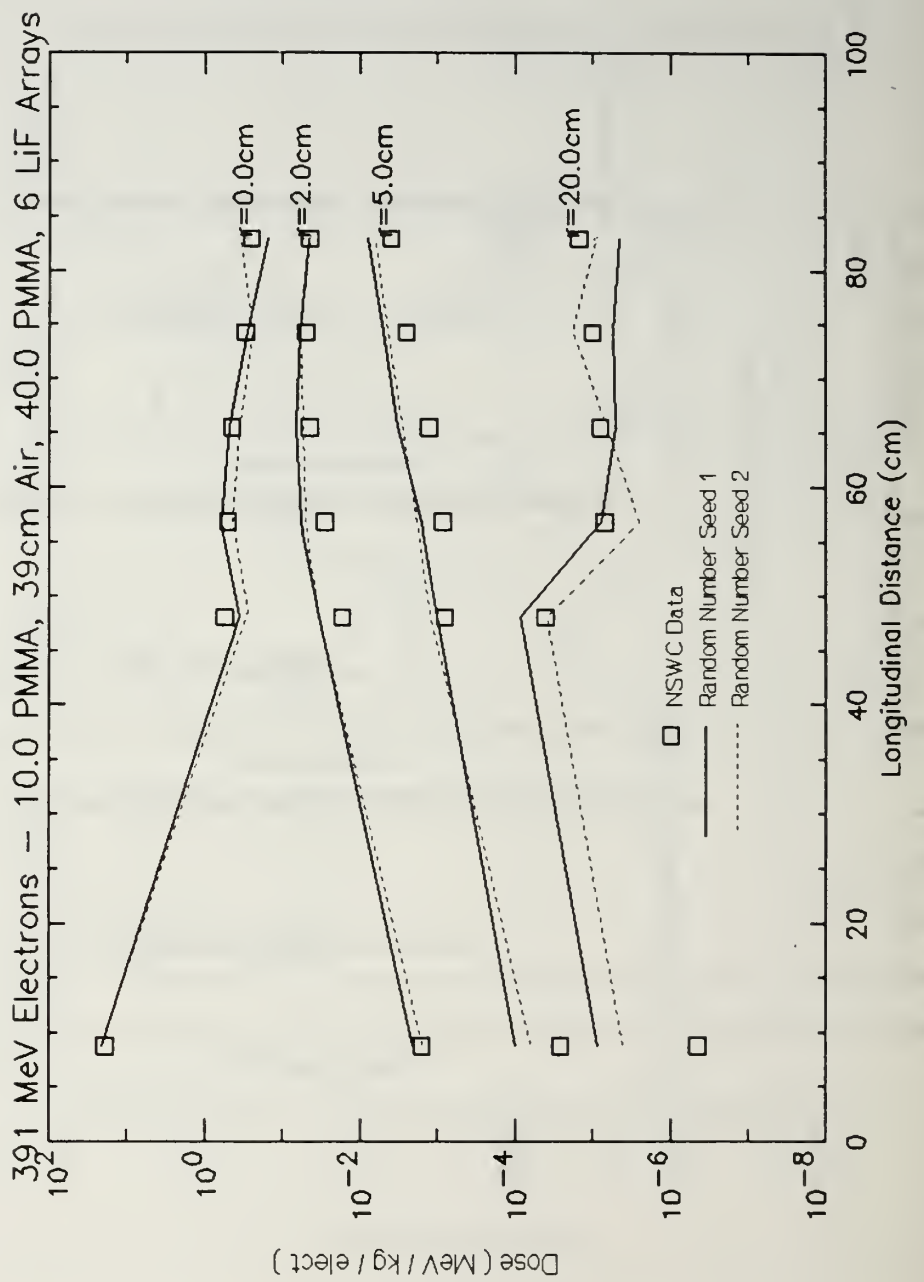

Figure C5. Low Resolution 391 MeV Dose Distribution for Target of Fig 4. Comparison of CYLTRAN calculations using 2 different random num seeds, all other parameters remaining the same.

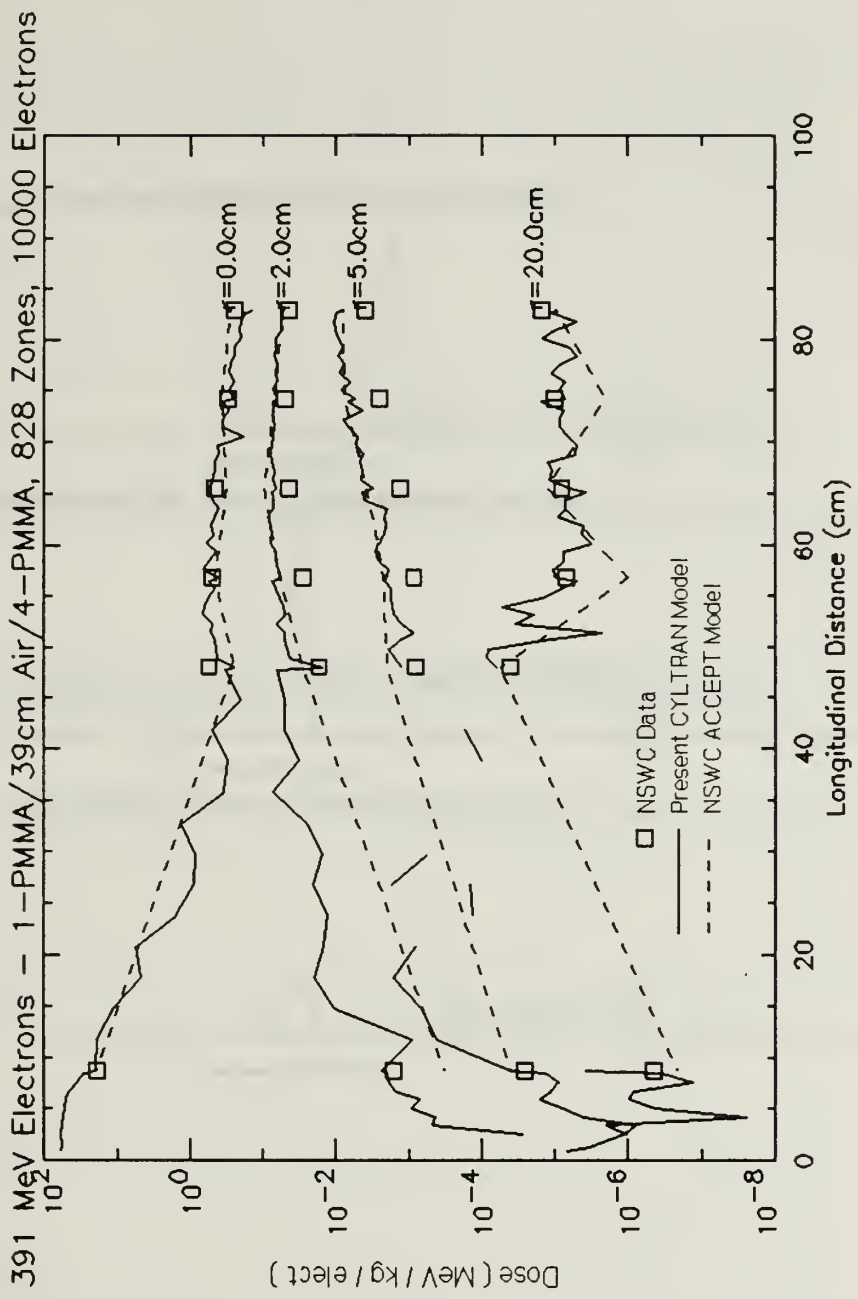

Figure C6. High Resolution Dose Distribution for Target of Figure 10 with Different Random Number Seed. Compare to figure 10 to see that the random number seed can cause the results to fluctuate about 20-50%.

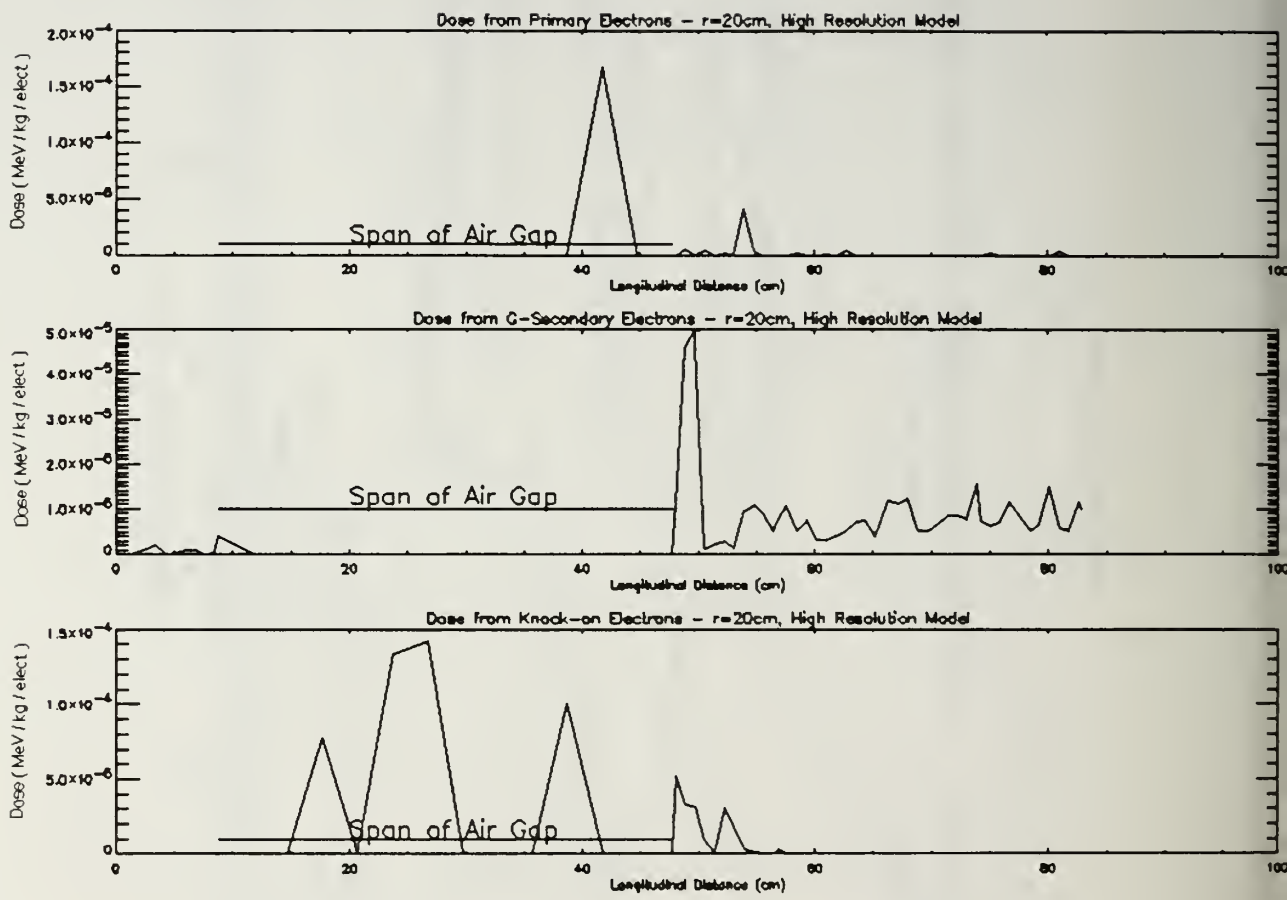

Figure C7. Dose Breakdown at 20cm Radius for Target of Figure 10 wi Different Random Number Seed. Notice the small number of collisio experienced in the air gap. The change in random number seed causes drastic change in the distribution in the air.

THIS PAGE INTENTIONALLY LEFT BLANK

LIST OF REFERENCES

1. Stern, S. H., Cha, M.H., Goktepe, O. F., Lindgren, R. A., and Haftel, M. I., "A Benchmark Experiment to Test Monte Carlo Electron-Photon Shower-Simulation Codes", Bates Linear Accelerator Center Annual Scientific and Technical Report, p. 9, 1986.

2. Stern, S. H., Cha, M.H., Goktepe, O. F., Lindgren, R. A., and Haftel, M. I., "A Benchmark Experiment with 391 MeV Electrons to Test Monte Carlo Electron-Photon Shower-Simulation Codes", Bates Linear Accelerator Center Annual Scientific and Technical Report, p. 197-198, 1987.

3. Stern, S. H., Cha, M.H., Goktepe, O. F., Lindgren, R. A., and Haftel, M. I., "A Benchmark Experiment to Test Radiation Shower Simulation Codes", paper presented at the BEAMS '88 Conference, p. 3-4, 1988.

4. Heilbleib, J.A., Mehlhorn, T.A., ITS: The Integrated Tiger Series of Coupled Electron/Photon Monte Carlo Transport Code, Sandia National Laboratories, Report SAND84-0573, November, 1984.

5. Jensen, D.C., Monte Carlo Calculation of Electron Multiple Scattering in Thin Foils, Master's Thesis, Naval Postgraduate School, Monterey, California, p. 12, June 1988.

6. Nahum, A.E., "Overview of Photon and Electron Monte Carlo", Monte Carlo Transport of Electrons and Photons, edited by Jenkins, T.M., Nelson, W.R., Rindi, A., Plenum Press, p. 4, 1988.

7. Seltzer, S.M., "An Overview of ETRAN Monte Carlo Methods", Monte Carlo Transport of Electrons and Photons, edited by Jenkins, T.M., Nelson, W.R., Rindi, A., Plenum Press, p. 156, 1988.

8. U.S. Department of Energy, Oak Ridge National Laboratory, Radiation Shielding Information Center, Report CCC-467, ITS 2.1, Integrated TIGER Series of Coupled Electron/Photon Monte Carlo Code System, p.16, 1991.

9. University of California-Berkeley, Lawrence Berkeley Laboratory, Berkeley Particle Data Group, Particle Properties Data Booklet, pp. 99-100, 170-171, 1988.

10. Bielajew, A.F, and Rogers, D.W.O., "Electron Step-Size Artefacts and PRESTA", Monte Carlo Transport of Electrons and Photons, edited by Jenkins, T.M., Nelson, W.R., Rindi, A., Plenum Press, p. 156, 1988.

INITIAL DISTRIBUTION LIST

1.	Defense Technical Information Center Cameron Station Alexandria, VA 22304-6145	2
2.	Library, Code 52 Naval Postgraduate School Monterey, CA 93943-5002	2
3.	Prof. Xavier K. Maruyama Department of Physics, Code Ph/Mx Naval Postgraduate School Monterey, CA 93943-5000	4
4.	Prof. K.E. Woehler, Code Ph/Wh Physics Department Chairman Naval Postgraduate School Monterey, CA 93943-5000	1
5.	Prof. John R. Neighbours Department of Physics, Code Ph/Nb Naval Postgraduate School Monterey, CA 93943-5000	1
6.	CPT Richard N. Yaw 100 Malloway Lane Monterey, CA 93940	3
7.	Dr. Joseph Mack Code P-4 Mail Stop E554 Los Alamos National Laboratory Los Alamos, NM 87545	1
8.	Dr. Steven Seltzer Center for Radiation Research National Bureau of Standards Gaithersburg, MD 20899	1
9.	R. A. Lindgren University of Virginia Charlottesville, VA 22901	1
10.	Director Bates Linear Accelerator Center Massachusetts Institute of Technology Cambridge, MA 02139	1

11. M. I. Haftel 1
Naval Research Laboratory
Washington, D.C. 20375

12. S. H. Stern 1
Naval Surface Weapons Center
Silver Spring, MD 20903

229.546

Thesis
Y328 Yaw
c.1 Monte Carlo analysis of energy deposition in solid state materials by 400 and 200 MeV electrons.

Thesis
Y328 Yaw
c.1 Monte Carlo analysis of energy deposition in solid state materials by 400 and 200 MeV electrons.

AMERICAN BINDERY 1 10-93

DUDLEY KNOX LIBRARY
3 2768 00033192 0